

Proceedings of the One-day Symposium

2nd Contemporary Seismic Engineering - 2011

Organized by

The Hong Kong Institute of Steel Construction

Sponsored by

Department of Civil and Structural Engineering, The Hong Kong Polytechnic University

Joint Structural Division, The Hong Kong Institution of Engineers



Edited by
Ir Dr. C.M. Koon

21 March 2011

Chiang Chen Studio Theatre, The Hong Kong Polytechnic University

NIDA – Innovative Second-Order Design Software Without Effective Length

Features: Advanced Solutions in Structural Design with *Curved* Element to Simulate Imperfections

- Second-Order Analysis & Design to Eurocode3 (2005)/HK Steel Code (2005)

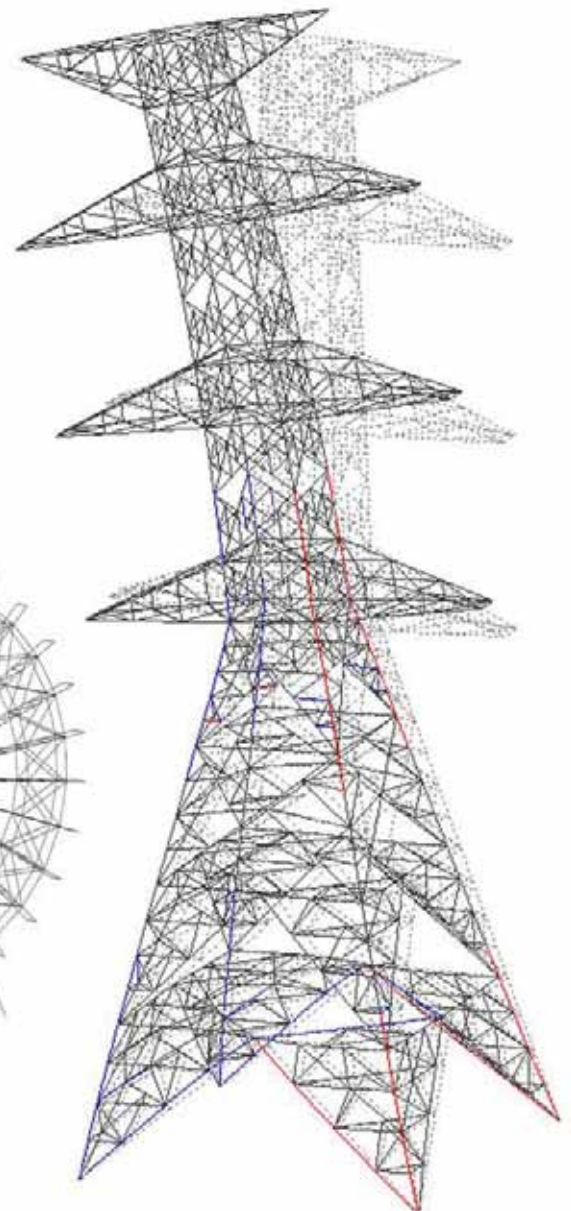
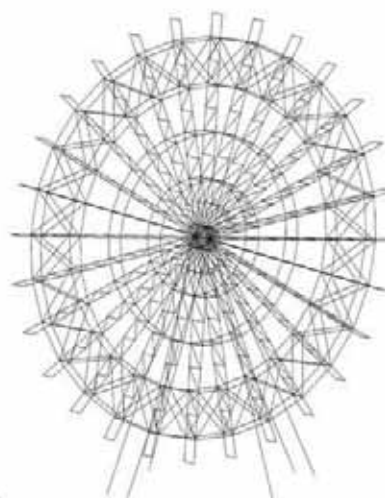
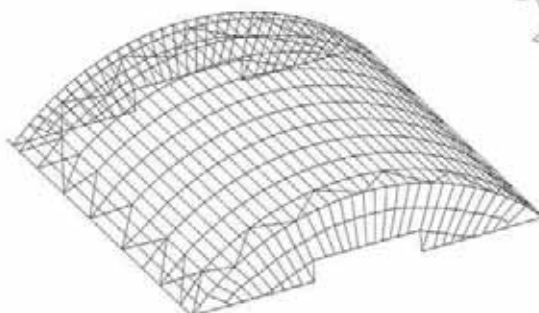
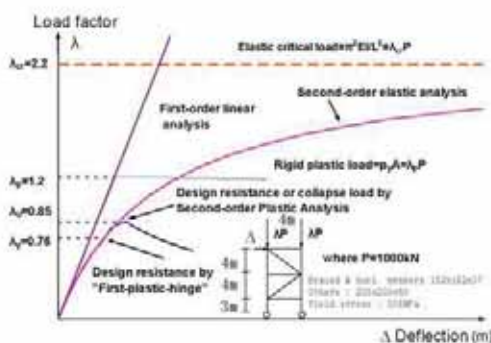
Second-order elastic and plastic analysis with allowance of global and member imperfections.

- Consideration of P- Δ , P- δ effects and Imperfections

Simulation of member imperfection to Table 5.1 in Eurocode3 or Table 6.1 in CoPHK

- Elimination of Effective Length Assumption
- Semi-rigid Connection and Plastic Hinge Method
- Load and Construction Sequences Analysis
- Large Deflection Analysis of Shell Structures
- Elastic Buckling and Vibration Analysis
- Seismic Performance Evaluation

Response Spectrum, Pushover, Time-History Analysis



CONTENTS

	Pages
Programme	i
Message from Chairman of the Structural Division of HKIE	iii
中国“建筑抗震设计规范 GB50011-2010”简介 王亚勇	1
Principles of Seismic Design with an Overview of Eurocode 8 A.Y. Elghazouli	13
Collapse Modes of Low-rise Masonry Infilled RC Frame Buildings under Strong Earthquakes C.L. Lee and R.K.L. Su	35
新型組合構件在高層建築中的應用 何偉明, 劉鵬, 鐘聰明, 劉光磊, 殷超及程鎮遠	57
Second Order Plastic Hinge Analysis for Seismic and Static Design of Building Structures Y.P. Liu and S.L. Chan	71
Seismic Strengthening of Reinforced concrete Structures S.S.E. Lam, Y.L. Wong, M.Z. Zhang, C.S. Li, B. Wu, A. Chen, Z.D. Yang, Y.Y. Wang, F.Y.I. Ho and B. Li	99
Acknowledgements	122

Disclaimer

No responsibility is assumed for any injury and/or damage to persons or property as a matter of products liability, negligence or otherwise, or from any use or operation of any methods, products, instructions or ideas contained in the material herein. The Institute of Steel Construction, the authors and the reviewers assume no responsibility for any errors in or misinterpretations of such data and/or information or any loss or damage arising from or related to their use.

Copyright © 2011 reserved by The Hong Kong Institute of Steel Construction

All rights reserved. No part of this publication may be produced, stored in a retrieval system, or transmitted in any form or by any means, electronic, mechanical, photocopying, recording or otherwise, without the prior written permission of the copyright holder. The authors retain the right to republish their contributions consisting solely of their own work.

Printed in Hong Kong

Programme

Date: 21st March 2011 (Monday)

Venue: Chiang Chen Studio Theatre, The Hong Kong Polytechnic University

Time: 8:30 am (registration) for 9:00 am to 5:15 pm

Time	Program	Session Chairmen
08:45 am	Registration	
09:00 am	Welcoming Speech Ir Dr. C.M. Koon Chairman, Joint Structural Division, The Hong Kong Institution of Engineers (HKIE) and The Institution of Structural Engineers (IStructE)	Ir C.K. Lau
Lecture 1 09:30 am	Brief of Chinese Code for Seismic Design of Buildings B50011-2010 Professor Y.Y. Wang, Professor of CABR, National Master of Building Design, main editor, Chinese Code for Seismic Design of Buildings.	
11:00 am	Tea Break	
Lecture 2 11:30 am	Principles of seismic design with overview of Eurocode 8 Professor A. Y. Elghazouli, Professor of Structural Engineering, Head of Structures Section, Department of Civil & Environmental Engineering, Imperial College London, U.K.	Ir Dr. WT Chan
Lecture 3 12:15 am	Collapse modes of low-rise masonry infilled RC frame buildings under strong earthquakes. Dr. C.L. Lee, University of Hong Kong, HK	
1:00 pm	Lunch	
Lecture 4 2:15 pm	Application of modern composite components in high-rise construction Ir Dr. Goman Ho, Ove Arup and Partners Limited	Ir Aldows Tang
Lecture 5 3:00 pm	Second-order plastic hinge analysis for seismic and static design of building structures Dr. Y.P. Liu & Prof. S.L. Chan, Hong Kong Polytechnic University, HK	
3:45 pm	Tea Break	
Lecture 6 4:15 pm	Seismic Strengthening of reinforced concrete structures Ir Dr.S.S. Lam, Hong Kong Polytechnic University, Hong Kong	Ir Adam Choy
5:00 pm	Closing remarks Ir Prof. Paul Pang Chairman of Sub-Committee of IStructE Matters in HK, Past Chairman of Joint Structural Division of HKIE and and IStructE	
5:15 pm	End	

(Blank)

Message from Chairman of the Structural Division of HKIE

I have great pleasure in handing this symposium proceeding to you. The Hong Kong Institute of Steel Construction (HKISC) has been organizing seminars and symposiums on various subjects, which help practicing engineers and engineering students, not only to enrich their knowledge, but also to broaden their approach to building design. It makes the process of design and analysis enjoyable and creative.

The HKISC is having its symposium on “2nd Contemporary Seismic Engineering 2011”, which is very timely, relevant, and of concern to every one of us. The 6.3 magnitude earthquake on 22 February 2011 rocked New Zealand’s Christchurch, causing widespread damage and took away over 200 lives. The 5.4 magnitude Yunnan earthquake on 10 March 2011 caused 25 people died and 250 injured. On the next day, 11 March 2011, the biggest 9.0 magnitude earthquake to hit Japan on record struck the northeast coast, triggering a 10-metre tsunami that swept away everything in its path, including houses, ships, cars and caused farm buildings on fire. The actual casualties are yet known and may be more than 25 000 people.

The theme of this year’s symposium is uniquely positioned at the crossroads between basic science research and practicality of seismic engineering, ready to use new knowledge gleaned from the advancement of knowledge and scientific discovery. Classical and modern philosophical concepts of seismic engineering will be discussed along with evidential findings and applications. This symposium is facilitated by experts in their chosen field and will inspire you to have a better understanding on structural responses in quake.

I congratulate the HKISC in particular the Organizing Committee on selecting such an important and timely topic. I also welcome all delegates and speakers who have come from China and Hong Kong.

KOON Chi Ming

Chairman

Structural Division of HKIE

(Blank)

中国“建筑抗震设计规范 GB50011-2010”简介

王亚勇

中国建筑科学研究院 工程抗震研究所 北京 100013

yayongwang@sina.com

摘要

新的国家标准“建筑抗震设计规范 GB50011-2010”已于 2010 年 5 月 31 日由中华人民共和国住房和城乡建设部与国家质量监督检验检疫总局联合发布，2010 年 12 月 1 日起实施。在规范修订过程中，2008 年 5 月 12 日汶川地震和 2010 年 4 月 14 日玉树地震中各类建筑震害提供了重要的经验。本文简要介绍修订的主要内容，包括：地震动区划的修改、关于地震次生地质灾害和场地选址的要求、场地分类和设计反应谱、防震缝设置、楼梯间的计算分析和构造、楼层最小地震剪力要求、多道抗震防线要求、结构时程分析和输入地震动、大跨空间结构和地下建筑抗震设计等。

关键词：建筑抗震设计规范 GB50011-2010；建筑震害

1. 前言

2008年5月12日汶川地震和2010年4月14日玉树地震中,各类建筑受到不同程度的破坏,对建筑震害的总结和分析研究,促进了规范修订工作。国家标准“建筑抗震设计规范 GB50011-2010”(以下简称“新规范”)于2010年5月31日由中华人民共和国住房和城乡建设部与国家质量监督检验检疫局联合发布,2010年12月1日起实施。按原建设部建标[2006]77号文件通知,国家标准“建筑抗震设计规范”修订的指导原则是“依据我国国情,适当调整提高抗震设防标准”。新规范继承了原规范的“三水准设防”和“两阶段抗震验算”的抗震设计理念和基本要求。但是,在抗震设防标准和具体抗震措施等方面,新规范有所提高和改进;基于性能的抗震设计方法也正式引入新规范;新规范还增加了大跨空间结构和地下建筑抗震设计的内容。本文主要介绍建筑抗震设计的基本要求,对各类建筑结构的具体条文将另文叙述。

2. 新规范对 89 规范和 2001 规范的延续

新规范在以下几方面延续了 1989 规范和 2001 规范的基本原则:

- 1) 遵守“三水准设防和两阶段抗震验算”的抗震设计基本原则,以“小震不坏,中震可修,大震不倒”为三水准设防目标,进行“小震”作用下的结构强度和弹性变形验算和“大震”作用下的弹塑性变形验算。
- 2) 保留 7 度 0.15g 和 8 度 0.30g 的设计地震分区及相应的抗震设计要求。
- 3) 保留设计反应谱(地震影响系数曲线)的骨架曲线形状,周期延长到 6s,并提供不同阻尼比的调整方法。
- 4) 保留楼层最小剪力系数强制性要求。
- 5) 保留建筑规则性定性和定量化的定义。
- 6) 保留钢筋混凝土结构抗震等级划分和相应的计算与构造要求。
- 7) 保留砌体结构设置圈梁和构造柱以提高结构延性和整体性的要求。
- 8) 保留并细化隔震和消能减震设计内容。
- 9) 保留非结构抗震设计内容。

3. 抗震设计采用的设计地震分组

设计地震分组完全照《中国地震动参数区划图 GB18306-2001》的定义,不再进行调整。这样,与 2001 规范相比,在新规范的附录 A 中,全国 2500 个抗震设防城镇中设防烈度不变而设计地震分组上升的城镇有 1000 多个,占 40%以上。变化较多的省份和所占城镇的比例如下:

河北：74%，山西：55%，福建：54%，山东：75%，河南：45%，四川：76%，云南：82%，西藏：82%，陕西：48%，甘肃：92%，青海：88%，宁夏：81%，新疆：82%。

其中，设计地震分组上升的省会城市和直辖市有：

天津、石家庄、福州、郑州、银川、乌鲁木齐，由设计一组升为设计二组；
济南、昆明、兰州、西宁、拉萨、台北，由设计二组升为设计三组；
成都，由设计一组升为设计三组；

设计地震分组的上升表明对应的场地特征周期 T_g 有所加大，地震作用相应增大。

4. 关于建筑形体的规则性

建筑形体的规则性包含建筑平、立面尺寸、抗侧力构件布置和楼层质量、侧向刚度、抗剪承载力分布等诸多方面。由于建筑造型和使用功能的要求，可能设计出形体不规则的建筑，对结构抗震带来不利影响。

1) 不规则建筑

新规范第 3.4.3 条的表 3.4.3-1，2 基本保留 2001 规范关于平面和竖向不规则性类型的定义，适用于钢筋混凝土结构、混合结构和钢结构，其它类型房屋有各自的规定。

2) 特别不规则建筑

对于存在多项不规则或不规则性超过规定的参考指标较多的建筑，新规范参照《超限高层建筑工程抗震设防专项审查技术要点》提出以下三类判定为“特别不规则”建筑：

- (a) 同时具有规范表 3.4.3-1，2 所列六项主要不规则类型的三项或三项以上；
- (b) 具有表 1 所列一项不规则类型；
- (c) 具有规范表 3.4.3-1，2 所列两项、且其中一项接近表 1 的不规则指标。

对于特别不规则建筑，应运用合理的计算模型和分析方法，对结构薄弱部位采取加强措施。必要时，也可设置防震缝将其划分为较规则的若干部分。

3) 严重不规则建筑

建筑形体复杂，两项不规则指标超过新规范第 3.4.4 条所定义的扭转不规则和楼层承载力突变的上限值、或某一项超过较多，以及超过规定的刚度比突变的上限，均属于严重不规则建筑。原则上，不允许采用严重不规则的建筑设计，或要对建筑布置进行调整和改变结构体系后，才能采用。

表 1 特别不规则结构类型

特别不规则	简要定义
扭转偏大	考虑偶然偏心时，较多楼层的扭转位移比大于 1.4。
抗扭刚度弱	普通结构的平动与扭转振型周期比 >0.9 ，混合结构的周期比 >0.85 。
层刚度偏小	本层侧向刚度小于相邻上层的 50%。
高位转换	框支墙体的转换层位置：7 度超过 5 层，8 度超过 3 层。
厚板转换	7~9 度设防区的厚板转换结构。
塔楼偏置	单塔或多塔合质心与大底盘的质心偏心距大于底盘相应边长 20%。
复杂连接	两端塔楼高度、体型差别较大，或沿大底盘两个主轴方向的振动周期显著不同的连体结构。
多重复杂	同时带转换层、加强层、错层、连体、多塔等 5 种复杂类型的 2 种以上。

5. 关于防震缝的设置

对于特别不规则的建筑，通常采用防震缝分割，形成若干较为规则的结构单元，以求得“完美”的计算结果和避免采用额外的加强措施。但是，大量的建筑震害表明，防震缝的设置有利有弊。新规范对防震缝的设置作了修订，第 3.4.5 条规定，体型复杂、平立面不规则的建筑，应根据不规则程度、地基基础条件和技术经济等因素的比较分析，确定是否设置防震缝，并分别符合下列要求：

- 1) 当不设置防震缝时，应采用符合实际的计算模型，分析判明其应力集中、变形集中或地震扭转效应等导致的易损部位，采取相应的加强措施。
- 2) 当在适当部位设置防震缝时，宜形成多个较规则的抗侧力结构单元。防震

缝应根据抗震设防烈度、结构材料、结构类型、结构单元的高度和高差以及可能的地震扭转效应情况，留有足够的宽度，其两侧的上部结构应完全分开。新规范将钢筋混凝土框架结构防震缝的最小宽度加大到 100mm，规定大跨屋盖结构防震缝最小宽度为 150mm，并要求计算中震作用下防震缝两侧结构的相对位移，使之不发生碰撞；如果缝宽不够，则要求设置长度不大于层高 1/2 的防撞墙。

6. 关于结构多道抗震防线

多道抗震防线是建筑抗震概念设计的主要要求之一。钢筋混凝土结构中的框-剪、框-筒、框架-支撑、剪力墙-连梁（联肢墙）结构；砌体结构中的砌体墙-构造柱、圈梁；钢结构中的框架-支撑（中心、偏心、消能支撑）；空旷房屋所采用的排架-支撑（竖向、水平支撑）等，均是具有多道抗震防线的结构形式。

大震作用下，具有多道抗震防线结构的第一道防线承受了主要的地震作用，产生塑性破坏，吸收地震能量；同时使结构内力重分布，地震作用转移到第二道抗震防线。因此，应考虑第一道防线失效后的内力重分布对第二道防线的内力调整，第二道抗震防线应具备足够的承载力和延性，防止结构倒塌。例如，框-剪、框-筒结构中，任一层框架承担的剪力按底部总剪力 20%和框架部分的各楼层剪力最大值 1.5 倍二者的较小值控制；砌体结构中，墙体破坏后，地震作用转由圈梁和构造柱组成的延性构架承担，保证建筑不倒；框架-支撑和排架-支撑结构中，作为第一道防线的支撑体系屈曲耗能，保证框架和排架柱的安全。

7. 关于楼梯间的抗震安全性

在 2008 年 512 汶川地震和 2010 年 414 玉树地震中，框架结构和砌体结构建筑中的楼梯间遭受严重破坏，暴露出对楼梯间地震安全重视不足的问题。为此，新规范规定，进行结构抗震计算时，楼梯间构件应参与建模计算。对于钢筋混凝土框架结构，楼梯间的布置不应导致结构平面特别不规则，抗震计算应考虑楼梯构件的影响，同时应对楼梯构件的抗震承载力进行验算。对于多层砌体房屋，要求在楼梯间四角和梯段上、下端对应的墙体处增设构造柱。

对钢筋混凝土框架结构，分别构建了六层单跨、三跨、五开间、七开间，楼梯间布置在一端、两端和中间等十四模型，与不考虑楼梯构件影响的四个计算模型进行对比。结果表明，楼梯构件参与计算使结构周期变短；基底剪力，除单侧设置楼梯外，顺梯方向增大：三跨为 1.1~1.2 倍，单跨 1.2~1.4 倍；层间位移：单侧设置楼梯为 1.4~1.5 倍，中间设置约为 1.1~1.2 倍，两侧布置的基本不变；与楼梯构件相连的框架柱内力增大：轴力为 3~4 倍，剪力 2~3 倍，弯矩 1.0~1.5 倍；框架梁端弯矩增大为 1.25~1.6 倍；与楼梯间不相连的框架构件，影响可忽略。楼梯构件本身受力比较复杂，梯板应计入轴力和弯矩的影响，顺梯方向的休息平台梁应计入轴力影响，横梯方向的休息平台梁应计入剪力和扭矩的影响，支承平台梁的柱子应考虑短柱效应。

8. 关于场地分类的调整

新规范对岩土类型与剪切波速的关系有所调整, 将坚硬土和硬岩石分开, 新增波速大于 800m/s 为岩石类(坚硬和较硬岩石), 保留波速为 500m/s~800m/s 的软基岩和坚硬土类。这个规定基本上与我国核电站抗震设计规范的 700 m/s, 美国规范的 760 m/s, 欧洲规范的 800 m/s 相近。中软土与软弱土的剪切波速分界, 由 140m/s 改为 150m/s (中软土中的可塑新黄土指的是 Q₃ 以来的黄土)。这样, 新的场地分类标准如表 2 所示:

表 2 场地分类标准

岩石的剪切波速或土的等效剪切波速 (m/s)	场地类别				
	I ₀	I ₁	II	III	IV
$V_s > 800$	0				
$800 \geq V_s > 500$		0			
$500 \geq V_{se} > 250$		<5	≥ 5		
$250 \geq V_{se} > 150$		<3	3~50	>50	
$V_{se} \leq 150$		<3	3~15	>15~80	>80

注: 表中 V_s 系岩石的剪切波速

9. 关于地震次生地质灾害和建筑选址

汶川地震和玉树地震中, 次生地质灾害产生了严重的人员伤亡和财产损失。新规范提出, 建筑物应避开地震时可能发生滑坡、崩塌、地陷、地裂、泥石流等及发震断裂带上可能发生地表位错的危险地段。特别强调建筑要避开发震断裂附近而且可能引发滑坡、崩塌等具有双重危险的地段, 严禁在危险地段建造甲、乙类设防的建筑。但是, 考虑到山区建设用地的困难, 新规范将发震断裂的最小避让距离由 200~500m 改为 100~400m。如果确有必要在断裂范围内建房, 只允许建造 1-2 层分散的单体建筑(农房), 而且要尽量采用整体基础, 不用独立柱基, 还应加强上部结构整体性。

山区建筑场地的勘察应对边坡的稳定性作出评价, 边坡设计应符合国家标准《建筑边坡工程技术规范》的要求。边坡附近的建筑, 也应对地基基础进行稳定性设计。建筑基础与土质、强风化岩质边坡的边缘应留有足够的距离, 不允许将建筑的外墙作为挡土墙, 或把山坡挡土墙作为建筑基础, 在其上建造房屋。

10 · 三水准抗震 设防地震动参数

为了适应不同设防水准下抗震性能化设计的要求，新规范分别给出了 6~9 度的三水准地面加速度峰值和地震影响系数最大值，如表 3 和表 4 所示。

表 3 地震烈度 I 与地面加速度峰值 A_{\max} (cm/s^2)

地震影响	6 度	7 度	8 度	9 度
多遇地震	18	35 (55)	70 (110)	140
设防地震	50	100 (150)	200 (300)	400
罕遇地震	125	220 (310)	400 (510)	620

注：括弧中的数据分别对应 7 度 0.15g 和 8 度 0.30g

表 4 地震影响系数最大值 α_{\max}

地震影响	6 度	7 度	8 度	9 度
多遇地震	0.04	0.08 (0.12)	0.16 (0.24)	0.32
设防地震	0.12	0.23 (0.34)	0.45 (0.67)	0.90
罕遇地震	0.28	0.50 (0.72)	0.90 (1.20)	1.40

注：括弧中的数据分别对应 7 度 0.15g 和 8 度 0.30g

11 · 关于设计反应谱骨架曲线的调整

规范反应谱（地震影响系数）是在大量实测的强震加速度记录统计平均基础上得到的，如图 1 所示。但是，由于强震仪频带范围的局限和加速度反应谱在长周期段下降速度太快，以致对高层建筑等长周期结构的抗震计算得到的地震响应小到根本不起控制作用。出于工程安全的考虑，我国的抗震设计规范在构建反应谱时，将反应谱的速度控制段和位移控制段人为抬升了，得到了如图 2 所示的规范反应谱骨架曲线。

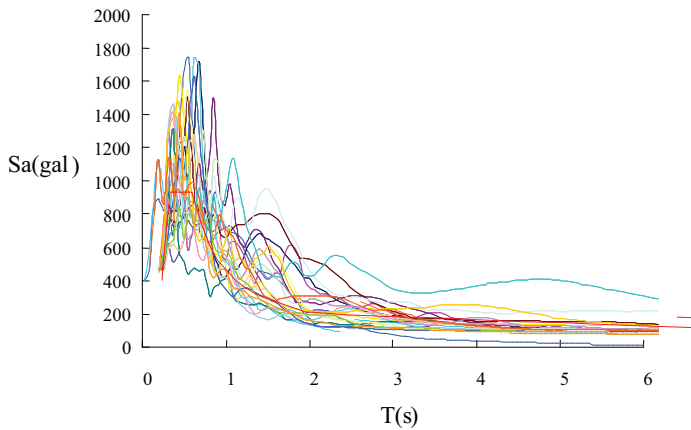


图 1 统计得到的加速度反应谱骨架曲线

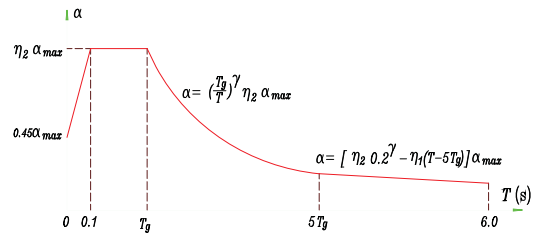


图 2 中国规范的设计反应谱

新规范对反应谱的曲线下降段的衰减指数 γ ，直线下降段的斜率调整系数 η_1 和阻尼调整系数 η_2 进行如下调整：

$$\begin{aligned} \gamma &= 0.9 + \frac{0.05 - \zeta}{0.5 + 5\zeta} \implies \gamma = 0.9 + \frac{0.05 - \zeta}{0.3 + 6\zeta} \\ \eta_1 &= 0.02 + \frac{0.05 - \zeta}{8} \implies \eta_1 = 0.02 + \frac{0.05 - \zeta}{4 + 32\zeta} \\ \eta_2 &= 1 + \frac{0.05 - \zeta}{0.06 + 1.7\zeta} \implies \eta_2 = 1 + \frac{0.05 - \zeta}{0.08 + 1.6\zeta} \end{aligned}$$

做此调整的目的是消除 2001 规范所构建的不同阻尼比反应谱骨架曲线在长周期段交叉的问题，这种交叉使得阻尼比大的反应谱值高于阻尼比小的反应谱值，如图 3 所示。调整后的反应谱如图 4 所示，在长周期段反应谱曲线交叉的现象有所改善，但是，在周期超过 6 秒之后，这种交叉又重新出现。因此，新规范规定，对于基本周期超过 6 秒的结构抗震验算，所采用的反应谱应专门研究。

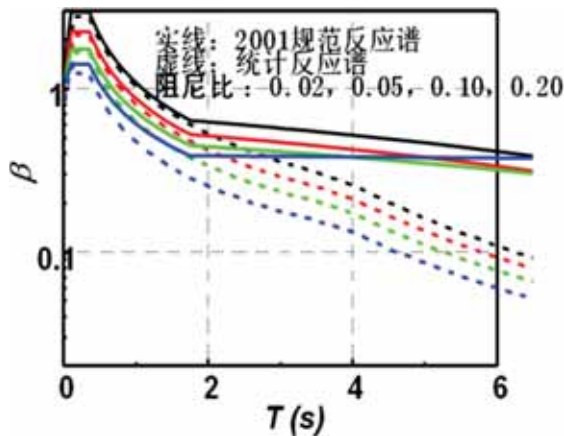


图 3 2001 规范反应谱

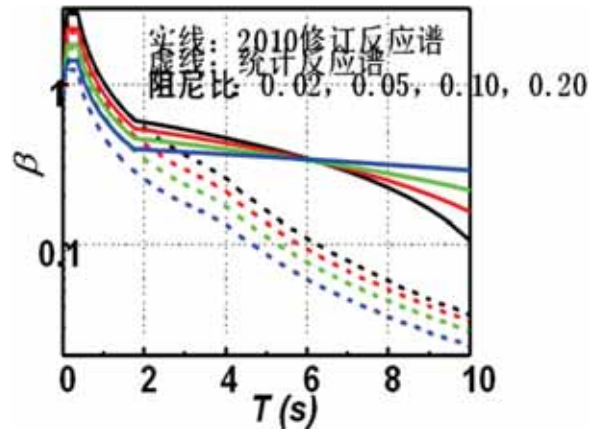


图 4 2010 规范反应谱

12 · 关于最小楼层剪力系数的要求

新规范 5.2.5 条强制规定，抗震验算时，结构任一楼层的水平地震剪力应符合下式要求：

$$V_{EKi} > \lambda \sum_{j=i}^n G_j \quad (1)$$

式中 λ 为剪力系数，不应小于表 5 规定的楼层最小地震剪力系数值（剪重比）。

表 5 楼层最小地震剪力系数值

地震影响	6 度	7 度	8 度	9 度
结构扭转 效应明显 或基本周 期<3.5s	0.00 8	0.016 (0.024)	0.032 (0.048)	0.06 4
结构基本 周期>5.0s	0.00 6	0.012 (0.018)	0.024 (0.036)	0.04 8

注：括弧中的数据分别对应 7 度 0.15g 和 8 度 0.30g

表 5 表明，为了保证结构的抗震安全，有必要规定一个楼层的最小地震剪力。但是，由于加速度反应谱在长周期段迅速下降，对于长周期结构，计算的楼层剪力系数很难满足规范要求，宜适当调低。当结构基本周期达到 6s 以上，还允许计算的楼层剪力系数（剪重比）再降低 10% 左右。所有不满足最小地震剪力系数的楼层地震剪力均应乘以相应的放大系数，以提高楼层抗侧力构件的承载力。但是，不满足最小地震剪力系数的楼层数不宜超过建筑总楼层数的 10%。计算的楼层剪力系数太低、或不满足要求的楼层数太多，表明结构刚度不足或重量太大，应对结构体系进行调整，提高结构刚度，而不应单纯采用乘以地震剪力增大系数提高结构构件强度的办法。

13 · 关于结构时程分析和输入地震波

结构时程分析即结构直接动力分析，与振型分解反应谱法一样，是经典的结构动力学方法之一。

1) 时程分析法的适用范围

新规范仍将时程分析法作为振型分解反应谱法的补充计算手段，小震作用下弹性时程分析的适用范围与 2001 规范相同。按照《高层建筑工程超限抗震设防审查

技术要点》要求，大震作用下弹塑性时程分析的适用范围扩大到高度超过 200m 的各类建筑结构。

2) 输入地震波的“选波”原则

结构时程分析法中，输入地震波的确是时程分析结果能否既反映结构最大可能遭受的地震作用，又能满足工程抗震设计基于安全和功能要求的关键。在工程实际应用中经常出现对同一个建筑结构采用时程分析时，由于输入地震波的不同造成计算结果的数倍乃至数十倍之差，使工程师无所适从。为此，新规范作了比较明确的规定。

(a) 数量要求

对于高度不高、体型比较规则的高层建筑，取 2+1，即选用不少于 2 条天然地震波和 1 条拟合目标谱的人工地震波，出于安全考虑，计算结果宜取包络值。对于超高、大跨、体型复杂的建筑结构，需要更多的地震波输入进行时程分析，规范规定 5+2，即不少于 7 组，其中，天然地震波数量不少于总数的 2/3，计算结果取平均值。

(b) 持续时间要求

为了充分地激励建筑结构，一般要求输入的地震动有效持续时间为结构基本周期的 5 倍左右。时间短了不能使结构充分振动起来，时间太长则会增加计算时间。对于结构动力时程分析，只有加速度记录的强震部分的长度、即有效持续时间才有意义。最常用的有效持续时间定义是：取记录最大峰值的 10%~15%作为起始峰值和结束峰值，在此之间的时间段为有效持续时间。

(c) “选波”原则

新规范规定，应按建筑场地类别和设计地震分组选用实际强震记录和人工模拟的加速度时程曲线、即通常所说的地震波。所选地震波反应谱的特征应与规范设计反应谱在统计意义上一致。对选波结果的评估标准是，以时程分析所得到的结构基底总剪力和振型分解反应谱法的计算结果进行比较，用一组（单向或两向水平）地震波输入进行时程分析，结构主方向基底总剪力为同方向反应谱计算结果的 65~130%，多组地震波输入的结果平均值为反应谱计算结果的 80~120%。不要求结构主、次两个方向的基底剪力同时满足这个要求。一组地震波的两个水平方向记录数据无法区分主、次向，通常可取加速度峰值较大者为主向。

14·大跨屋盖建筑抗震设计的地震作用和抗震验算

1) 大跨屋盖建筑的定义

大跨空间结构通常由下部钢筋混凝土支承结构和大跨度钢屋盖组成。新规范定义大跨度钢屋盖包括：拱、平面桁架、立体桁架、网架、网壳、张弦梁和弦支穹顶等七类基本形式。支承条件有：周边支撑、两线边支撑、长悬臂等。

跨度大于 120m、结构单元长度大于 300m 或悬挑长度大于 40m 的屋盖结构，以及除上述七类外新的屋盖结构形式，抗震设计应做专门研究。

2) 地震作用

一般情况下，大跨度空间结构除了考虑水平地震作用外，还应考虑竖向地震作用。两向水平与竖向地震作用的比例通常取 1.00 : 0.85 : 0.65。

3) 抗震验算

抗震验算要考虑多向地震效应的组合，特别增加了以竖向地震效应为主的组合，即取水平地震作用分项系数 $\gamma_{Eh}=0.5$ 和竖向地震作用分项系数 $\gamma_{Ev}=1.3$ 。

4) 地震动输入方式

抗震验算时，应根据屋盖尺度大小和支承条件，采用单点一致、多向单点、单向多点、多向多点等地震动输入方式。必要时，应考虑地震行波效应和局部场地效应。在 6、7 度 I，II 类场地时，可采用简化计算方法，对建筑短边的抗侧力构件的内力乘以放大系数 1.15~1.30。

15. 地下建筑抗震设计的地震作用和抗震验算

1) 地下建筑的定义

新规范定义的地下建筑仅限于单建式建筑，不包括地下铁道和城市公路隧道。单建式地下建筑可用于服务于人流、车流，或物资储藏，抗震设防应有不同的要求。

2) 地震作用

地下建筑结构的地震作用方向与地面建筑有所区别。

(a) 水平地震作用

对于长条形的地下结构，与其纵轴方向斜交的水平地震作用，可分解为沿横断面和沿纵轴方向的水平地震作用，一般不能单独起控制作用。因而在按平面应变问题分析时，一般可仅考虑沿结构横向的水平地震作用。对于地下空间综合体等体型复杂的地下建筑结构，宜同时计算结构横向和纵向的水平地震作用。

(b) 竖向地震作用

对于体型复杂的地下空间结构或地基条件复杂的长条形地下结构，都容易产生不均匀沉降并导致结构破坏，因而在 7 度及 7 度以上，有必要需考虑竖向地震作用效应为主的组合。

3) 抗震验算

地下建筑应进行多遇地震作用下构件承载力和结构变形验算。

考虑到地下建筑修复难度较大，对于不规则的地下建筑以及地下变电站和地下空间综合体等，尚应进行罕遇地震作用下的抗震变形验算，混凝土结构弹塑性层间位移角限值宜取 1/250。

在存在液化危害性的地基中建造地下建筑时，应验算其抗浮稳定性，必要时应采取抗液化措施。

参考文献

1. 中华人民共和国国家标准，GB50011-2010 建筑抗震设计规范，2010，中国建筑工业出版社
2. 国家标准建筑抗震设计规范管理组，建筑抗震设计规范（GB50011-2010）统一培训教材，2010，地震出版社

PRINCIPLES OF SEISMIC DESIGN WITH AN OVERVIEW OF EUROCODE 8

A.Y. Elghazouli
Imperial College London, UK
a.elghazouli@imperial.ac.uk

ABSTRACT

This paper provides an overview of the main principles of seismic design for buildings with particular emphasis on the guidance provided in the European seismic code of practice, Eurocode 8. After giving a brief introduction to previous developments and current considerations in seismic design, the fundamental approaches and key provisions employed in Eurocode 8 are summarised. Typical procedures for determining seismic actions are presented including recommended response spectra. In addition, general requirements for the design of buildings, such as the implementation of capacity design, assessment of regularity, and considerations related to stiffness, are highlighted. The paper also outlines the principal features for the design of reinforced concrete and steel structures according to the European seismic code.

Keywords: Earthquake loading; Seismic design; Capacity design; reinforced concrete structures; steel structures; Eurocode 8.

1. INTRODUCTION

Design requirements for lateral loads, such as wind or earthquakes are fundamentally different to those for gravity (dead and live) loads. Whilst design for wind loads may be a primary requirement, due to the frequency of the loading scenario, earthquake design may have to deal with relatively rare events. It may therefore be highly uneconomical to design structures to resist earthquake forces for the same level of internal stress used for wind design.

The first concepts for structural design in seismic areas were developed from experience gained in major events such as the San Francisco earthquake in 1906 and the Messina earthquake in 1908. At the very beginning, in the absence of experimental data, the method used was to design structures to withstand uniform horizontal accelerations of the order of 0.1g. After the Long Beach earthquake in 1933, experimental data showed that ground accelerations could be much higher, even in excess of 0.5g. Consequently, the resistance of certain structures could be explained only by the energy dissipation which occurred by response well into the inelastic range.

The 'second generation' of codes took into account the amplification due to the dynamic behaviour of the structures as well as indirectly the energy dissipation. However, such approaches remained rather elementary and did not appropriately differentiate between the behaviour of the various materials and types of lateral resisting systems. On the other hand, current 'third generation' of codes makes it possible to specify appropriate mechanisms for utilising energy dissipation, according to the type of lateral resistance and the type of structural material used. It also widens the scope of codes, for instance by dealing with geotechnical aspects. Moreover, current rules typically take into account the semi-probabilistic approach for verification of safety [1]. The emergence of displacement-based analysis methods makes it possible to foresee an evolution towards a 'fourth generation' of seismic design codes, where the various components of the seismic behaviour would be better controlled, in particular those which relate to energy dissipation.

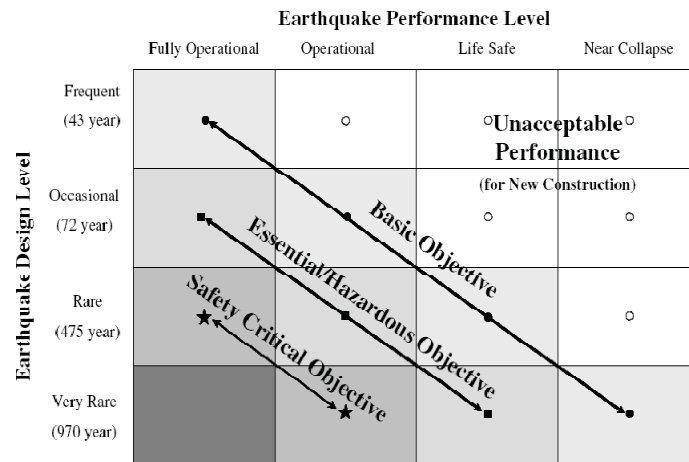


Figure 1 Seismic performance levels and objectives [2]

Modern trends utilise a number of performance targets, as opposed to design force levels, to control the level of damage inflicted on structures by earthquakes. In this context, ‘performance-based seismic design’ may be considered as a framework relating specific seismic hazard levels to carefully selected performance targets with defined levels of reliability and consequences. By definition, it requires a proper assessment of seismic hazard and detailed simulation of structural response, to realise its benefits. It also calls for involvement and decisions by owner/community with consideration of aspects of life safety/business disruption/repair costs within the nominal life time of the structure. However, performance-based design approaches have not yet been fully incorporated as such in codes of practice, with the level of implementation varying from one code to the other – an example of performance objectives and design levels for buildings, as defined by SEAOC [2] are depicted in Figure 1. However, even single design scenario codes purport to satisfy other limit states by recommending a number of checks on the structure resulting from the design process.

Table 1 Parts of Eurocode 8

Title	Reference
Part 1: General Rules, Seismic Actions and Rules for Buildings	EN 1998-1
Part 2: Bridges	EN 1998-2
Part 3: Assessment and Retrofitting of Buildings	EN 1998-3
Part 4: Silos, Tanks and Pipelines	EN 1998-4
Part 5: Foundations, Retaining Structures & Geotechnical Aspects	EN 1998-5
Part 6: Towers, Masts and Chimneys	EN 1998-6

This brief paper provides an overview of the main seismic design principles with particular emphasis on the provisions adopted in the recent European seismic design code [3], Eurocode 8, or EC8 for short. As indicated in Table 1, EC8 comprises six parts relating to different types of structures. Parts 1 and 5 form the basis for the seismic design of new buildings and its foundations; their rules are aimed both at protecting human life and also limiting economic loss. For brevity, this paper only summarises selected fundamental concepts covered within a number of sections within Part 1: General Rules, Seismic Actions and Rules for Buildings [3]. Particular focus is given to several main aspects within Sections 1-6 of Part 1 of EC8, covering loading and spectra, general considerations for buildings, and an outline of the underlying principles for the design of reinforced concrete and steel structures.

2. LOADING AND SPECTRA

Seismic analysis is normally a two-stage process: first estimating the dynamic properties of the structure (natural frequencies and mode shapes) by analysing it in the absence of external loads, then using these properties in the determination of earthquake response. Economical seismic design for severe events often entails non-linear response in structures. However, most practical seismic design continues to be based on linear analysis. The effect of non-linearity is generally to reduce the seismic demands on the structure, and this is normally accounted for by a simple modification to the linear analysis procedure. This section is limited to these simplified approaches, yet more detailed information on other seismic analysis procedures can be found elsewhere [1].

Figure 1 shows the elastic response spectra defined by Eurocode 8. EC8 specifies two categories of spectra: Type 1 for areas of high seismicity (defined as $M_s > 5.5$), and Type 2 for areas of moderate seismicity ($M_s \leq 5.5$). Within each category, spectra are given for five different soil types: A – rock; B – very dense sand or gravel, or very stiff clay; C – dense sand or gravel, or stiff clay; D – loose-to-medium cohesionless soil, or soft-to-firm cohesive soil; E – soil profiles with a surface layer of alluvium of thickness 5 to 20 m. The vertical axis is the peak, or spectral acceleration of the elastic structure, denoted by S_e , normalised by a_g , the design peak ground acceleration on Type A ground. The spectra are plotted for an assumed structural damping ratio of 5%.

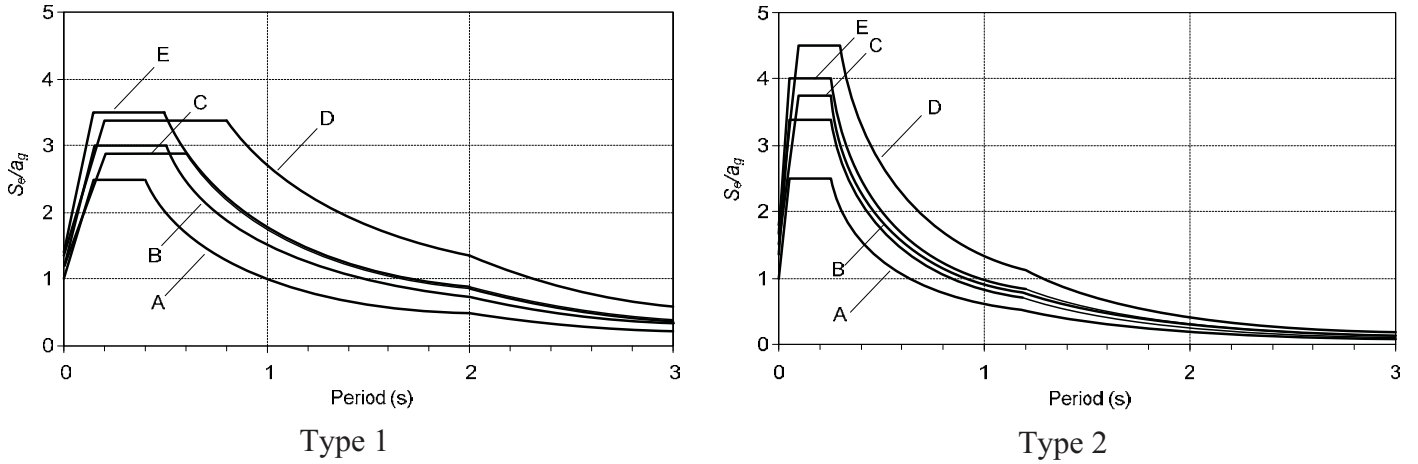


Figure 2 EC8 Type 1 and Type 2 elastic spectra (shown for 5% damping)

The underlying method of analysis in EC8 is the spectral modal analysis procedures, for which details can be found elsewhere [1], together with a description of other methods such as nonlinear static (push-over) analysis and time-history analysis. As with other codes, for structures satisfying a set of regularity criteria specified in EC8, it can reasonably be assumed to be dominated by a single (normally the fundamental) mode and a simple static analysis procedure can be used which involves only minimal consideration of the dynamic behaviour. In this case, the period of the fundamental mode T_1 is estimated – usually by simplified approximate methods given in EC8 rather than a detailed dynamic analysis.

For the calculated structural period, the spectral acceleration S_e can be obtained from the design response spectrum. The base shear F_b is then calculated as:

$$F_b = \lambda m S_e \quad (1)$$

where m is the total mass; λ takes the value 0.85 for buildings of more than two storeys with $T_1 < 2T_C$, and is 1.0 otherwise. The total horizontal load is then distributed over the height of the building in proportion to (mass \times mode shape). For simple regular buildings, EC8 permits the assumption that the first mode shape is a straight line (i.e. displacement is directly proportional to height). This leads to a storey force at level k given by:

$$F_k = F_b \frac{z_k m_k}{\sum_j z_j m_j} \quad (2)$$

where z represents storey height. Finally, the member forces and deformations can be calculated by static analysis.

To make use of ductility requires the structure to respond non-linearly. As in other codes, and for relatively regular structures, a ductility-modified response spectrum can be used such that linear analysis can be retained in design and more complex dynamic analysis procedures are avoided. This procedure requires the use of the behaviour factor (referred to as force reduction or forced modification factor in other seismic codes), which can be defined as the peak force that would be developed in the system if it responded elastically, to the yield load of the system.

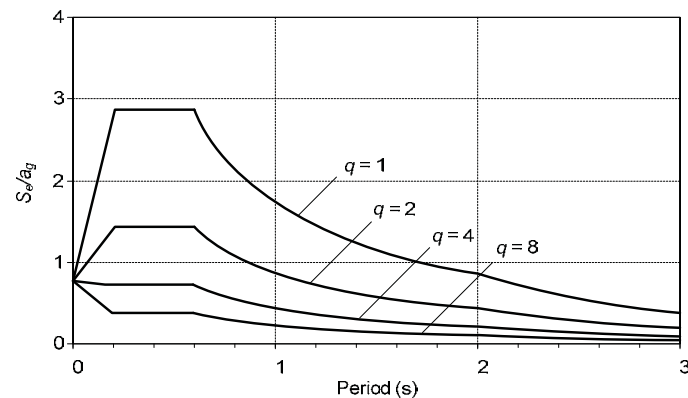


Figure 3 EC8 design response spectra (shown for Type 1 spectrum, Soil Type C)

In EC8, this is implemented within the *design spectrum*, S_d . For example, Figure 3 shows EC8 design spectra based on the Type 1 Spectrum and Soil Type C, for a range of behaviour factors. Over most of the period range (for $T \geq T_B$) the spectral accelerations S_d (and hence the design forces) are a factor of q times lower than the values S_e for the equivalent elastic system. Clearly, after calculating displacements using the design spectrum within an elastic analysis procedure, these must be magnified to account for the inelastic deformations that would occur in the structure.

3. GENERAL REQUIREMENTS FOR BUILDINGS

3.1 Fundamental Principles

There are two main fundamental requirements in EC8. The first is to meet a ‘no collapse’ performance level, which requires that the structure retains its full vertical load bearing capacity after an earthquake with a recommended return period of 475 years (probability of exceedence of 10% in 50 years); longer return periods are given for special structures, for example casualty hospitals or high risk petrochemical installations. After this earthquake, there should also be sufficient residual lateral strength and stiffness to protect life even during strong aftershocks. The second main requirement is to meet a ‘damage limitation’ performance level, which requires that the cost of damage and associated limitations of use should not be disproportionately high, in comparison with the total cost of the structure, after an earthquake with a recommended return period (for normal structures) of 95 years (probability of exceedence of 10% in 10 years).

At a conceptual design stage, six general guiding principles are given EC8 Part 1: (i) structural simplicity; (ii) uniformity, symmetry and redundancy; (iii) bi-directional resistance and stiffness; (iv) torsional resistance and stiffness; (v) adequacy of diaphragms at each storey level; (vi) adequate foundations. More detailed information on these aspects can be found elsewhere [1].

3.2 *Siting Considerations*

Within an area of uniform regional hazard, the level of expected ground shaking is likely to vary strongly, and so is the threat from other hazards related to seismicity, such as landslides or fault rupture. The most obvious cause of local variation in hazard arises from the soils overlying bedrock, which affect the intensity and period of ground motions. It is not only the soils immediately below the site which affect the hazard; the horizontal profiles of soil and rock can also be important, due to 'basin effects'. Topographic amplification of motions may be significant near the crest of steep slopes. Fault rupture, slope instability, liquefaction, and shakedown settlement are other hazards associated with seismic activity which may also need to be considered.

By ensuring that these potential hazards at a site are identified, the designer can take appropriate actions to minimise those hazards. In some cases, the choice of a different site may be the best approach is feasible, for example to avoid building on an unstable slope or crossing a fault assessed as potentially active. If the hazard cannot be avoided, appropriate design measures must be taken to accommodate or mitigate it. For example, ground improvement measures may be one option for a site assessed as susceptible to liquefaction, and suitable articulation to accommodate fault movements may be possible for extended structures such as pipelines and bridges.

3.3 *Regularity in Plan and Elevation*

EC8 Part 1 sets out quantified criteria for assessing structural regularity, complementing the qualitative advice on symmetry and uniformity. Irregular configurations are allowed by EC8, but lead to more onerous design requirements.

A classification of 'non-regularity' in plan requires the use modal analysis, as opposed to equivalent lateral force analysis, and generally a 3D as opposed to a 2D structural model. For a linear analysis, a 3D model may usually be chosen for convenience, even for regular structures. However, a non-linear static (pushover) analysis becomes much less straightforward with 3D analysis models, and should be used with caution if there is plan irregularity, because of the difficulty in capturing coupled lateral-torsional modes of response. Other consequences of non-regularity in plan are the need to combine the effects of earthquakes in the two principal directions of a structure and for certain structures (primarily moment frame buildings) the q

factor must be reduced. Moreover, in ‘torsionally flexible’ concrete buildings, the q value is reduced to 2 for medium ductility and 3 for high ductility, with a further reduction of 20% if there is irregularity in elevation. A classification of ‘non-regular’ in elevation also requires the use of modal analysis, and leads to a reduced q factor, equal to the reference value for regular structures reduced by 20%.

According to EC8, classification as regular in plan requires the following: (i) *nearly* symmetrical distribution of mass and stiffness in plan; (ii) a *compact* shape, i.e. one in which the perimeter line is always convex, or at least encloses not more than 5% re-entrant area, as indicated in Figure 4; (iii) the floor diaphragms shall be sufficiently stiff in-plane not to affect the distribution of lateral loads between vertical elements - EC8 warns that this should be carefully examined in the branches of branched systems, such as L, C, H, I and X plan shapes; (iv) the ratio of longer side to shorter sides in plan does not exceed 4; (v) limits on the torsional radii in both planar directions must satisfy specified limits with respects to the eccentricity between centres of stiffness and mass in both directions; (vi) the torsional radii must exceed the radius of gyration, otherwise the building is classified as ‘torsionally-flexible’, and the q values particularly for concrete buildings are greatly reduced. Further information is available in EC8 [3] and in a recent design manual produced by IStructE [4].

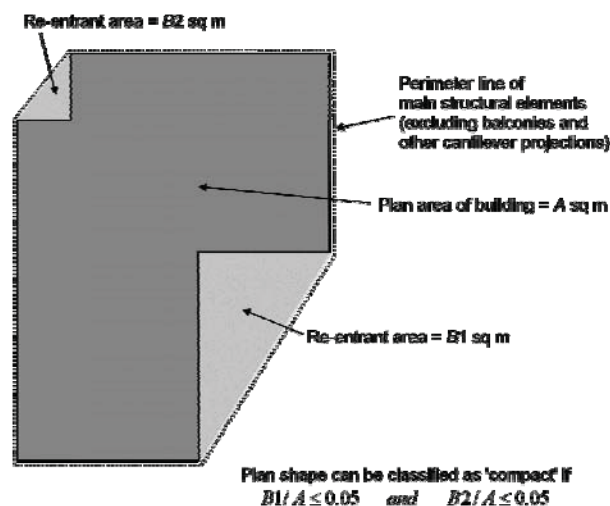


Figure 4 Definition of compact shapes in plan according to EC8

For the regularity in elevation, a building should satisfy the following according to EC8: (i) all the vertical load resisting elements must continue uninterrupted from foundation level to the top of the building, or where setbacks are present to the top of the setback; (ii) mass and stiffness must either remain constant with height or reduce only gradually, without abrupt changes; (iii) in buildings with moment-resisting frames, the lateral resistance of each storey should not vary disproportionately between storeys; (iv) buildings with setbacks are generally irregular, but may be classified as regular if less than limits defined in the code – in general, a total reduction in width from top to bottom on any face not exceeding 30%, with not more than 10% at any level compared to the level below, would conform; however, an overall reduction in width of up to half is permissible within the lowest 15% of the

height of the building. Further details on regularity criteria is available in EC8 [3] and in the design manual produced recently by IStructE [43].

3.4 Capacity Design

EC8 contains specific design measures for ensuring that structures meet the performance requirements of the code. These apply to all structures, not just buildings, and a crucial requirement concerns capacity design, which determines much of the content of the material specific rules for concrete, steel and composite buildings in sections 5, 6 and 7 of EC8 Part 1. EC8 [1,3] states clearly that ‘in order to ensure an overall dissipative and ductile behaviour, brittle failure or the premature formation of unstable mechanisms shall be avoided. To this end, where required in the relevant Parts of EC8, resort shall be made to the capacity design procedure, which is used to obtain the hierarchy of resistance of the various structural components and failure modes necessary for ensuring a suitable plastic mechanism and for avoiding brittle failure modes.

The principle of capacity design is illustrated in Figure 5. The idea is that the ductile link yields at load which is well below the failure load of the brittle links. Although most building structures are somewhat less straightforward than the chain idealisation, one of the main merits of the capacity design principle is that it relies on simple static analysis to ensure good performance, and is not dependent on the complexities of dynamic analysis.

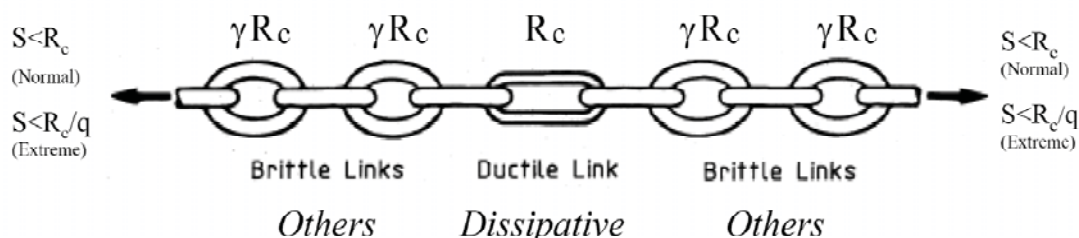


Figure 5 Idealised illustration of the capacity design concept

Ensuring that columns are stronger than beams in moment frames, concrete beams are stronger in shear than in flexure and steel braces buckle before columns are three examples of capacity design requirements. A general rule for all types of frame building given in EC8 is that the moment strength of columns connected to a particular node in RC moment frames be 30% greater than the moment strength of the beams:

$$\sum M_{Rc} \geq 1.3 \sum M_{Rb} \quad (3)$$

One feature of capacity design is that it ensures that designers identify clearly which

parts of the structure will yield in a severe earthquake (the “critical” regions) and which will remain elastic.

3.5 Primary and Secondary Members

EC8 distinguishes between primary and secondary elements. Primary elements are those which provide the main contribution to the seismic resistance of the structure. Some structural elements can however be designated as ‘secondary’ elements, which are taken as resisting gravity loads only. Their contribution to seismic resistance is typically neglected. These elements must be shown to be capable of maintaining their ability to support the gravity loads under the maximum deflections occurring during the design earthquake. This may be performed by showing that the actions (moments, shears, axial forces) that develop in them under the calculated seismic deformations do not exceed their design strength, as determined as other non-seismic loading conditions. Otherwise, no further seismic design or detailing requirements are required.

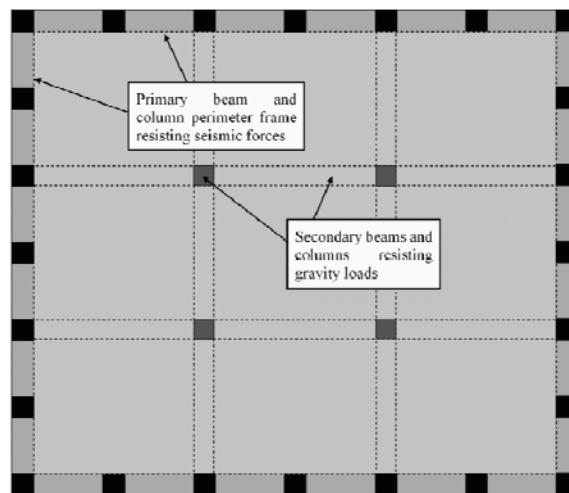


Figure 6 Example of primary and secondary elements in plan

An example of the use of secondary elements occurs in a frame building is depicted in Figure 6. The perimeter frame is considered as the primary seismic resisting element, and is designed for high ductility while the internal members are considered secondary. This gives considerable architectural freedom for the layout of the internal spaces; the column spacing can be much greater than would be efficient in a moment resisting frame, while closely spaced columns on the perimeter represents much less obstruction.

3.6 Stiffness Considerations

Apart from its major influence in determining the magnitude of inertial loads, structural stiffness is important in meeting the damage limitation provisions of EC8

and in assessing the significance of P- δ effects. Both effectively place limits on storey drift, the former explicitly albeit for a lower return period earthquake, and the latter implicitly through the inter-storey drift sensitivity coefficient, θ . In both cases, the relative displacements between storeys, d_r , if obtained from a linear analysis, should be multiplied by a displacement behaviour factor q_d . When the period of response of the structure is greater than T_C (i.e. on the constant displacement or constant velocity portion of the response spectrum), q_d is equal to the behaviour factor q , so that the plastic displacement is equal to the elastic displacement obtained from the unreduced input spectrum. However, q_d exceeds q at lower periods as defined in Appendix B of the code.

In calculating displacements, EC8 requires that the flexural and shear stiffness of concrete structures reflect the effective stiffness consistent with the level of cracking expected at the initiation of yield of the reinforcement. If the designer does not take the option of calculating the stiffness reduction directly through push-over analysis, for example, the code allows the effective stiffness to be based upon half of the gross section stiffness to account for softening of the structure at the strain levels consistent with reinforcement yield. It is acknowledged that the true stiffness reduction would probably be greater than this but the value chosen is a compromise; lower stiffness being more onerous for P- δ effects but less onerous for calculation of inertial loading on the structure. The EC8 approach, whilst similar to performance-based methodologies elsewhere, differs in applying a uniform stiffness reduction independent of the type of element considered. Paulay and Priestley [5] proposes greater stiffness reductions in beams than in columns, reflecting the weak beam/strong column philosophy and the beneficial effects of compressive axial loads.

Checks on damage limitation aim to maintain the maximum storey drifts below limiting values set between 0.5% and 1% of the storey height, dependent upon the ductility and fixity conditions of the non-structural elements. The amplified displacements for the design earthquake are modified by a reduction factor, v , of either 0.4 or 0.5, varying with the Importance Class of the building, to derive the displacements applicable for the more frequent return period earthquake considered for the damage limitation state.

The inter-storey drift sensitivity coefficient, θ , used to take account of P- δ effects, is defined as:

$$\theta = (P_{tot} d_r) / (V_{tot} h) \quad (4)$$

P_{tot} is the total gravity load at and above the storey, V_{tot} the cumulative seismic shear force acting at each storey and h the storey height. If the maximum value of θ at any level is less than 0.1, then P- δ effects may be ignored. If θ exceeds 0.3, then the frame is insufficiently stiff and an alternative solution is required. For values of θ between 0.1 and 0.2, an approximate allowance for P- δ effects may be made by increasing the analysis forces by a factor of $1/(1-\theta)$ whilst, for values of θ of between 0.2 and 0.3, a second order analysis is required.

4. MAIN FEATURES OF REINFORCED CONCRETE DESIGN TO EC8

4.1 *Design Concepts*

This section introduces few of the main features of seismic design of RC structures in EC8 (Section 5 of Part 1). It is beyond the scope of this brief paper to discuss these design aspects in detail. As noted earlier, EC8 aims to ensure life safety in a large earthquake together with damage limitation following a more frequent event. Whilst the code allows these events to be resisted by either dissipative (ductile) or non-dissipative (essentially elastic) behaviour, there is a clear preference for resisting larger events through dissipative behaviour. Hence, much of the code is framed with the aim of ensuring stable, reliable dissipative performance in pre-defined 'critical regions'. The design and detailing rules are formulated to reflect the extent of the intended plasticity in these critical regions, with the benefits of reduced inertial loads being obtained through the penalty of more stringent layout, design and detailing requirements. This is particularly the case for reinforced concrete structures where such performance can only be achieved if strength degradation during hysteretic cycling is suppressed by appropriate detailing of these critical zones to ensure that stable plastic behaviour is not undermined by the occurrence of brittle failure modes such as shear or compression in the concrete or buckling of reinforcing steel.

In light of the above discussion, three dissipation classes are introduced:

- Low (DCL) in which virtually no hysteretic ductility is intended and the resistance to earthquake loading is achieved through the strength of the structure rather than its ductility.
- Medium (DCM) in which quite high levels of plasticity are permitted and corresponding design and detailing requirements are imposed.
- High (DCH) where very large inelastic excursions are permitted accompanied by even more onerous and complex design and detailing requirements.

EC8 classifies concrete buildings into the following structural types:

- Frame system
- Dual system which may be either frame or wall equivalent
- Ductile wall system
- System of large lightly reinforced walls
- Inverted pendulum system
- Torsionally flexible system

Apart from torsionally flexible systems, buildings may be classified as different systems in the two orthogonal directions.

Frame systems are defined as those systems where moment frames carry both vertical and lateral loads and provide resistance to 65% or more of the total base shear. Conversely, buildings are designated as wall systems if walls resist 65% or more of the base shear. Walls may be classed as either ductile walls, which are designed to respond as vertical cantilevers yielding just above a rigid foundation, or as large lightly reinforced walls. Ductile walls are further subdivided into coupled or uncoupled walls. Coupled walls comprise individual walls linked by coupling beams, resisting lateral loads through moment and shear reactions in the individual walls together with an axial tensile reaction in one wall balanced by an axial compressive reaction in the other to create a global moment reaction. The magnitude of these axial loads is limited by the shear forces that can be transferred across the coupling beams. In order to qualify as a coupled wall system, the inclusion of coupling beams must cause at least a 25% reduction in the base moments of the individual walls from that which would have occurred in the uncoupled case. As coupled walls dissipate energy, not only in yielding at the base but also in yielding of the coupling beams, buildings with coupled walls may be designed for lower inertial loads than buildings with uncoupled walls to reflect their greater ductility and redundancy.

Large lightly reinforced walls are a category of structure introduced in EC8 and not found in other national or international seismic codes. These walls are assumed to dissipate energy, not through hysteresis in plastic hinges, but by rocking and uplift of the foundation, converting kinetic energy into potential energy of the structural mass and dissipating this through radiation damping. The dimensions of these walls or their fixity conditions or the presence of stiff orthogonal walls effectively prevent plastic hinging at the base. These provisions are likely to find wide application in heavy concrete industrial structures.

Dual systems are structural systems in which vertical loads are carried primarily by structural frames but lateral loads are resisted by both frame and wall systems. From the earlier definitions, it is clear that, to act as a dual system, the frame and wall components must each carry more than 35% but less than 65% of the total base shear. When more than 50% of the base shear is carried by the frames, it is designated a frame-equivalent dual system. Conversely, it is termed a wall-equivalent dual system when walls carry more than 50% of the base shear.

Torsionally flexible systems are defined as those systems where the radius of gyration of the floor mass exceeds the torsional radius in one or both directions. An example of this type of system is a dual system of structural frames and walls with the stiffer walls all concentrated near the centre of the building on plan.

Inverted pendulum systems are defined as systems where 50% of the total mass is concentrated in the upper third of the height of the structure or where energy dissipation is concentrated at the base of a single element. A common example would normally be one storey frame structures. However, single storey frames are specifically excluded from this category provided the normalised axial load does not exceed 0.3.

4.2 Behaviour Factors

Table 2 shows the basic values of q factors for reinforced concrete buildings. These are the factors by which the inertial loads derived from an elastic response analysis may be reduced to account for the anticipated non-linear response of the structure, together with associated aspects such as frequency shift, increased damping, overstrength and redundancy. The factor, α_u/α_1 , represents the ratio between the lateral load at which the ultimate capacity occurs and that at which first yield occurs in any member. Default values of between 1.0 and 1.3 are given in the code with an upper limit of 1.5. Higher values than the default figures may be utilised but need to be justified by push-over analysis.

Table 2 Basic value of behaviour factor, q_0 , for RC systems regular in elevation

Structural Type	DCM	DCH
Frame system, dual system, coupled wall system	$3.0\alpha_u/\alpha_1$	$4.5\alpha_u/\alpha_1$
Uncoupled wall system	3.0	$4.0\alpha_u/\alpha_1$
Torsionally flexible system	2.0	3.0
Inverted pendulum system	1.5	2.0

For walls or wall-equivalent dual systems, the basic value of the behaviour factor then needs to be modified by a factor, $k_w = (1 + \alpha_0)/3$ where α_0 is the prevailing aspect ratio, h_w/l_w , of the walls; k_w accounts for the prevailing failure mode of the wall, the q factors being reduced on squat walls where more brittle shear failure modes tend to govern the design. A lower limit of 0.5 is placed on k_w for walls with an aspect ratio of 0.5 or less, with the basic q factor being applied unmodified to walls with an aspect ratio of 2 or more.

The basic q_0 factors tabulated are for structures which satisfy the EC8 regularity criteria, the basic factors needing to be reduced by 20% for structures which are deemed to be irregular in elevation according to the criteria given in EC8 [3,4].

4.3 Local Ductility and Detailing Provisions

EC8 design rules take account of the fact that, to achieve the global response reductions consistent with the q factor chosen, much greater local ductility has to be available within the critical regions of the structure. Design and detailing rules for these critical regions are therefore formulated with the objective of ensuring that: (i) sufficient curvature ductility is provided in critical regions of primary elements, and

(ii) local buckling of compressed steel within plastic hinge regions is prevented.

This is fulfilled by special rules for confinement of critical regions, particularly at the ends of beams and columns, within beam/column joints and in boundary elements of ductile walls, which depend, in part, on the local curvature ductility factor μ_Φ . This is related to the global q factor as follows:

$$\mu_\Phi = 2q_0 - 1 \quad \text{if } T_1 \geq T_C \quad (5)$$

$$\mu_\Phi = 1 + 2(q_0 - 1)T_C/T_1 \quad \text{if } T_1 < T_C \quad (6)$$

where q_0 is the basic behaviour factor shown in Table 2 before any reductions are made for lack of structural regularity or low aspect ratio of walls. T_1 is the fundamental period of the building and T_C is the period at the upper end of the constant acceleration zone of the input spectrum as shown in Figure 2. Additionally, if Class B reinforcement is chosen rather than Class C in DCM structures, the value of μ_Φ should be at least 1.5 times the value given by the above equations.

Several detailing provisions in EC8 revolve around the inclusion of transverse reinforcement to provide a degree of triaxial confinement to the concrete core of compression zones and restraint against buckling of longitudinal reinforcement. As confinement increases the available compressive capacity, in terms of both strength and more pertinently strain, increases, and it has direct benefits in assuring the availability of local curvature ductility in plastic hinge regions. Figure 7 depicts relationships for increased compressive strength and available strain associated with triaxial confinement. These indicate that for the minimum areas of confinement reinforcement, the ultimate strain available would be between about 2 and 4 times that of the unconfined situation, dependent on the effectiveness of the confinement arrangement [3, 4].

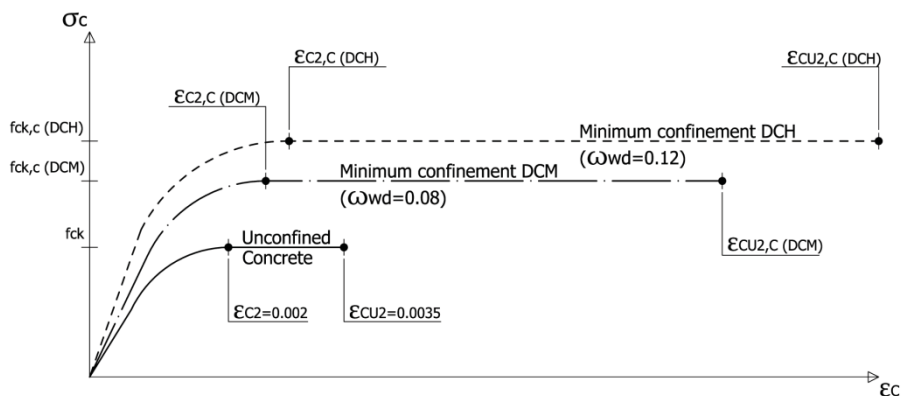


Figure 7 Stress strain relationships for confined concrete

To reflect the above, specific detailing rules are typically required in the critical regions of beams, where plastic flexural hinges are expected to form. These are defined as the region extending a specific length away from the face of the support, as indicated for example in Figure 8. Typical rules include maximum and minimum ratios for the main (longitudinal) reinforcement, and minimum diameter and spacing for the hoop (transverse) reinforcement.

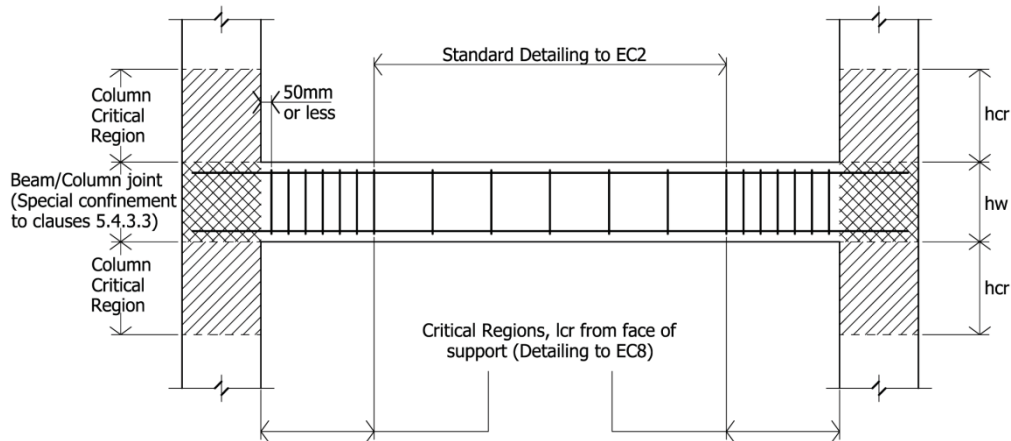


Figure 8 Example of transverse reinforcement requirements in beams to EC8 [1]

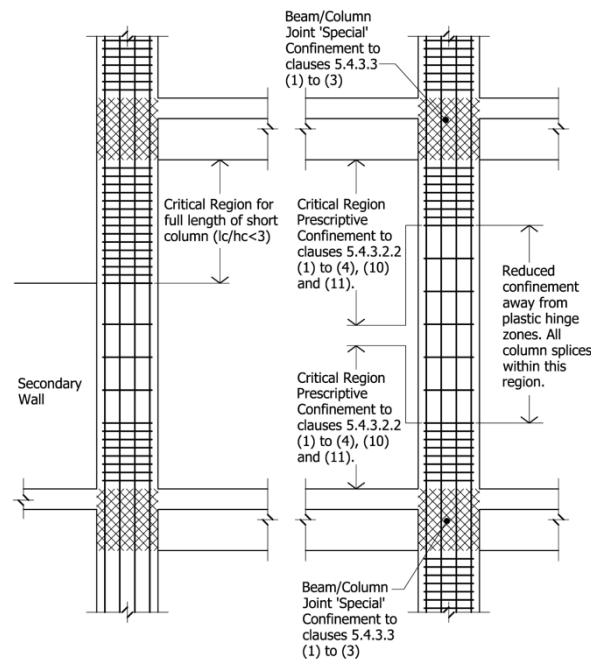


Figure 9 Example of typical column detailing requirements to EC8 [1]

Requirements are also typically given for columns, where a critical region is defined in which specific detailing requirements of ductility, in terms of longitudinal and transverse reinforcement as well as anchorage/splicing, need to be considered, as indicated for example in Figure 9. Another important consideration in columns is that the normalised axial compression force (v_d) should be limited to a specified value (0.6

in DCM and 0.55 in DCH). Specific rules are also given for beam-column joints; these are generally straightforward in DCM, but are much more demanding in DCH.

EC8 additionally provides specific rules for reinforced concrete walls. The rules cover slender walls, where the height is at least twice the wall width at its base. The code also covers squat shear walls, coupled shear walls, dual or frame-wall structures and large lightly reinforced walls. In ductile walls, the member is required to yield in bending, at a level of the wall that has been provided with suitable detailing, and this yielding in flexure must occur before shear failure occurs. In most cases, flexural yielding will be chosen to occur at the base of the wall, requiring that premature bending failure should not first occur in the upper part of the wall. To achieve this EC8 requires that the upper portions of the wall have suitable excess bending strength, by requiring design for possible 'tension shift'. As in columns, a limit is also imposed on v_d (0.4 in DCM and 0.35 in DCH). Special confining reinforcement is required in 'boundary elements' to sustain the large compressive strains due to flexure. EC8 requires this to extend over the length of wall for which the concrete strain exceeds 0.35%; appropriate expressions for calculating this length are provided. The height of wall over which the special confinement steel is required is also defined. Otherwise, the confinement steel follows similar rules to those for confinement in columns.

More detailed information on the design of reinforced concrete structures to EC8 can be found elsewhere [1,4].

5. MAIN FEATURES OF STEEL DESIGN TO EC8

5.1 Structural Types and Behaviour Factors

There are essentially three main structural steel frame systems used to resist horizontal seismic actions, namely moment resisting, concentrically braced and eccentrically braced frames. Other systems such as hybrid and dual configurations can be used and are referred to in EC8. It should also be noted that other configurations such as those incorporating buckling restrained braces or special plate shear walls, which are covered in the most recent North American Provisions, are not directly addressed in the current version of EC8.

As noted before, unless the complexity or importance of a structure dictates the use of non-linear dynamic analysis, regular structures are designed using the procedures of capacity design and specified behaviour factors. These factors (also referred to as force reduction factors) are recommended by codes of practice based on background research involving extensive analytical and experimental investigations. Table 3 shows the main structural types together with the associated dissipative zones according to the provisions and classification of EC8. The upper values of q allowed for each system, provided that regularity criteria are met, are also shown in Table 3. The ability of the structure to dissipate energy is quantified by the behaviour factor;

the higher the behaviour factor, the higher is the expected energy dissipation as well as the ductility demand on critical zones.

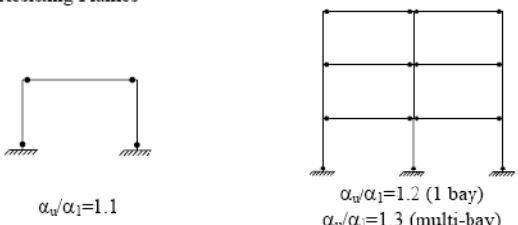
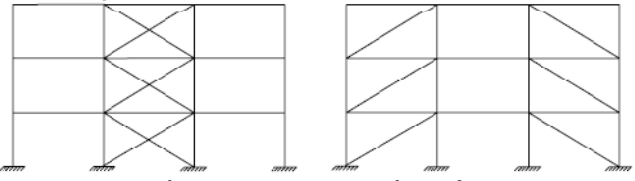
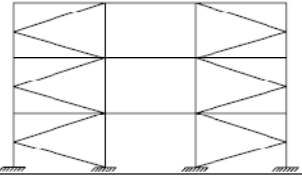
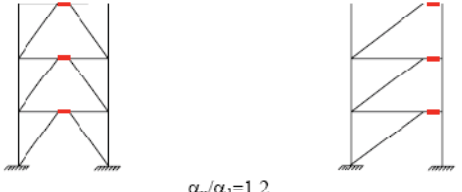
Structural Type	q-factor	
	DCM	DCH
<p>Moment-Resisting Frames</p>  <p>$\alpha_w/\alpha_1=1.1$</p> <p>$\alpha_w/\alpha_1=1.2$ (1 bay) $\alpha_w/\alpha_1=1.3$ (multi-bay)</p> <p><i>dissipative zones in beams and column bases</i></p>	4	$5\alpha_w/\alpha_1$
<p>Centrally-Braced Frames</p>  <p><i>dissipative zones in tension diagonals</i></p>	4	4
<p>V-Braced Frames</p>  <p><i>dissipative zones in tension and compression diagonals</i></p>	2	2.5
<p>Frames with K-bracings</p> 	Not allowed in dissipative design	
<p>Eccentrically-Braced Frames</p>  <p>$\alpha_w/\alpha_1=1.2$</p> <p><i>dissipative zones in bending or shear links</i></p>	4	$5\alpha_w/\alpha_1$

Table 3 Structural types and behaviour factors for steel structures in EC8
(continued below)

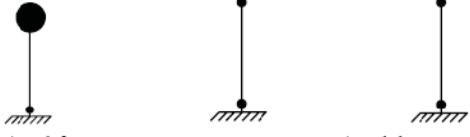
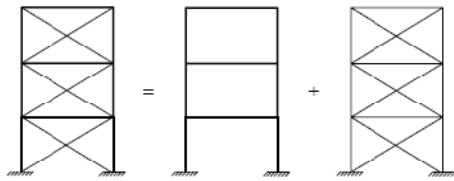
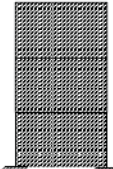
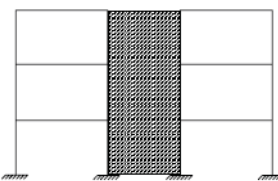
Structural Type	q-factor										
	DCM	DCH									
Inverted Pendulum Structures  $\alpha_u/\alpha_1=1.0$ <i>dissipative zones in column base, or column ends ($N_{Ed}/N_{pl,Rd}<0.3$)</i>	2	$2\alpha_u/\alpha_1$									
Moment-Resisting Frames with Concentric Bracing  $\alpha_u/\alpha_1=1.2$ <i>dissipative zones in moment frame and tension diagonals</i>	4	$4\alpha_u/\alpha_1$									
Moment Frames with Infills  <table border="1" data-bbox="694 851 1220 1019"> <tr> <td>Unconnected concrete or masonry infills, in contact with the frame</td> <td>2</td> <td>2</td> </tr> <tr> <td>Connected reinforced concrete infills</td> <td colspan="2">See concrete rules</td> </tr> <tr> <td>Infills isolated from moment frame</td> <td>4</td> <td>$5\alpha_u/\alpha_1$</td> </tr> </table>	Unconnected concrete or masonry infills, in contact with the frame	2	2	Connected reinforced concrete infills	See concrete rules		Infills isolated from moment frame	4	$5\alpha_u/\alpha_1$		
Unconnected concrete or masonry infills, in contact with the frame	2	2									
Connected reinforced concrete infills	See concrete rules										
Infills isolated from moment frame	4	$5\alpha_u/\alpha_1$									
Structures with Concrete Cores or Walls 	See concrete rules										

Table 3 (continued) Structural types and behaviour factors for steel structures in EC8

The multiplier α_u/α_1 depends on the failure/first plasticity resistance ratio of the structure. A reasonable estimate of this value may be determined from conventional nonlinear ‘push-over’ analysis, but should not exceed 1.6. In the absence of detailed calculations, the approximate values of this multiplier given in Table 3 may be used. If the building is irregular in elevation, the listed values should be reduced by 20%, as noted before.

The values of the structural behaviour factor given in the code should be considered as an upper bound even if in some cases non-linear dynamic analysis indicates higher q factors. For regular structures in areas of low seismicity having standard structural systems with sections of standard sizes, a behaviour factor of 1.5-2.0 may be adopted (except for K-bracing) by satisfying only the resistance requirements of Eurocode 3.

Although a direct comparison between codes can only be reliable if it involves the full design procedure, the reference q factors in EC8 appear generally lower than R values

in US provisions for similar frame configurations. It is also important to note that the same force-based behaviour factors (q) are proposed as displacement amplification factors (q_d). This is not the case in US provisions where specific seismic drift amplification factors (C_d) are suggested; these values are generally lower than the corresponding R factors for all frame types.

5.2 Ductility Classes and Rules for Cross-Sections

To achieve some consistency with other parts of the code, the most recent version of EC8 explicitly addresses the three ductility classes, namely DCL, DCM and DCH referring to low, medium and high dissipative structural behaviour, respectively. For DCL, global elastic analysis and the resistance of the members and connections may be evaluated according to EC3 without any additional requirements. The recommended reference ' q ' factor for DCL is 1.5-2.0. For buildings which are not seismically isolated or incorporating effective dissipation devices, design to DCL is only recommended for low seismicity situations. In contrast, structures in DCM and DCH need to satisfy specific requirements primarily related to ensuring sufficient ductility in the main dissipative zones. Some of these requirements are general rules that apply to most structural types whilst others are more relevant to specific configurations.

Ductility Class	Reference q-factor	Cross-Section Class
DCM	$1.5 < q < 2$	Class 1, 2 or 3
	$2.0 < q < 4$	Class 1 or 2
DCH	$q > 4$	Class 1

Table 4 Cross-section requirements based on ductility class and reference q-factor

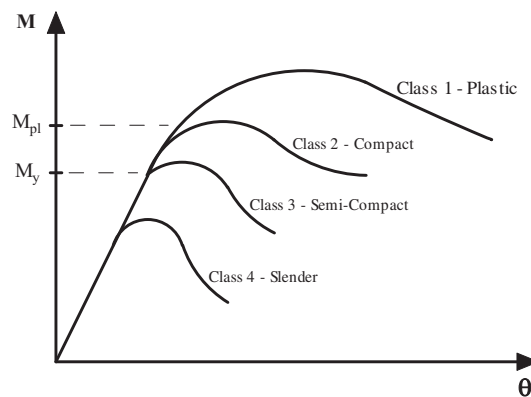


Figure 10 Moment-rotation characteristics for different cross section classes

The application of a behaviour factor larger than 1.5-2.0 must be coupled with sufficient local ductility within the critical dissipative zones. For elements in compression or bending (under any seismic loading scenario), this requirement is ensured in EC8 by restricting the width-to-thickness (b/t) ratios to avoid local buckling. An increase of b/t ratio results in lower element ductility due to the occurrence of local buckling (as illustrated in Figure 10) leading to a reduction in the energy dissipation capacity, which is expressed by a lower q factor. The classification used in EC3 is adopted but with restrictions related to the value of q factor as given in Table 4. It is worth noting that the seismic cross-section requirements in US practice imply more strict limits for certain section types.

The cross-section requirements apply to all types of frame considered in EC8. These provisions implicitly account for the relationship between local buckling and rotational ductility of steel members.

More detailed information on the performance and design of moment and braced forms of steel and composite structures according to the provisions of EC8 to can be found elsewhere [1, 4, 6, 7].

6. CLOSURE

This brief paper has provided an overview of the main principles of seismic design with focus on Eurocode 8. This covered the loading and spectra specified in the code, as well as general requirements for buildings including the fundamental principles, siting considerations, regularity criteria, capacity design provisions, primary and secondary members, and stiffness-related considerations. The main features for the design of reinforced concrete and steel buildings were also pointed out, including, the overall design concepts, structural types and behaviour factors, as well as local ductility and detailing provisions.

REFERENCES

1. Elghazouli, A.Y., Editor. "Seismic Design of Buildings to Eurocode 8", Taylor and Francis, Spon Press, 2009.
2. SEAOC. "Vision 2000, Performance Based Seismic Engineering of Buildings", Structural Engineers Association of California, CA, 1995.
3. Eurocode 8. "Design of Structures for Earthquake Resistance", Part 1: General Rules, Seismic Actions and Rules for Buildings, EN1998-1-2004, European Committee for Standardization, CEN, Brussels, 2005.
4. IStructE, Manual for the Design of Steel and Concrete Buildings to Eurocode 8, Institution of Structural Engineers, UK, 2010.
5. Paulay, T. and Priestley, M.J.N. "Seismic Design of Reinforced Concrete and Masonry Buildings. Wiley, 1992.
6. Fardis M.N. et al. "Designers' Guide to EN 1998-1 and EN 1998-5 Eurocode 8: Design of structures for earthquake resistance. General rules, seismic actions, design rules for buildings, foundations and retaining structures". Thomas Telford, London, 2005.
7. Elghazouli, A. Y. "Assessment of European Seismic Design Procedures for Steel Framed Structures", Bulletin of Earthquake Engineering, 8(1), pp. 65-89. 2010.

COLLAPSE MODES OF LOW-RISE MASONRY INFILLED RC FRAME BUILDINGS UNDER STRONG EARTHQUAKES

C.L. Lee¹, R.K.L. Su²

^{1,2} *Department of Civil Engineering, The University of Hong Kong, China*

¹ *clee63@hku.hk*

² *klsu@hkucc.hku.hk*

ABSTRACT

Confined masonry structures are a widely applied structural system in many developing countries. During the past Wenchuan Earthquake in 2008, numerous confined masonry buildings collapsed, while many others suffered damage. This study reviews the construction practices of confined masonry buildings in China. Simple models and hand calculation methods are proposed for quantifying the tearing failure of diaphragms, the tensile failure of tie-columns and the sway-mode strength of masonry buildings. The results indicate very good agreement with field observations. The seismic measures that are stipulated in the seismic design codes are very effective for increasing the strength and integrity, but not the ductility of masonry buildings. For those buildings that survived the earthquake, strength rather than ductility protected the confined masonry from collapse or serious damage. Design recommendations are suggested for preventing various types of premature failures and enhancing the lateral strength of masonry buildings.

Keywords: Collapse, Ductility, Integrity, Masonry, Strength, Tie-system

1. INTRODUCTION

The past 2008 Wenchuan earthquake occurred in Sichuan province in China (see Fig. 1) led to around seventy thousand deaths and numerous injuries. The majority of the deaths and injuries were in Dujiangyan, Mianyang and Deyang. More than 216,000 buildings collapsed, including 6898 schools, and countless buildings were damaged to varying extents.

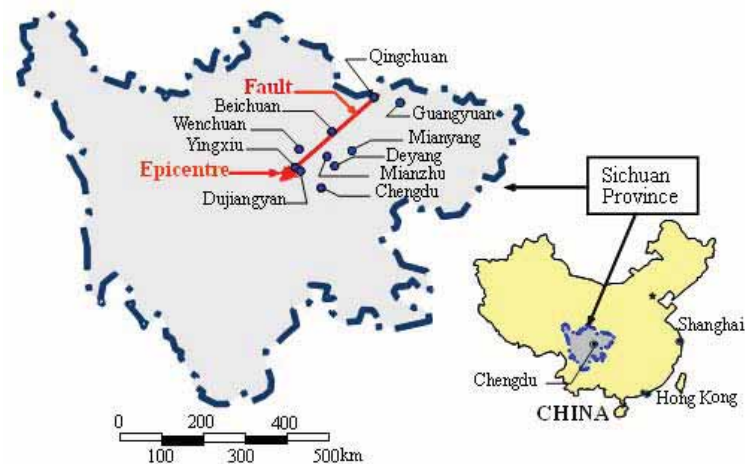


Figure 1. Location of the epicentre and major affected cities

Confined masonry structures, which are widely used in China, consist of tie-columns, reinforced concrete (RC) beams and precast concrete hollow floor planks in the upper floors and RC infill frames on the bottom floor. Approximately 70% of residential buildings in China are made of confined masonry (see Fig. 2). During the Wenchuan Earthquake, numerous confined masonry buildings failed and caused a large number of casualties. Table 1 shows the proportion of masonry buildings destroyed during the earthquake (China Earthquake Administration [1]). In Dujiangyan, about 55% of the masonry buildings collapsed or were seriously damaged.

Table 1. The proportions of the destruction of masonry and bottom frame masonry buildings in the Wenchuan Earthquake

City / town	Intact	Slightly to Moderately damaged	Severely damaged to collapsed
Chengdu	96.8	3.21	0.033
Deyang	50.3	47.2	2.5
Mianyang	55.9	33.8	10.3
Mianzhu	20.4	47.0	25.6
Dujiangyan	27.7	24.1	55.2

In the study reported here, different collapse models of masonry buildings were proposed. The predicted results are compared with field observations to validate the proposed models. The key findings and main design considerations for the collapse prevention of masonry buildings are presented in this paper. Some misconceptions of

the Chinese seismic design codes in the design of seismic resistant masonry buildings are highlighted.



Figure 2. Typical confined masonry buildings in Sichuan

2. TYPICAL CONFINED MASONRY STRUCTURES IN CHINA

In China, confined masonry structures are widely used in the construction of low-rise residential buildings in the regions with the basic design peak ground acceleration (PGA) less than or equal to 0.3g. Various types of brickwork, such as fired clay bricks, fired clay perforated bricks, and small hollow concrete blocks, are commonly used in building construction. Most of the collapsed buildings were constructed from fired clay bricks. According to the Chinese design code GB50011-2001 [2], masonry brickwork must be restrained by cast-in-situ RC ring-beams and tie-columns. The required member sizes and RC details are dependent on the basic design PGA. In the earthquake affected regions, where the basic design PGA is 0.05g to 0.1g, the minimum size of the tie-columns is 240 mm×180 mm and the minimum depth of the tie beams is 180 mm. A typical construction detail of the brick walls, ring-beams, and tie-columns is shown in Fig. 3. The beams and columns are required to be reinforced by four longitudinal high yield steel bars (nominal yield stress $f_y \geq 335$ MPa) with diameters of 12 mm. Horizontal tie-bars (two 6 mm diameter bars, 1 m long at 500 mm vertical spacing) are used to improve the structural integrity between the tie-columns and the brickwork. To further enhance the bonding between the tie-system and the masonry walls, the tie-columns and beams have to be cast after laying the adjacent brickwork. The concrete used should have a cube strength of at least 20 MPa.

The Chinese design code GB50011-2001 (clause 7.3) [2] stipulates that tie-columns must be provided at the four corners of the exterior walls, at intersections of the transverse wall in the slit-level portion and the exterior longitudinal wall, at both sides of large openings, and at intersections of interior walls and exterior longitudinal walls in large rooms. The code also states that columns should be provided at the four corners of staircases and elevator shafts, and at intersections of each 15 m or unit transverse wall and exterior longitudinal wall. Wang [3] reported that the buildings which strictly adhered to the design code performed satisfactorily under the Wenchuan earthquake load.

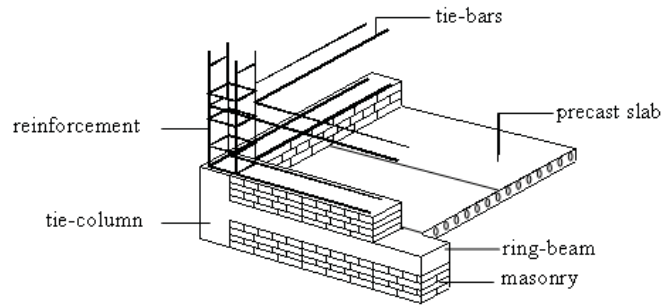


Figure 3. A typical construction detail of confined masonry structures

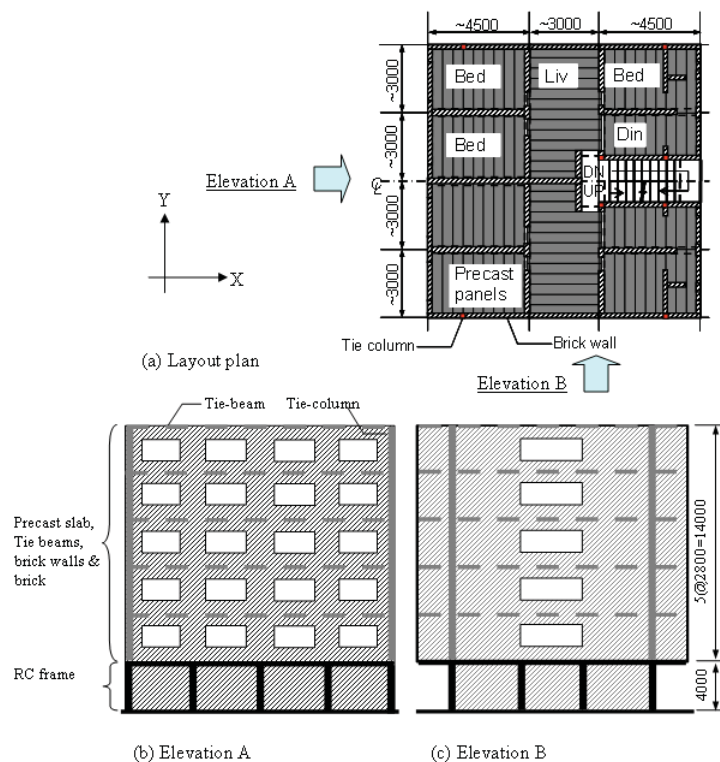


Figure 4. Typical structural arrangements of masonry residential buildings

The structural arrangements of a typical collapsed residential masonry building in Dujiangyan are illustrated in Fig. 4. Hollow precast panels were adopted for the floor supporting system. Infilled reinforced concrete frames were used in the first storey, while confined masonry was used in the second storey and above to resist gravity and lateral loads. The field investigation conducted by the University of Hong Kong revealed that many of the collapsed buildings did not follow the design code requirements. Tie-columns were not usually provided at the intersections of transverse and longitudinal walls, and neither at both sides of bigger openings (e.g., window and door openings). Without sufficient tie-columns and adequate confinement to masonry walls, the load-carrying capacity, the energy dissipation ability and the strength retention of masonry walls were substantially impaired.

3. COLLAPSE MODES OF CONFINED MASONRY STRUCTURES

3.1 Estimation of Basic Design Earthquake Load

The basic design spectral acceleration and the characteristic periods of the regions affected by the earthquake can be found in the Chinese Seismic Zoning Maps GB18306-2001 [4], which are shown in Figs. 5(a) and 5(b), respectively. It can be observed that the basic design PGA in the affected areas is relatively low: 50 gal for Mianyang and Deyang and 100 gal for Chengdu, Dujiangyan, Yingxiu, Wenchuan, Beichuan, and Qingchuan.

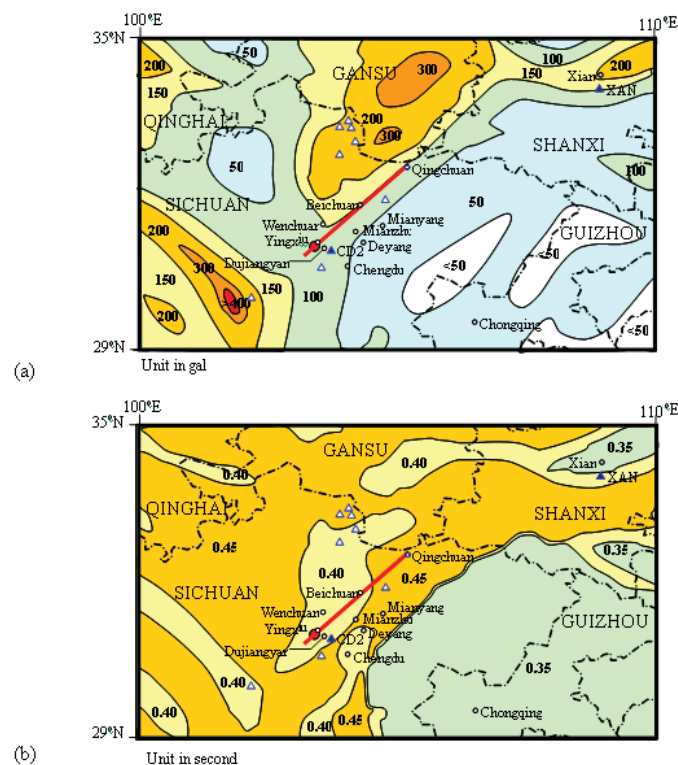


Figure 5. Distributions of (a) basic design *PGA* and (b) characteristic period in the earthquake affected areas

The Chinese seismic design code adopts the widely used concepts of designing structures to allow no damage during frequent earthquakes, repairable damage during occasional earthquakes and no collapse during rare earthquakes. The frequent, occasional (basic design), and rare earthquakes correspond to earthquakes with a 63%, 10%, and 2% probability of exceedance in 50 years, respectively. Ultimate design earthquake forces are obtained by multiplying the loading demand of frequent earthquakes by a partial safety factor of 1.3. The spatial distributions of recorded PGAs in both E-W and N-S directions of the Wenchuan Earthquake [1] were combined and are plotted in Fig. 6. The PGA in the affected area ranged from 100 gal to 958 gal and the maximum PGA of the Wenchuan Earthquake was located near Yingxiu and Beichuan.

Table 2 compares the ultimate design PGA and the measured PGA in various affected regions. The measured PGA is found to be about 8 times higher than the ultimate design PGA in most of the affected regions, except at Chengdu, which is only 2.2. It is worth noting that although the design overstrength ratios, which are defined as dividing the measured PGA by the design ultimate PGA, are quite similar for Deyang, Mianyang, Mianzhu, and Dujiangyan, serious damage to buildings (see Table 1) was only observed at Dujiangyan and Mianzhu (as well as Yingxiu), where the PGA demands were higher than 290 gal. The design overstrength ratio, which can be related to the global ductility demand, was not a good indicator for quantifying earthquake damage. The high PGA demand was the major factor accounting for the serious damage and widespread collapse of the buildings in the affected areas. Further explanations will be given in Sections 3.2 to 3.4.

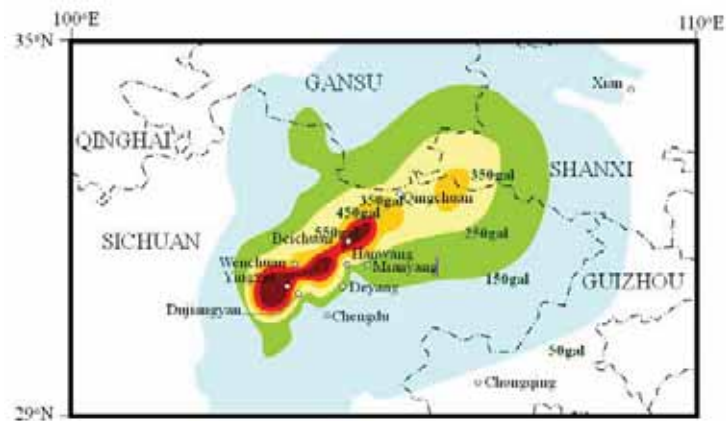


Figure 6. Spatial distribution of PGAs of the Wenchuan Earthquake

Table 2. A comparison of the ultimate design and recorded PGAs in various affected regions

City / town	Ultimate design PGA (gal)	Measured PGA* (gal)	Design overstrength ratio ⁺
Cheungdu	35.6	80	2.2
Deyang	17.8	150	8.4
Mianyang	17.8	160	9.0
Mianzhu (Hanwang City)	35.6	290	8.1
Dujiangyan	35.6	320	9.0
Yingxiu	35.6	550	15.1

Note: * The values were interpolated from Fig. 6

⁺ Design overstrength ratio is obtained by dividing the design ultimate PGA with the measured PGA

3.2 Tearing Failure of Floor Diaphragms

Under earthquake load, cyclic tensile forces are generated in floor diaphragms. When masonry infill walls are added in a frame building, the structure resists the lateral earthquake load mainly by the strut and tie action. Very high tensile forces can be induced in the diaphragms, in particular at the first floor of the building. Sufficient reinforcements have to be provided to resist the forces. Horizontal ties should not yield earlier than the occurrence of the ductile beam-sway mechanism for the building.

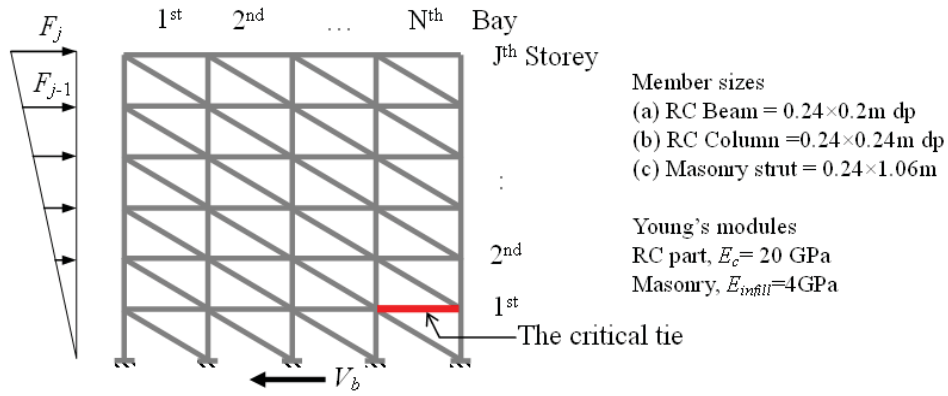


Figure 7. Strut and tie model for an infilled frame building subjected to lateral earthquake loads

Fig. 7 shows a strut and tie model for simulating an infilled frame building of N bays and J storeys subjected to lateral earthquake loads. In this model, the length of each bay and the floor to floor height are both taken as 3m. The member sizes and material properties are presented in Fig. 7. This model should be applicable to rigid buildings of which the higher mode effect is not significant. Hence, assuming the fundamental mode shape is approximately by horizontal displacements increasing linearly along the height, the seismic shear distribution can be determined by Eq. (1).

$$F_i = V_b \frac{h_i \cdot w_i}{\sum_{j=1}^J h_j \cdot w_j} \quad (1)$$

where h_i is the level at the i^{th} floor, V_b is the seismic base shear, w_i is the weight at the typical floor and w_j is the weight at the roof which is taken as $w_i/2$. The effective uniformly distributed weight on the diaphragm may be taken as 10 kPa for the masonry buildings in China. The lateral earthquake load V_b , which is same as the base shear force, is expressed in Eq. (2):

$$V_b = W_{eq} S_a \quad (2)$$

where W_{eq} is the equivalent weight of the building, which is equal to $0.85W$ according to the Chinese seismic code GB50011-2001 (clause 5.2.1) [2], and S_a is the spectral acceleration.

By considering that the number of storeys of the building varied from two to ten ($J=2$ to 10) and the number of bays was either two or four ($N=2$ or 4), a finite element analysis using the finite element package ETABS [5] was conducted. The internal forces (F_t) in the critical tie as highlighted in Fig. 7 were determined. The normalized tie forces ($F_t N/V_b$) are represented in Fig. 8. Using the regression analysis, the normalized tie force was expressed in terms of the number of storeys. The normalized tie force can be estimated by Eq. (3).

$$\frac{NF_t}{V_b} = 0.417 + 0.14J - 0.0066J^2 \quad (3)$$

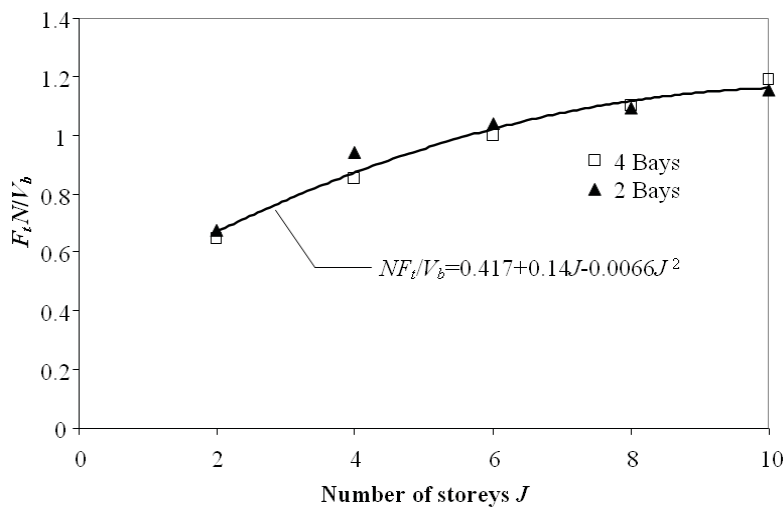


Figure 8. Normalized tensile force in the critical tie

For a six-storey building with two bays only, the maximum tie force F_t can be as high as $0.51 V_b$. For cast-in-situ floors, the flexural reinforcement provided is often sufficient for serving as ties. However, for restraining precast floor systems, sufficient ties or tie beams have to be installed to prevent the premature tearing failure of the floor diaphragm.

Considering the horizontal force equilibrium, the total required steel area A_s in the diaphragm at the first floor can be estimated as,

$$A_s = F_t / f_y \quad (4)$$

where f_y is the yield strength of the tie reinforcement.

The field investigation revealed that tearing failures of floor diaphragms are not uncommon. An example collapsed building in Dujiangyan is shown in Fig. 9 was resulted from a lack of tie beams. Pre-cast slabs together with tie beams have been pulled down at the failure zone.

Although the Chinese design code GB50011-2001 (clause 3.5.5) [2] mentions that precast structures should be properly and firmly connected to the other structural components to ensure the integrity of the structure, our field investigations revealed that many simply supported precast slabs did not comply with this design regulation and were directly seated on tie-beams without any mechanical connections. Only tie beams were provided to resist the tensile force generated by the earthquake loads. To demonstrate the significance of the tearing failure of pre-cast floor slabs, the critical spectral acceleration required to tear up the pre-cast floors of the six-storey masonry building with four bays is shown in Fig. 4 is estimated based on the proposed equations. As the building has four tie beams along the Y-direction and each tie beam contains four reinforcing bars with a diameter of 12 mm, the total area of tie reinforcement provided on each floor is $1809 \text{ mm}^2 (=6^2\pi \times 4 \times 4)$. The tie force capacity, according to Eq. (4), is 606 kN ($=1809\text{mm}^2 \times 335\text{Nmm}^{-2}/1000$). By Eqs. (2) and (3), the spectral acceleration capacity S_a is found to be 0.3 g which is much less than the peak spectral acceleration demand of around 0.9 g in Dujiangyan. Although the estimated value should be on the conservative side, as the tension stiffening effect of the concrete and brickwork has not been considered in the calculation, the large difference between the demand and capacity demonstrates that the installation of tie beams alone is not sufficient for preventing tearing failure of the floor diaphragm. Precast slabs have to be firmly connected to the other structural components to increase the tension capacity in high seismicity regions.



Figure 9. A 4-storey building without sufficient tie beams collapsed at Dujiangyan

3.3 Tensile Failure of Tie Columns

Under the seismic actions, reversed cyclic axial forces are generated in tie columns. Such actions could cause the yielding of vertical ties and debonding between tie-beams and infill masonry walls. More importantly, the loss of confinement for the infill masonry walls could significantly weaken the lateral stability of the load-bearing walls. The extent and importance of such an effect could be investigated through the following simple analysis.

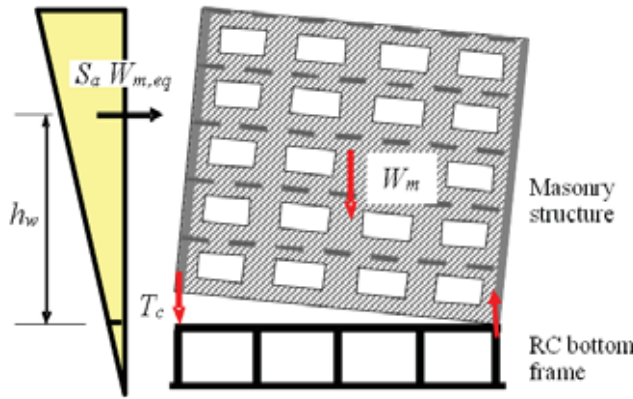


Figure 10. Free body diagram of the masonry structure above the RC bottom frame

The masonry building with a bottom frame, as shown in Fig. 4, is considered again. Knowing that the bottom reinforced concrete frame, which is provided with more tension reinforcement, is much stronger than the masonry superstructure on top of the frame, tension failure usually occurs at the interface between the reinforced concrete frame and the confined masonry structure (i.e., at the top of the first floor). Fig. 10 shows a free body diagram of the masonry structure above the bottom frame. The average bearing stress developed in the load-bearing masonry walls at the first floor can be obtained from Eq. (5).

$$\sigma_{avg} = \frac{W_m + T_c}{A_w} \quad (5)$$

where W_m is the effective weight of the superstructure above the first floor, T_c is the total tensile forces developed in the tension ties, and A_w is the total sectional area of load-bearing walls. Under strong lateral earthquake loads, uplifting could occur at the exterior masonry walls. Assuming that the masonry body deforms rigidly, when the tension stress σ_b , developed by the overturning earthquake moment, just balances the average bearing stress, one can have,

$$\sigma_{avg} = \sigma_b = \frac{(M - T_c D / 2) D}{2I_w} \quad (6)$$

where I_w is the second moment of the area of load-bearing walls, D is the depth of the building and M is the critical earthquake moment, above which could lead to tension failure of the confined masonry walls. Under reversed cyclic earthquake loads, debonding of the mortar between the bricks and the tie beams, could easily and quickly take place. Hence, the tensile strength provided by the masonry walls is conservatively ignored in the calculations. The critical moment M is expressed in terms of spectral acceleration capacity in Eq. (7).

$$M = S_a W_{m,eq} h_w \quad (7)$$

where $W_{m,eq} \approx 0.85 W_m$ is the equivalent building weight above the first floor and h_w is the moment arm of the resultant lateral forces measured from the first floor. Assuming that the seismic lateral force is triangularly distributed for the low-rise masonry building considered, and h_1 and h_2 are the levels at the first and roof floors, respectively, the moment arm can be expressed as,

$$h_w = \frac{(h_2 - h_1)(h_1 + 2h_2)}{3(h_2 + h_1)} \quad (8)$$

Taking the thickness of the masonry walls to be 240 mm, and following the building arrangements as shown in Fig. 4, the total sectional area A_w , second moment of area I_w and effective weight above the first floor W_m are estimated to be 17 m², 380 m⁴ and 7200 kN, respectively. When h_1 and h_2 are 4 m and 18 m, respectively (see Fig. 4), Eq. (8) gives $h_w = 8.48$ m. Furthermore, when the two edge tie columns are both yielded, the total tie force T_c provided is 303 kN ($=6^2\pi \times 8\text{mm}^2 \times 335\text{N/mm}^2$). Using Eq. (5), the average bearing stress is 0.44MPa, which is much less than the nominal compressive brickwork strength of 10MPa and the nominal compressive mortar strength of 5 MPa. Hence, the compressive failure of the masonry walls was unlikely when the walls were properly restrained. By using Eqs. (6) and (7), the spectral acceleration capacity S_a is found to be 0.57 g. It is worth noting that under strong reversed cyclic earthquake loads, tension cracking (see Fig. 11(a)) or even out-of-plane dislocations of masonry walls could occur. Those types of damage could severely weaken the integrity and stability of the masonry walls, and hence the gravity load-bearing system. Fig. 11(b) shows a nearly collapsed 6-storey building that suffered from out-of-plane failure of the masonry walls above the first floor of the concrete frame.



Figure 11. Damage to exterior masonry walls on top the first floors (a) extensive cracks and (b) out-of-plane dislocations



Figure 12. Damage of confined masonry buildings (a), (b), and (c) partial collapses, (d) collapse of simply supported hollow precast slabs, and (e) pullout failure of a beam

As evidenced by the extensive collapse of multi-storey masonry buildings in Dujiangyan and Yingxiu, the peak spectral acceleration demands for buildings are likely to be higher than 1.0 g (further details will be given in Section 4). The small tie-columns or ring-beams were too weak to contribute to the resistance of lateral and gravity loads. Thus, the collapse of the masonry walls triggered the progressive collapse of the buildings (see Figs. 12(a) to 12(d)). Fig. 12(e) shows a pullout failure of a tie-beam from a beam-column joint. The lack of redundancy of simply supported precast slabs and the insufficient strength of the tie-beam and column systems are believed to be the two major causes of the widespread collapse of confined masonry residential buildings. To improve the integrity and hence the load-bearing capacity of

the masonry walls, it is strongly recommended adding vertical ties (two 6mm diameter bars, 1 m long at 500 mm spacing) to attach the masonry infill to the top and bottom tie beams to restrain all four edges of the infill walls and prevent out-of-plane dislocations. Furthermore, larger diameter bars (e.g., T16) with higher yield stress (e.g., 460 MPa) should be used in tie beams and tie-columns to improve the integrity of the building and to avoid the premature tearing failure of buildings.

3.4 Sway Mode Failure Strength

Previous earthquakes and extensive studies (Dolšek *et al.* [6], Kwan *et al.* [7], Fajar *et al.* [8]) have revealed that masonry buildings, even those designed with ductility considerations and with uniform storey stiffness, create a soft storey at the bottom of the building if the ground motion is strong enough. When the strength is inadequate, deformations of the building will concentrate in the weakest storey and will increase rapidly. The PGA increasing ratio from the beginning of the formation of a soft storey to the collapse of the structure is only around 1.1 to 1.2 (Dolšek *et al.* [6], Kwan *et al.* [7]), which is much smaller than the strength reduction factor of 4 or higher that is typically used in the seismic design of buildings in China. Although it is difficult to accurately determine when a structure collapses, a masonry structure with a soft storey is dangerous enough in a normal design sense. Hence, the non-collapse design of low-rise masonry buildings should make sure that the structure has sufficient lateral strength. To ensure the whole building resists the seismic induced loading, good structural integrity is vitally important. When premature failures such as those mentioned in Sections 3.2 and 3.3 have been effectively controlled, the entire building can undergo swaying deformations. The ultimate lateral strength associated with swaying is defined as the inherent lateral strength. The inherent strength considers the strengths from both non-structural and structural components, and can be estimated at peak loading (or yielding) status.

In this section, a simple model proposed by Su *et al.* [9] was adopted to estimate the inherent strength of masonry buildings. The key element of the model is that stiffness and damping of the structure are characterized by secant properties at maximum response, rather than based on initial elastic properties. The building is assumed to fail in shear mode and the structure is represented as an equivalent single degree of freedom (SDOF) system under seismic attack (See Fig. 13). In such case, the spectral acceleration capacity S_a can be calculated using Eq. (9):

$$S_a = S_d \left(\frac{2\pi}{T} \right)^2 \quad (9)$$

where S_d is the spectral displacement at the peak load of the structure and T is the lengthened structural period at the peak load.

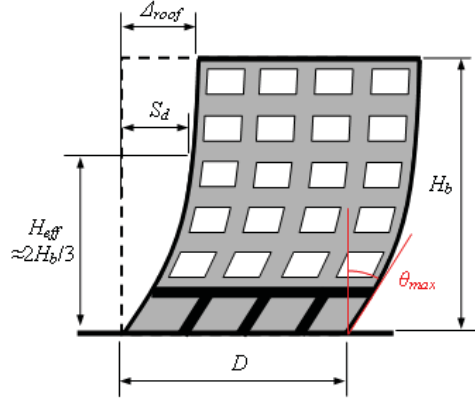


Figure 13. Lateral deformation of a low-rise building

The structural period of a building can be conveniently estimated from ambient vibration test data. Based on 12 dynamic test results of low-rise masonry buildings in China, Liang and Chen [10] reported that the structural period T of masonry buildings may be expressed as,

$$T = 0.0463\beta H_b / \sqrt{D} \quad (10)$$

where D is the depth of the building and β is the period shift factor. Under seismic actions, masonry buildings undergo inelastic deformations due to, for instance, cracking and sliding brickwork. The reduction in stiffness leads to lengthening of the structural period under strong shakings. As the structural period can be related to the structural stiffness through the well-known relationship ($T=2\pi\sqrt{M/K}$), the period shift factor can be obtained from the stiffness degradation factors. According to the shaking table analyses (Kwan *et al.* [7], Zheng *et al.* [11]) of confined masonry structures, the period shift factor (β) of infilled frames is found to range from 1.66 to 2.23 with a mean around 1.9.

As the vibration shapes of various shear-mode dominant low-rise buildings are very similar under earthquake excitations, S_d can be related to the maximum inter-storey drift ratio θ_{max} by Eq. (11) as:

$$S_d = \frac{H_b \theta_{max}}{\lambda} \quad (11)$$

where H_b is the height of the building and λ is the drift factor depending mainly on the height and type of the building. Miranda and his co-worker [12,13] have determined the drift factor explicitly. By substituting Eq. (11) into Eq. (9), one can obtain Eq. (12):

$$S_d = \frac{H_b \theta_{max}}{\lambda} \left(\frac{2\pi}{T} \right)^2 \quad (12)$$

Eq. (12) summarizes the key parameters that affect the lateral inherent strength of a building. Under the peak loading condition, θ_{max} is equal to the yield inter-story drift ratio. Previous experimental studies [Kwan *et al.* [7], Zheng *et al.* [11], Gao [14], Jin *et al.* [15]) of confined infill walls reported that the yield drift ratio primarily depends on the geometry and configuration of walls, the confinement steel content and the construction methods, and typically ranges between 0.5% and 0.9%.

To illustrate the application of the abovementioned theory, the masonry building as depicted in Fig. 4 is considered again. Assuming a global ductility capacity of 2.5 for brittle masonry buildings, the variations of drift factor to the number of storeys with building depth varying from 6m to 18m determined according to references (Miranda [12], Miranda and Reyes [13]) are shown in Fig. 14. For the building with a depth of 12m and 6 storeys, λ is found to be 2.50. The corresponding structural period T is found to be 0.457 sec ($=0.0463 \times 1.9 \times 18 / \sqrt{12}$) according to Eq. (10). Assuming the yield inter-storey drift θ_{max} is equal to 0.7% and using Eq. (12), the spectral acceleration capacity S_a is equal to 0.97 g (or $9.52 \text{ ms}^{-2} = 18 \times 0.007 \times (2\pi/0.457)^2 / 2.5$) is obtained. This implies that when stronger tie-columns and tie-beam systems are provided, a more deformable sway failure mode could be enhanced. The lateral strength, in terms of spectral acceleration capacity, could be increased remarkably from 0.57 g to around 1.0 g for 6-storey masonry buildings.

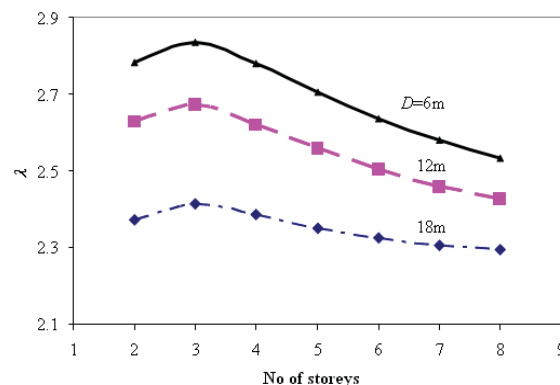


Figure 14. Variations of drift factor λ against the number of storeys

4. ESTIMATED RESPONSE SPECTRA

The response acceleration spectra of some of the affected areas, such as Zengjia, Bajiao, Qingping and Wolong, were given by Li *et al.* [16]. From these spectra, one can find that the dominant characteristic period of the ground motions was at 0.4 sec, the acceleration spectral ratio ranged from 2.7 to 5.4 with an average of 3.5, and the descending branch of the acceleration spectra in the range of 0.4 sec to 1 sec was roughly proportional to the function $T^{-1.4}$. Based on these parameters, together with the recorded PGA as shown in Fig. 6, the response acceleration spectra at various earthquake affected areas were estimated and presented in Fig. 15.

By considering the masonry building as shown in Fig. 4 and assuming the number of storeys varies from 2 to 7, and $\beta=1.9$, the structural period and spectral acceleration capacity of multi-storey masonry buildings were calculated. Fig. 15 shows the comparison between the failure strengths, design capacity and the estimated seismic loads (all in terms of spectral accelerations). To take into account the variations of material properties, yield rotations of 0.5% and 0.8% were considered. The design capacity was calculated according to the Chinese seismic design code GB 50011-2001 Clauses 5.1.4 and 5.1.5 [2]. The results show that buildings generally have sufficient lateral strengths in Chengdu, Deyang and Mianyang, while three- to seven-storey buildings in Dujiangyan, Hanwang and Yingxiu could have insufficient strength. Furthermore, the results show that the lateral strength of masonry buildings is very sensitive to building heights. Low-rise masonry buildings with three or fewer storeys are more robust under seismic attacks. Diaphragm failure of these buildings is the most common failure mode. The tie-columns of taller (and usually more slender) masonry buildings are likely to fail under tension due to the high over-turning effect. The loss of confinement to the infill walls could trigger the walls to detach from the main structures and the subsequent out-of-plane displacements. The structural period of an unrestrained infill wall could be a few seconds, and the displacement demands for long-period structural components in the affected areas could be much higher than 200 mm. Bearing in mind that the actual displacement demands experienced by the infill walls are calculated by adding up the spectral floor displacements and the ground displacements, the peak ground displacements were 200 mm in Chengdu and Mianyang, more than 500 mm in Dujiangyan and around 1000 mm in Yingxiu (Chen *et al.* [17]).

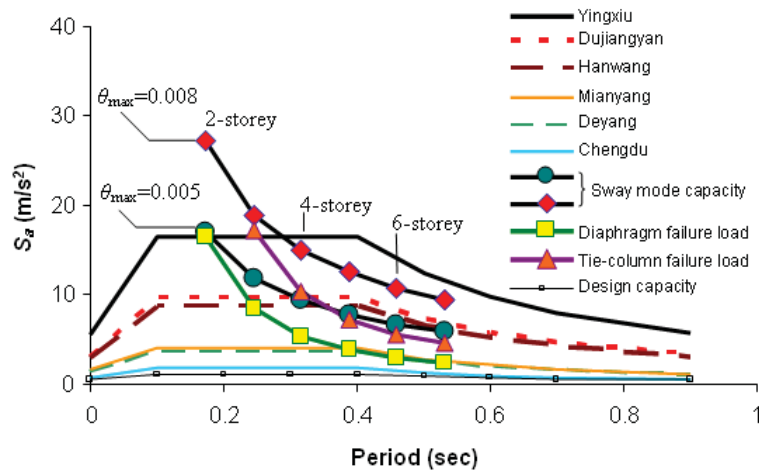


Figure 15. A comparison of spectra acceleration demands and capacities of masonry buildings in various earthquake affected areas

It should be noted that this paper has no intention of using the aforementioned simple analyses to explain all the possible causes of the collapse of a large variety of masonry buildings in the Wenchuan Earthquake. It is very difficult, but not impossible, to obtain all the essential material and geometric parameters to define the pre-earthquake conditions of individual buildings for conducting detailed collapse analyses. However, the above simple analyses did explain the damage and collapse of

the buildings in the Wenchuan Earthquake very well, and are worth considering in future seismic resistant design.

There are a number of possible ways to prevent the premature failure of masonry walls: for example, one can (1) reduce the height-to-depth ratio of the buildings, (2) add more tie-columns and tie-reinforcement, and (3) connect the infill walls to the tie-beams using tie-bars. The above provisions are very effective for improving the integrity of masonry buildings under seismic loads.

Finally, if the premature failures could be controlled for a multi-storey masonry building, a more deformable sway mode failure would probably happen. To further increase the lateral strength of the sway mode, one could (1) increase the yield inter-storey drift ratio of the building by using higher strength construction materials, (2) increase the initial stiffness (or shorten the initial period) of the buildings by increasing the size of structural members, and (3) avoid having structural irregularities so that the drift factor λ would not be larger than 2.5. Based on the above discussions, providing lateral strength should be a viable solution for the seismic resistant design of masonry buildings.

5. FIELD OBSERVATIONS

In our post-earthquake field investigations, we visited the Chengdu and Mianyang urban areas, as well as Dujiangyan and Yingxiu cities. Our observations broadly agreed with the damage data presented in Table 1. The main findings are,

- 1) No building collapses were observed in the Chengdu urban area;
- 2) Only one partially collapsed 6-storey building resulting from the failure of load-bearing masonry walls was found at the Mianyang urban centre (see Fig. 16);
- 3) Numerous partial collapses of 5- to 6-storey buildings occurred in Dujiangyan; and
- 4) Widespread collapse of buildings occurred in Yingxiu.

Fig. 15 shows that the proposed simple strength calculations explain our field observations very well. Apparently, strength, rather than ductility, protected the confined masonry buildings from collapse or serious damage.



Figure 16. A partial collapsed 6-storey building due to collapse of load-bearing masonry walls at Mianyang city

6. THE EFFECTIVENESS OF CHINESE SEISMIC DESIGN CODE ON PREVENTION OF BUILDING COLLAPSE

The effectiveness and importance of the seismic measures in the Chinese seismic design code have been evidenced in the Wenchuan earthquake. However, there is a different understanding regarding the real effect of the seismic measures, in particular the efficacy of tie-systems. Wang [3] reported that, for masonry structures designed and constructed according to the Chinese design code, tie-columns and tie-beams succeeded in acting as the second line of defence after the damage of the masonry walls. However, as demonstrated by the present study, many tie-systems were too weak to contribute to the resistance of gravity and earthquake loads in high seismic intensity areas. We believe that the real effect of the tie-columns and tie-beams system is to restrain infill walls and resist the tensions generated in the global lateral load structural systems. The tie-system can enhance the integrity of the entire building and effectively avoided premature failures under cyclic earthquake loads. However, the restraining frame of tie-columns and tie-beams cannot be considered as a second defence line.

In Section 3.1, earthquake load demands were found to be about 8 times higher than the corresponding design ultimate strength in many seismic affected areas. In the cities such as Chengdu and Mianyang, despite the high PGA demands and design overstrength ratios, almost all of the buildings could avoid collapse under the Wenchuan Earthquake. As mentioned in previous sections, the good performance of the buildings in these areas is mainly attributed to the high inherent strengths of the masonry buildings (see Fig. 15), but not the ductility capacity. In fact, the actual overstrength ratio (using the inherent lateral strength as the denominator) of masonry buildings is very small, around 1.15 according to Dolšek *et al.* [6] and Kwan *et al.* [7]. The seismic measures presented in the Chinese design code show the efficacy of increasing the lateral strength, but not ductility. Hence, the damage to buildings has a better correlation with PGA demands, but not the design overstrength ratios. When the seismic loading demands in terms of PGA is higher than the inherent spectra acceleration capacity of the buildings, extensive damage or even collapse of the

buildings occurs. The seismic measures defined in the Chinese seismic design code are quite effective in ascertaining the required integrity (as demonstrated in Section 3.2), but not the ductility of structures. Nonetheless, the tie-columns and tie-ring system, and other ductile detailing requirements, are still considered to be of vital importance for increasing the yield rotation and hence the inherent strength of a building.

Our post-earthquake field investigations further revealed that the ductile swaying failure mode of masonry buildings was rarely seen in the earthquake-affected areas. This is because in real construction of masonry buildings, reinforced concrete beams were often strengthened and stiffened by the adjacent slabs, masonry walls, and other non-structural components. The principle of strong column-weak beam was difficult to implement in real masonry buildings. If ductility design is difficult to implement, should we look for an alternative? Sufficient strength rather than ductility should be considered as the decisive factor in the design of masonry buildings. If rare earthquake loads are used for the non-collapse design of low-rise masonry buildings—judging from the variations between inherent strength and the rare earthquake loads the increase in the construction costs for masonry buildings should not be substantial.

Furthermore, many current seismic design codes adopted component-based seismic design without adequate considerations of the global integrity of the entire structures, and the limited ductility capacity of brittle construction materials and global collapse mechanism should be thoroughly reviewed. The proposed simple analyses in light of global collapse mechanisms warrant further refinement and improvement.

7. CONCLUSIONS

Based on field studies of the areas affected by the Wenchuan Earthquake and the subsequent seismic assessments of masonry buildings, the major findings are summarised as follows. The major factors influencing the inherent strength and preventing premature failures have been briefly discussed. Various failure models have been presented to quantify the tearing failure of floor diaphragms, the tension failure of tie-columns and the sway-mode failure of masonry buildings. The strength calculations explain our field observations very well. The substantial under-design of strength is found to be the primary reason for the widespread collapse of masonry buildings. For those masonry buildings that survived in this earthquake, their inherent strength, rather than their ductility, protected them from collapse. Moreover, the seismic measures stipulated in the Chinese seismic design code are very effective for increasing the strength and integrity of structures (but not ductility), and should be followed during design and construction. Furthermore, design recommendations have been given for preventing premature failures and increasing the inherent lateral strength of masonry buildings. The strength-based approach should be used in the design of low-rise masonry buildings. However, the ductility design approach is preferable for the design of medium and high-rise buildings. Rare earthquake loads could be used directly in the design of masonry buildings to achieve the objective of “no collapse in rare earthquakes”. Because the inherent strength of the buildings

constructed according to the current Chinese seismic code is already very high, the increase in construction costs should not be significant.

ACKNOWLEDGEMENTS

The research described here was supported by The University of Hong Kong through the Small Project Funds (2008) and the Sichuan Earthquake Roundtable Fund.

REFERENCES

1. China Earthquake Administration, “General introduction to the engineering damage during Wenchuan Earthquake”, *Journal of Earthquake Engineering and Engineering Vibration*, 28(supplementary), 2008, pp. 1-114.
2. National Standard of PRC, National Standard of the People’s Republic of China, Code for Seismic Design of Buildings GB 50011-2001 (English version), Ministry of Construction of the People’s Republic of China, China Architecture & Building Press, Beijing, 2005.
3. Wang, Y., “Lessons learned from the “5.12” Wenchuan Earthquake: evaluation of the earthquake performance objectives and the importance of seismic conceptual design principles”, *Earthquake Engineering and Engineering Vibration*, 7, 2008, pp. 255-262.
4. National Standard of PRC, National Standard of the People’s Republic of China, Seismic Ground Motion Parameter Zonation Map of China GB18306-2001, Zhongguo biao zhun chu ban she, Beijing, 2001.
5. Habibullah, A., ETABS (version 7.22) Three Dimensional Analysis of Building Systems, User’s Manual, Computers & Structures Inc, University of California, 1999.
6. Dolšek, M. and Fajfar, P., “Soft storey effects in uniformly infilled reinforced concrete frames”, *Journal of Earthquake Engineering*, 5, 2000, pp. 1-12.
7. Kwan, A.K.H. and Xia, J.Q., “Study on seismic behavior of brick masonry infilled reinforced concrete frame structures”, *Earthquake Engineering and Engineering Vibration*, 16, 1996, pp. 87-98.
8. Fajfar, P., Gašperšič, P. and Drobnič, D., “A simplified nonlinear method for seismic damage analysis of structures”, *Seismic Design Methodologies for the Next Generation of Codes*, Bled, Slovenia, Balkema, Rotterdam, 1997, pp. 183-194.
9. Su, R.K.L., Lee, C.L. and Wang, Y.P., “Seismic spectral acceleration assessment of masonry in-filled reinforced concrete buildings by a coefficient-based method”, *Structural Engineering and Mechanics* (submitted).
10. Liang, S.H. and Chen, Z.F., “Research on the formula of vibration period about masonry structure supported by frame”, *Jiangsu Jian Zhu* (in Chinese), 107, 2006, pp. 18-20.
11. Zheng, S., Yang, Y. and Zhao, H., “Experimental study on aseismic behavior of masonry building with frame – shear wall structure at lower stories”, *China Civil Engineering Journal*, 37, 2004, pp. 23-31.

12. Miranda, E., "Approximate seismic lateral deformation demands in multistory buildings", *Journal of Structural Engineering*, ASCE, 125, 1999, pp. 417-425.
13. Miranda, E. and Reyes, C.J., "Approximate lateral drift demands in multistory buildings with nonuniform stiffness", *Journal of Structural Engineering*, ASCE, 128, 2002, pp. 840-849.
14. Gao, J.P., "Structural analysis for storey-adding of existing brick masonry buildings by incorporated masonry-in-frame system", *Journal of East China Jiaotong University*, 24, 2007, pp.40-43.
15. Jin, W., Xu, Q., Pan, J., Yan, J. and Ye, J., "Experimental study on lateral resistance behaviour of small concrete hollow block wall with difference constructional measures", *Journal of Building Structures*, 22, 2001, pp. 64-72.
16. Li, X., Zhou, Z., Huang, M., Wen, R., Yu, H., Lu, D., Zhou, Y. and Cu, J., "Introduction and preliminary analysis of strong motion recordings from the 12 May 2008 M28.0 Wenchuan Earthquake of China", *Proceedings of the 14th World Conference on Earthquake Engineering*, Beijing; 2008, 16 pages.
17. Chen, Y.T., Xu, L.S., Zhang, Y., Du, H.L., Feng, W.P., Liu, C. and Li, C.L., *Report on the Source Characteristics of the Great Wenchuan Earthquake on 12 May 2008*. Institute of Geophysics China Earthquake Administration, (in Chinese), 2008.

(Blank)

新型組合構件在高層建築中的應用

何偉明¹ 劉鵬² 鐘聰明³ 劉光磊⁴ 殷超⁵ 程鎮遠⁶

奧雅納工程顧問

goman.ho@arup.com

提要

隨著中國大陸經濟的發展，高層建築在高度上也高速發展，由於組合構件同時具有較好的經濟性和結構性能，在中國大陸近年的高層建築中得到了廣泛的應用，組合的形式由於專案的而不同要求而各種各樣，本文介紹了一些項目中的一些為了配合建築及結構體系而發展出的新型組合構件的形式以及相應的應用範圍，為了考察這些構件的設計方法和性能所進行的數值模擬和模型試驗。

關鍵字： 高層建築 組合構件 組合鋼板牆 型鋼混凝土 鋼管混凝土

-
1. 董事，奧雅納工程顧問
 2. 助理董事，奧雅納工程顧問
 3. 高級工程師，奧雅納工程顧問
 4. 工程師，奧雅納工程顧問
 5. 工程師，奧雅納工程顧問
 6. 工程師，奧雅納工程顧問

1 概況

在中國大陸近年蓬勃興建的高層建築中，將傳統意義上的鋼結構/構件和鋼筋混凝土結構/構件以各種形式混合利用，已經成為主流的設計和建造的方法。

在一個基本結構構件中同時使用型鋼與鋼筋混凝土時稱為組合構件。在一個結構體系中，組合構件又可以與鋼構件和混凝土構件共同使用，視需要佈置於不同的部位，稱為混合結構^[5]，以達到結構安全性與造價經濟性的最佳平衡。

本文介紹的組合構件主要是結構的豎向構件。在高層建築中廣泛採用的壓型鋼板(profile decking)+混凝土樓板的組合樓板以及鋼樑+組合樓板的組合梁體系不在本文介紹範圍內。

2 組合構件

型鋼與混凝土的結合方式，應用於高層建築中，基本上可以分為鋼包裹於混凝土之內的型鋼混凝土(SRC, Steel Reinforced Concrete)和混凝土在鋼之內的鋼管混凝土(CFT, Concrete-filled Tube)兩大類：

項目	高度	組合構件形式	
		周邊結構	核心筒
北京中國國際貿易中心三期主塔樓	330m	矩形 SRC 組合柱 矩形 CFT 組合柱	異形 SRC 組合柱，組合鋼板牆，鋼斜撐
北京中央電視臺新台址主樓	234m	SRC 組合柱	
北京環球金融中心	100m	矩形 SRC 組合樑柱	
北京財富中心二期寫字樓	258m	圓形 CFT 柱	組合鋼板牆，混凝土牆內暗柱/暗梁，SRC 連梁，埋入式鋼桁架
天津嘉裡中心住宅樓	200m	矩形 SRC 組合樑柱	組合鋼板牆
廣州西塔	432m	圓形 CFT 斜撐	混凝土牆內暗柱/暗梁
大連裕景中心	380m	SRC 巨型柱	混凝土牆內暗柱/暗梁
深圳蔡屋圍京金融中心	439m	SRC 柱	混凝土牆內暗柱/暗梁

由於建築空間的需要，高層建築的豎向體系(vertical system)一般包括周邊結構(perimeter system)和核心筒體(core system)。雖然目前的全國性規範/規程中的混合結構只包含了周邊鋼框架+混凝土核心筒和周邊下拉式列示方塊架+混凝土核心筒兩種形式，事實上不同形式的組合構件應用於周邊結構和核心筒時，形成的結構形式更為多樣，見表中的專案實例。

3 型鋼混凝土(SRC)

型鋼混凝土組合構件巧妙的利用了鋼結構的強度及建造速度和混凝土結構的剛度及可成型性，從上世紀的 40 年代開始發展考慮混凝土作用的計算方法以來，日本及歐美在這方面進行了深入的研究，日本建築學會 1958 年制定了《鋼骨鋼筋混凝土計算標準及其說明》，此後經過數次修訂，基本形成較為完整的設計理論和方法。該標準的基本原理是在承載力計算方面採用了強度迭加理論，其基本假設為：不考慮型鋼與混凝土之間的粘結，截面的強度等於混凝土和型鋼分別計算強度的迭加。

美國涉及到型鋼混凝土構件的規範有 ACI318 和 AISC 的 LRFD。前者將寬翼緣鋼截面的作用假設為等值的鋼筋，然後採用與普通混凝土構件同樣的方法設計 SRC 構件，其基本假定與日本規範相同。後者採用極限強度設計法來設計 SRC 結構，將 RC 部分換算為等值型鋼，再按鋼結構的設計方法來計算組合構件。兩者均滿足變形協調和內力平衡條件，但後者考慮了型鋼材料本身的殘餘應力和初始位移。英國鋼結構設計規範按組合截面進行彈性設計，即取 0.7 倍型鋼屈服強度用彈性方法計算型鋼，然後按組合截面進行修正，忽略混凝土抗拉強度

中國大陸的設計方法基本體現於 YB9082-2006 及 JGJ138-2001 兩本規範中^[1,2]。YB9082 無論從承載力計算，還是到剛度、裂縫的計算，均採用了迭加原理。JGJ138 則採用平截面假定，鋼骨和混凝土之間協調變形，構件的承載力和裂縫是通過截面上受力平衡的條件得出來的。但在計算抗剪強度及剛度時，採用迭加原理。目前，JGJ138 在中國大陸的應用更廣泛一些。

從以上計算理論的描述中，我們可以注意到，保證這些計算模式成立的基本前提是在這種組合構件中，型鋼和混凝土之間的粘結性能能夠得到完全的保證，但事實往往並不盡如人意。越來越多的學者開始注意到型鋼混凝土組合構件中存在的粘結滑移問題，並進行了深入的試驗和理論研究。研究的結果是得到了眾多的粘結強度的統計計算公式和各受力構件的粘結滑移本構關係，但目前似乎尚沒有一個得到大多數人的一致認同。另一個值得注意的問題是，大部分的型鋼混凝土構件被應用在抗震的結構當中，因此低周反復荷載作用下的粘結滑移性能的退化規律也顯得特別重要，在這方面還沒有成熟的理論。經過試驗的合理驗證後，有限元數值模擬也許是處理問題的一種較為通用的方法。當然，具有較高可靠度的簡化計算方法仍然是工程實用中的有效工具。

但理論的不完備並不能延緩實踐的步伐，新型的各種複雜的組合方式層出不窮，如以下各小節中將要介紹的那些型鋼混凝土組合構件。它們形態各異，採用規範的計算方法很困難。而且要尋求這些組合構件在地震作用下的性能，通過足尺模型試驗來驗證其可靠性是必要的。同時，通過對試件滯回性能的研究，也便於進一步確認結構的性態水準及容許變形值。

3.1 高含鋼率SRC柱

位於北京的中國中央電視臺新台址主樓工程高 234m，包括兩座雙向傾斜 6 度的斜塔，頂部以 14 層高的懸臂結構相連(圖 1)。結構的抗側力體系為周邊支撐框筒，其鋼骨混凝土組合柱尺寸較大，鋼骨部分為多空腔的箱形截面，截面含鋼率最高達 24.3%，遠大於一般型鋼組合柱(圖 2)。



圖 1: 中國中央電視臺新台址主樓圖

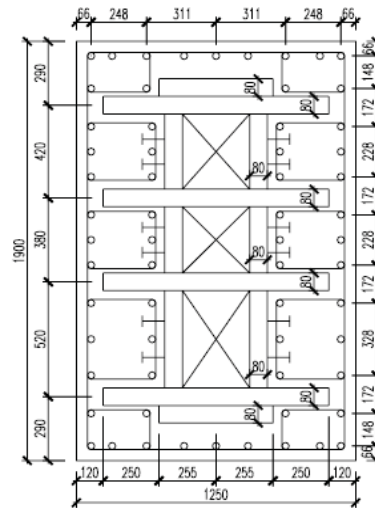


圖 2: CCTV 鋼骨混凝土柱截面

為了考察此大含鋼率及內有空腔的組合柱的軸力-彎矩承载力關係，在同濟大學進行了不同軸壓比的壓彎構件的滯回性能試驗^[10]。

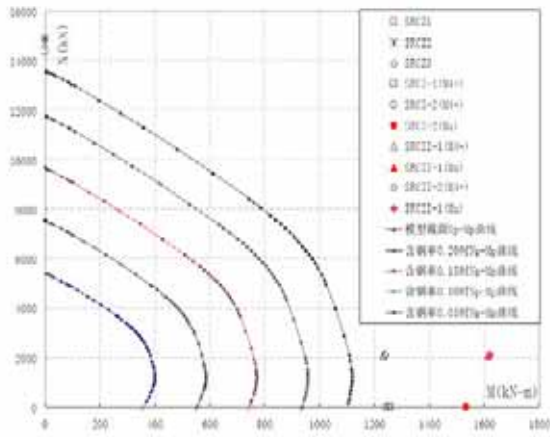


圖 3: 極限軸力-彎矩理論曲線與試驗資料比較 (相應於軸壓比 0.000~0.250)

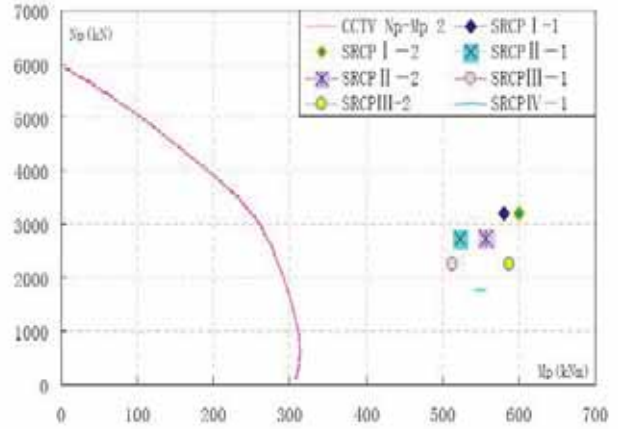


圖 4: 極限軸力-彎矩理論曲線與試驗資料比較 (相應於軸壓比 0.384~0.700)

試驗的結論是基於平截面假定的極限分析方法得到的承載力曲線是偏于安全的。試驗同時提出了為保證型鋼與混凝土共同作用，在上下兩端增設栓釘並改進箍筋佈置。

3.2 多型鋼 SRC 組合柱

對於異型和巨型 SRC 組合柱來說，很多情況下柱內採用多於一個的型鋼截面。基於型鋼的具體受力情況和抗震的考慮，各項目的處理不同。圖 5 顯示的香港國際金融中心二期工程巨型 SRC 柱。由於結構為抗風設計且巨型柱以承受軸力為主，柱內型鋼基本為離散佈置，只在伸臂桁架等節點處做整體處理。



a. 典型組合柱內型鋼佈置



b. 伸臂桁架節點

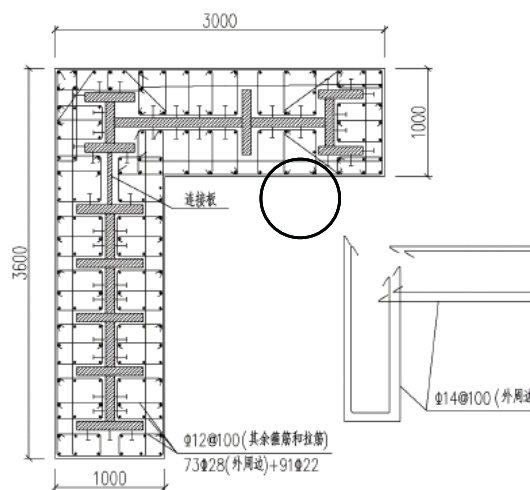
圖 5: 香港國際金融中心二期

北京中國國際貿易中心三期主塔樓工程(高330m, 見圖6a)的核心筒採用的異形型鋼混凝土柱亦是較為新型的組合構件的形式。混凝土柱的外形可能是L形, T形或其它形狀, 內含3~7根相連的工字形或箱形截面(圖6b)。由於起吊重量的限制, 初步設計中型鋼分成兩組, 擬在現場由間斷式的連接板相連(如圖6b中圓圈所示)。截面承載力曲線採用基於平截面假定的纖維有限元軟體分析得出, 同時亦進行了多組構件試驗以檢驗設計方法的可行性和構件的滯回性能^[9]。

試驗表明構件軸向受力性能達到設計要求。但在壓彎試驗時, 型鋼截面之間的連接板設計對於保持平截面假定相當重要。間斷式連接板且厚度不足時截面承載力須較平截面假定計算結果折減, 雖仍滿足大震設計要求, 但相應部位混凝土在極限荷載下產生通長裂縫(圖7a)。如加強連接板厚度和強度與工字鋼腹板相當, 則通長裂縫不再出現(圖7b)。



a.主塔樓外觀(2008年2月)



b.核心筒異型柱截面

圖6: 北京國際貿易中心三期

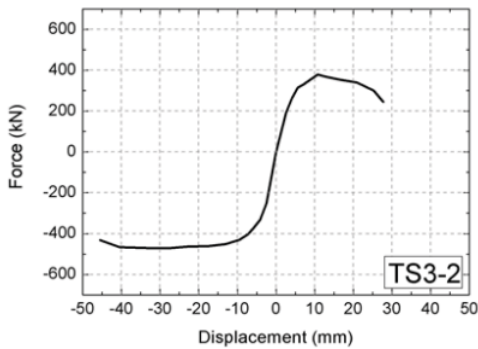


a: 原連接板設計

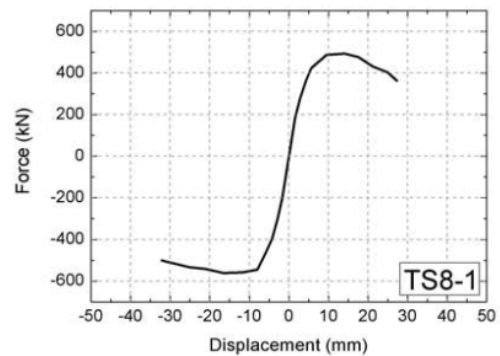


b: 加強連接板設計

圖 8: 試件縱向裂縫開展情況



a: 原連接板設計



b: 加強連接板設計

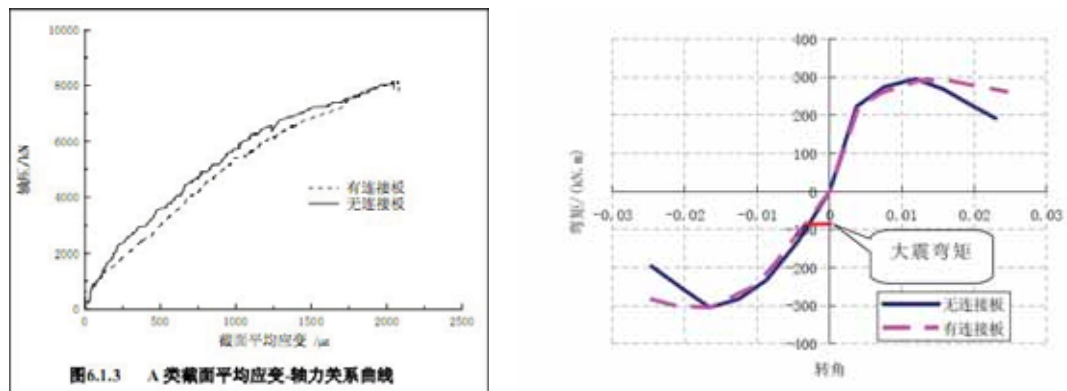
圖 8: 主軸方向載入滯回曲線

通過對比試驗結果和按平截面假定的數值計算結果，連接板的厚度和強度與工字鋼腹板相當時，平截面假定基本滿足，最終的設計也依此進行了修改。

大連中心裕景項目的超級塔 1 和超級塔 2 的建築高度分別為 383.2 米和 280 米。結構體系類似，均為筒中筒結構，內筒為鋼筋混凝土核心筒，外框筒由型鋼混凝土(SRC)巨型柱與內填混凝土箱形(CFB)大支撐形成。巨型柱截面接近五邊形，由於連接需要，巨型柱內埋鋼骨由多個不同截面的型鋼組成，各與巨型支撐以及樓面鋼樑連接。考慮到巨型柱受力以軸力為主而彎矩較小，從方便施工的角度我們在初步設計時仍希望採用離散型型鋼佈置或現場焊接間斷連接板將各截面聯繫起來。因此對型鋼的佈置方案進行了有無連接板的對比研究(見圖 10a 和 10b)。

試驗表明軸壓試驗下兩者結果基本接近(圖 9a)。往復側向荷載的壓彎試驗時，由於巨型柱主要承受軸力，在大震設計荷載時彎矩-轉角骨架曲線差別也很小(圖 9b)。在側移較大時均仍有縱向裂縫產生(見箭頭所示位置)，有連接板的裂縫出現時間遲且裂縫展開範圍較小。連接板上應變測試結果表明連接板起到了抗剪連接作用，但與各型鋼柱相比連接板仍偏弱。而縱向裂縫的出現表明鋼與混凝土之間的介面是任何型鋼混凝土截面設計需要重視的問題，即兩者之間的連接能否保證設計荷載下的共同工作以及平截面假定是否成立。對於本專案來說可以認為間斷連接板方案可保證結構的安全性，但最終作為對巨型柱整體性能的優化，在不加大用鋼量的基礎上將型鋼截面修改成為多腔整體式型鋼截面(見圖 10c)。

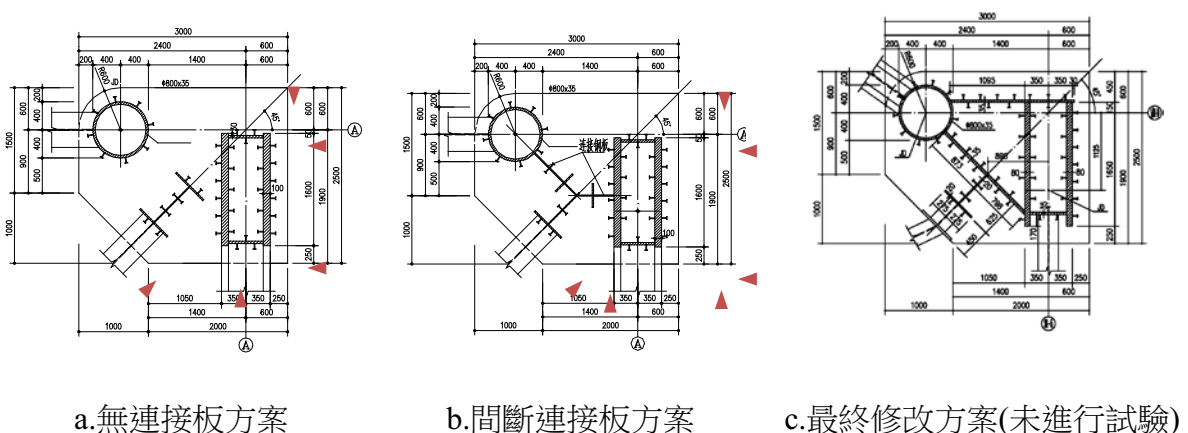
最近多個超高層項目均採用多腔體貫通整體式的型鋼佈置，截面整體性得以增強而施工上難度加大。但值得注意的是鋼與混凝土之間仍需要考慮介面連接強度。



a. 軸壓下平均應變-軸力關係曲線
(有無連接板比較)

b. 大震軸力下構件彎矩-轉角骨架曲線
(有無連接板比較)

圖 9: 大連中心裕景: 巨型柱有無連接板性能比較



a. 無連接板方案

b. 間斷連接板方案

c. 最終修改方案(未進行試驗)

圖 10: 大連中心裕景: 巨型柱內型鋼截面佈置(箭頭所示為縱向裂縫位置)

3.3 伸臂桁架區混凝土牆內的暗鋼桁架

在內筒與外框架之間加設伸臂桁架的結構，如內筒為混凝土，一般需在牆體內設置暗鋼桁架，從而有效傳遞兩側伸臂桁架中的巨大水準力。在北京財富中心二期寫字樓專案中按設計要求共設置了三層伸臂桁架，在核心筒牆體內加設了暗鋼桁架，如圖 11 所示(陰影內為核心筒區)。一般情況混凝土牆的抗剪能力有限，無法承受伸臂桁架中的巨大水準力，暗鋼桁架的設置可保證混凝土牆受拉開裂後仍可平衡伸臂桁架的水準荷載，需要按等強來對暗鋼桁架進行設計。

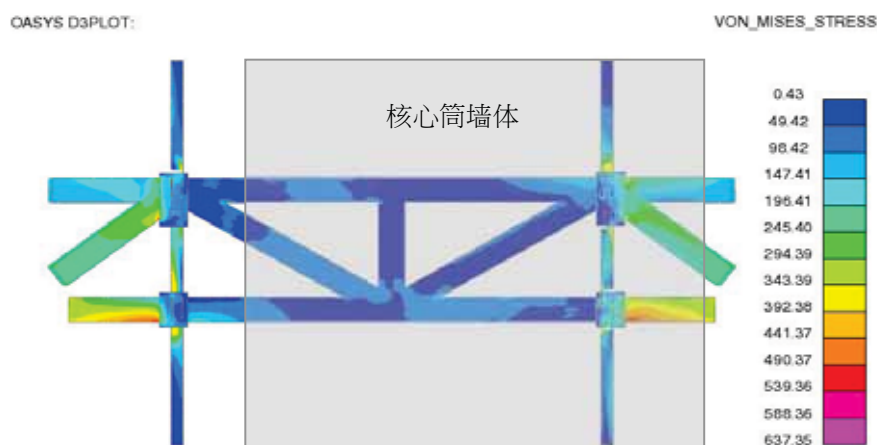
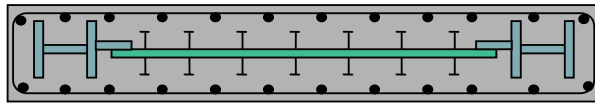


圖 11: 財富中心二期寫字樓暗桁架彈塑性分析結果

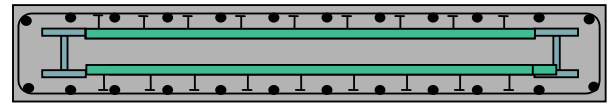
伸臂桁架與內筒混凝土牆及暗鋼桁架的連接處受力情況複雜，節點有限元分析的結果如圖 11 所示，伸臂桁架與暗柱/暗桁架相連的節點處有很大的應力傳遞，因此在這個範圍內不設置栓釘，而在暗桁架的構件上使型鋼的內力逐漸傳遞到牆體中。

4 組合鋼板剪力牆

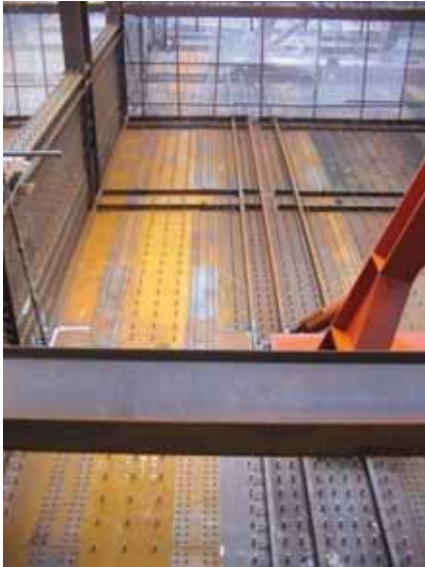
組合鋼板牆(C-SPW)在北美和日本的地震區已經得到了應用，在 AISC^[6]和日本規範中已經包含了相關規定。組合鋼板牆被定義為由鋼板以及鋼板一側或兩側的鋼筋混凝土組成的組合牆，並帶有型鋼或組合構件作為邊界構件。鋼板可能有一塊或兩塊(圖 12a 和 12b)在鋼筋混凝土的約束下，組合鋼板牆的整個鋼板可以達到抗剪屈服強度，遠遠優於純鋼板牆只有在對角受拉區域有效的抗剪承載力^[7]。組合鋼板牆的組合機制提供了很好的延性和抗側剛度。如果鋼板兩邊都有混凝土的話無需再做防火措施。



a. 單鋼板牆示意



b. 雙鋼板牆示意



c. 混凝土牆體施工前的鋼板牆圖



d. 綁紮混凝土牆體配筋後的鋼板牆

圖 12:組合鋼板牆

北京的中國國際貿易中心三期主塔樓工程是中國大陸首次大規模應用組合鋼板剪力牆這一新型結構體系^[8]，其後相繼應用於其它的超高層建築項目，例如北京財富中心二期寫字樓(258m)和天津嘉裡中心住宅樓(200m)。北美和日本的應用是以鋼框架+鋼板牆為基礎，加上混凝土部分作為屈曲約束和防火保護。但是這些結構裡的組合鋼板剪力牆基本上是在傳統的混凝土剪力牆+暗柱內加入鋼板+鋼暗柱+鋼暗梁形成的組合牆，因此混凝土部分發揮的作用要更大。這是由於在中國大陸混凝土核心筒是最為成熟的高層建築抗側力體系，而在混凝土牆內嵌入鋼板既可以大大提高其抗震性能，又保持了原體系剛度大的優點，因此預期在將來的超高層結構中這一組合結構體系將會有很大的發展。

中國建築科學研究院在 2007 年完成的研究報告^[9]對各種形式的組合剪力牆進行了試驗研究，結果表明在混凝土牆內加入四邊有型鋼邊緣構件(boundary members)的鋼板可大幅度提高牆的承載力而保持相當的延性。該研究建議的組合鋼板剪力牆的抗剪截面限值條件中計入鋼板及暗鋼柱的抗剪承載力，對於高層建築中剪力牆厚受抗剪截面條件控制時提供了有效的解決方法。

5 鋼管混凝土(CFT)

利用鋼管來約束混凝土形成的鋼管混凝土構件由於從字面上就能想得到的優點，被廣泛應用到大跨度橋樑和高層建築結構中。有關鋼管混凝土結構的理論研究也逐漸吸引了各國科研人員的興趣，並持續至今。目前的研究熱點主要集中在高強混凝土的應用、節點動力性能、耐火性能、鋼管混凝土結構體系抗震性能、預應力鋼管混凝土、矩形鋼管混凝土以及薄壁離心鋼管混凝土結構等方面。

關於鋼管混凝土結構的基本計算理論框架基本可分為以下三種^[15]：

1) 基於試驗回歸的“統一理論”，該理論最先由哈爾濱工業大學的鐘善桐教授提出，它的含義是“鋼管混凝土構件的性能，隨著物理參數、幾何參數、應力狀態及截面型式的改變而變化，變化是連續的、相關的和統一的。”^[14]該理論將鋼和混凝土混合成一種“組合材料”，不再對二者進行區分，從而擯棄了內力分配或迭加的概念。採用該理論的規範如電力行業標準 DL/T5085 和福建省標準 DBJ13-51-2003。

2) 折算理論，將混凝土折算成鋼，然後按純鋼結構設計。該理論的核心是“在不改變鋼管橫截面面積的前提下，將填充混凝土作為對鋼管壁的屈服強度和彈性模量的提高，以此來換算求得等效鋼管的性質，並以等效鋼管構件的承載力作為原型鋼管混凝土構件的承載力。”典型的規範如 AISC360、我國規範 CECS159:2004、CECS28:90 以及歐洲規範。

3) 迭加理論，其實質是將鋼管的承載力與混凝土的承載力迭加就得到鋼管混凝土結構的承載力。但該方法認為，如果軸壓力小於混凝土的承載力，則全部由混凝土部分承擔，否則，剩餘部分由鋼管承擔。這種混凝土優先受力的模式可能並不符合實際。日本的鋼管混凝土設計指南基本採用該原理。

不同國家規範的具體計算方法各異，但其理論基礎基本上是採用上述三種中的一種，以下小節將具體比較各規範間的差異。

5.1 中國現行 CFT 設計規範與各國規範之比較

很多國家都有鋼管混凝土的設計規範，但大都沒有非常明確的軸-彎、穩定性綜合設計和驗算方法。現時中國大陸對於鋼管混凝土的設計規程有中國工程建設標準化協會在 1990 年推出的《鋼管混凝土結構設計與施工規程》(CECS28:90)^[3]、2008 年推出的《高層建築鋼-混凝土混合結構設計規程》(CECS230:2008)^[22]和福建省建設廳 2003 年出版的《鋼管混凝土結構技術規程》(DBJ13-51-2003)^[17]，暫時還沒有由中國大陸建設部出版的全國通用規範。而國際規範有如美國鋼結構學會的 AISC360-05^[20]、澳洲橋樑設計規範 AS5100.6-2004^[21]，歐洲規範 EN-1994-1-1:2004^[13]和日本新都市房屋技術協會的鋼管混凝土設計指南^[18]，其中 AS5100.6-2004 和 EN-1994-1-1:2004 的設計方

法和要求是一模一樣的。

歐洲規範從力學原理出發，由截面反應計算出壓-彎曲線上四個代表受力狀態的承載力，考慮混凝土因鋼管約束效應而增加的混凝土受壓強度和鋼管壁因受雙向應力而產生的等效屈服值折減係數，並規定若是長細比超過 0.5 或偏心率超過 10%就不考慮約束效應[13]。受壓穩定性承載力可根據規範內公式計算，可是計算係數跟鋼材牌號有關，中國大陸的建築材料並不能完全對應計算公式要求。歐洲規範亦沒有提供對於構件受拉時的計算方法。

日本的設計指南也是從截面力學原理出發，不同之處是該指南將混凝土和鋼管受力分別考慮。混凝土約束效應值計算方法跟歐洲規範相似，鋼管雙向應力效應由 von Mises 屈服條件控制，所以其等效單向受拉和受壓的屈服值並不相同。軸-彎承載力曲線在有效設計長細比下並不會改變。

CECS28:90 規程是以概率理論為基礎發展出的設計公式，把鋼管等效作混凝土材料，其基本承載力由套箍效應來決定，然後乘上偏心(即壓彎)和長細比影響係數決定最終承載力。混凝土約束效應和鋼管雙向應力效應沒有直接體驗在公式上，但經過數學方法可以被分解出來。壓-彎承載力曲線呈雙折線形，明顯是經過工程簡化而得出。

最新出版的 CECS230:2008 規程在 CECS28:90 公式的基礎上對鋼管混凝土柱(考慮偏心影響的)軸向受壓承載力增加了 0.9 的修正係數，同時限制了管內混凝土在約束效應下的強度增幅，並另外提供了一個鋼管混凝土柱受彎承載力的公式。

福建省規範把鋼管等效作約束混凝土材料，然後按力學原理結合實驗資料制定出構件拉、壓、拉-彎、壓-彎和雙向受彎設計公式，並有構件的穩定性計算。混凝土約束效應和鋼管雙向應力效應可以經過數學方法被分解出來。

以下以一截 5m 長，1.5m 直徑，50mm 管厚，以中國大陸規範牌號的 Q345 鋼材和 C60 混凝土建成的鋼管混凝土柱在同時符合上述所有規範的設計條件下，根據 CECS230:2008，CECS28:90，福建規範，歐洲規範和日本鋼管混凝土設計指南規定下用材料標準值計算出來的軸-彎承載力曲線作比較。由於 CECS230:2008，CECS28:90 和歐洲規範沒有定義受拉承載力部份，所以在受拉情況下只考慮鋼材的貢獻。另外以 CECS28:90 在純軸向受壓的材料反應基準下基於平截面假定進行纖維截面積分作比較準則。

從圖 12 可見 CECS28:90 曲線把其它規範的曲線都包裹起來，CECS230:2008、日本設計指南和福建規範的最大軸壓承載力接近，而福建規範和歐洲規範的曲線形狀幾乎完全吻合，日本設計指南曲線則介乎 CECS28:90 和歐洲規範之間，但與 CECS230:2008 曲線接近。福建規範，歐洲規範和日本設計指南的最大軸壓承載力和純受彎承載力都很接近，可是 CECS28:90 曲線比其它規範的數值都要大。而 CECS230:2008 曲線利用受彎承載力設計公式結果跟歐洲規範考慮穩

定性計算後結果比較接近，但明顯比所有規範得出的結果要偏小很多。

根據 CECS230:2008 資料進行的纖維截面積分的純受彎承载力跟 CECS230:2008 算出來的數字很接近。由此可見福建規範和歐洲規範的設計結果總體比較保守，而 CECS28:90 的得出的承载力數值則偏大，可是 CECS230:2008 的受彎承载力公式明顯保守。

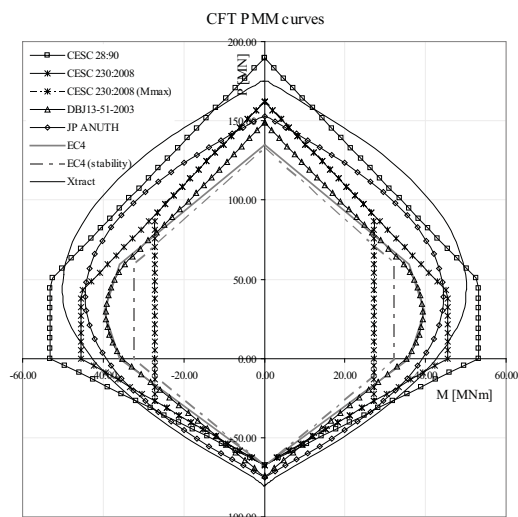


图 12 钢管混凝土柱在材料标准值下的轴-弯承载力曲线

6 結論

鋼構件具有高強度和良好的抗震性能，混凝土構件經濟性較好且剛度較大。組合構件兼具兩者的優勢，而組合形式十分靈活，重要的是可以針對不同的性能指標進行量化，達到安全性和經濟性的最佳平衡。相應於現在高層建築在高度或難度上不斷出現的新的挑戰，組合構件的應用因而愈加廣泛。正如本文所述，組合構件的靈活性也不斷帶來設計和研究上的未知性，包括組合構件兩種材料共同作用的性能，以及組合構件與組合構件、組合構件與其它構件之間的各種節點的性能。一個統一的設計理論最終是否有可能實現，需要設計界與科研界的共同努力。

參考文獻

1. 中華人民共和國行業標準 JGJ138-2001, 型鋼混凝土組合結構技術規程, 2001.
2. 中華人民共和國黑色冶金行業標準 YB9082-2006, 鋼骨混凝土結構技術規程, 2007.
3. 中國工程建設標準化協會標準 CECS28:90, 鋼管混凝土結構設計與施工規程, 1990.

4. 中華人民共和國電力行業標準 DL/T 5085-1999, 鋼-混凝土組合結構設計規程,1999.
5. 陳富生等, 高層建築鋼結構設計, 中國建築工業出版社,2000.
6. Seismic Provisions for Structural Steel Buildings, American Institute of Steel Construction Inc., Chicago, 2002.
7. Astaneh-Asl, A. (2002), Seismic Behaviour and Design of Composite Steel Plate Shear Walls, www.aisc.org.
8. 劉鵬等, 中國國際貿易中心三期主塔樓結構設計, 第二十屆全國高層建築結構學術交流會,2008.
9. 中國建築科學研究院等, 高層建築鋼-混凝土組合剪力牆受剪性能及設計方法的研究,2007.
10. 同濟大學鋼與輕型結構研究室, 中央電視臺新台址建設工程 SRC 組合柱試驗報告, 2006.
11. 日本建築學會,《鋼骨鋼筋混凝土計算標準及其說明》,1975 年日文修訂版。
12. 本格尼 . S . 塔拉納特,《高層建築鋼, 混凝土, 組合結構設計》, 羅福午等譯, 中國建築工業出版社, 1999.11
13. 趙均海等, 鋼管混凝土承載力的研究, 西北建築工程學院學報, 2001.6
14. 鐘善桐, 鋼管混凝土結構, 黑龍江科學技術出版社, 1994.12 第二版。
15. 陳志華等, 方鋼管混凝土柱的軸壓力分配係數研究, 天津大學。
16. 劉維亞等,《鋼與混凝土組合結構理論與實踐》, 中國建築工業出版社, 2008 年 6 月
17. 福建省工程建設地方標準 DBJ13-51-2003, 鋼管混凝土結構技術規程, 2003
18. Association of New Urban Housing Technology (ANUHT). (2002), Design Recommendations for Concrete Filled Steel Tube Structure, 4th Ed. (in Japanese)
19. Eurocode 4: Design of composite steel and concrete structures – Part 1-1: Genera; rules and rules for buildings EN 1994-1-1:2004, (2004)
20. Specification for structural steel buildings ANSI360-2005 (2005), American Institute of Steel Construction, Inc., Chicago
21. Austrian standard, Bridge design – Part6: Steel and composite construction (AS5001.6-2004). (2004), Standard Austrian International
22. 中國工程建設標準化協會標準 CECS230:2008, 高層建築鋼-混凝土混合結構設計規程,2008.

SECOND ORDER PLASTIC HINGE ANALYSIS FOR SEISMIC AND STATIC DESIGN OF BUILDING STRUCTURES

Y.P. Liu and S.L. Chan*

Department of Civil and Structural Engineering, The Hong Kong Polytechnic University, Hung Hom, Kowloon, Hong Kong, China

Corresponding author* ceslchan@polyu.edu.hk

ABSTRACT

Second-order elastic and plastic analysis as a new and robust design method has been introduced in many modern codes such as drafted LRFD (2010), Eurocode-3 (2005) and HKSC (2005) and becomes widely used in practice. This method considers the second-order effects, initial imperfections, material yielding, joint flexibility and so on in the process of analysis and as a result, it only needs the section design via the section capacity check rather than member design for safety and stability check. Thus, the reserved strength after yielding can be utilized and uncertainty in determination of effective length for member design under the framework of traditional linear design method is avoided. Strong earthquakes including the recent one on 11th March 2011 in Sendai, Japan and in different parts of the world led to severe damage of numerous buildings and loss of thousands of human lives. This paper extends the second-order elastic and plastic analysis used in numerous projects in Hong Kong since 2005 to push-over and time history analysis, which are expected to become more popular under the wide acceptance of performance-based seismic design in meeting multiple performance objectives. A simple and effective plastic hinge method is introduced in the second-order analysis to account for material yielding. Hence, the proposed second-order analysis method can be applied to seismic and static design of building structures. Unlike most software which could not design properly a structure without effective length under conventional static loads, the proposed computer method has been widely used in conventional design and therefore its application to seismic design is both consistent and natural since a structure will not be inconsistently designed by the linear analysis under conventional static load cases but checked by the nonlinear time history analysis under seismic actions.

Keywords: Second-order Analysis, Plastic Hinge, Time History Analysis, Performance-based Seismic Design, NIDA

1. INTRODUCTION

In the conventional linear analysis and design of building structures, the linearized response of a structure is used to construct the bending moment diagram of the structure from which the strength and stability of each member is checked and designed. As many practical columns are of modest to high slenderness that invalidates the assumption of an analysis considering only material yielding, the effective length factor, or the K-factor, is introduced to the design procedure for stability checking. Unfortunately, the determination of the effective length factor or the K-factor is based on the initial configuration under the linear analysis framework which ignores the change of structure geometry under external actions. This geometrical change alters the buckling length and thus the effective length factor assumed at undeformed geometry, making the effective length method inaccurate. Also, the contribution of the lateral stiffness from far end columns is normally ignored and therefore the effective length factor cannot be reliably determined. In many cases it is difficult and complicated to find the effective length factor even under the elastic theory for certain types of structures, for example, the dome structures and irregular frames.

Second-order analysis has been well researched for decades and becomes widely used in practical design in Hong Kong and Macau as a primary design method for member sizing and stability checking. In this computer age, the traditional tedious member design by hand is unjustifiable. On the other hand, the uncertainty of effective length method brings potential dangers in the design of fashionable and slender structures. The modern design codes such as Eurocode3 (2005) and HKSC (2005) explicitly require the second-order analysis for structures of high slenderness and irregular shape.

In this paper, a curved ability function element Chan and Gu (2000) allowing for initial bowing is used to simulate beam-column element. This element shows excellent accuracy under large axial force with the consideration of the interaction between axial force and bending moments and therefore one element per member is adequate without loss of accuracy which leads to much convenience in daily design.

Unlike previous second-order analysis which focuses only on P- Δ effect and ignores P- δ effect and initial imperfections, the proposed second-order analysis considers all second-order effects as well as initial imperfections and therefore meets the code requirement and can be used as a design tool. The proposed method has been extended to more common building structures with shear walls and floor slabs but not limit to bare steel frames, seen Liu and Chan (2009). With the consideration of member imperfection, the proposed method shows high accuracy in design of composite and reinforced concrete members with arbitrary shape subjected to axial force and biaxial bending (Chan *et al.* 2010).

It is noted that many strong earthquakes occurred in last two decades, for examples, Sendai Japan on 11th March 2011, USA Northridge 1994, Japan Kobe 1995, Taiwan Chi-Chi 1999, China Wenchuan 2008, Haiti 2010, Chile 2010 and China Yushu 2010. The development of modern seismic design codes is to reduce repair cost of building and to maintain their safety during earthquake. The traditional seismic design is significantly upgraded to performance-based seismic design (PBSD) which is believed to be a general design philosophy in future. The design criteria will be expressed in terms of performance objectives such as operational, immediate occupancy, life safety, collapse prevention associated with seismic hazard levels like frequent, occasional, rear and very rear opportunity under the framework of performance-based design. A performance objective is essentially associated with an acceptable risk meeting the community and owner's expectations. It is a future trend that the seismic design should permit multiple performance and hazard levels according to these expectations.

There are four well-known analysis methods specified in seismic codes for seismic performance evaluation, i.e. linear static analysis, modal response spectrum analysis, nonlinear static (pushover) analysis and nonlinear dynamic (time history) analysis. The first and second methods are based on linear theory without consideration of geometrical and material nonlinearities and therefore cannot be applied logically to multiple performance objectives seismic design. The pushover analysis estimates seismic demands on buildings by monotonically increasing lateral forces until a target displacement is reached. The basic assumption behind this method is that the response of the structure is controlled by its fundamental mode which is not the case for many structures. This paper is mainly focused on time history analysis (THA) which is deemed to be an "exact" method in predicting the structural behavior while more details about pushover analysis can be referred to (Liu *et al.* 2010).

In many codes, time history analysis is compulsively used for high-rise or important buildings and long-span bridges. To consider the inelastic behavior in a time history analysis, a plastic hinge method by inserting two end section springs into the curved stability function element Chan and Gu (2000) is adopted for simplicity and fast convergence. The Newmark (1959) method is utilized for step-by-step integration of the motion of equation. Due to the use of same nonlinear theoretical background, the static second-order analysis and time history analysis can be carried out in a unified platform. Nonlinear-based software NIDA (2010) has an inherent advantage for both second-order nonlinear design for conventional load cases and nonlinear dynamic seismic design.

2. NONLINEAR INTEGRATED DESIGN AND ANALYSIS

The conventional linear design method divides the whole design procedure into two stages: (1) determination of the internal forces and moments acting on each member of the structural system by elastic linear analysis; (2) assessment of the strength and stability of each member treated in isolation by plastic analysis. Compatibility between the isolated member and the structural system is doubtful. There has been an increasing awareness for the use of second-order analysis that simulates directly the behavior of structural members, connections, and other components in the determination of overall system response.

The new and advanced nonlinear integrated design and analysis method is very different from the conventional linear design since the nonlinear analysis model contains more factors which may significantly affect the structural behavior. Also, the interaction between the structural members and the structural system can be considered. In other words, the second-order design method is a “system-based” holistic approach, in contrast to the traditional “member-based” localized design method.

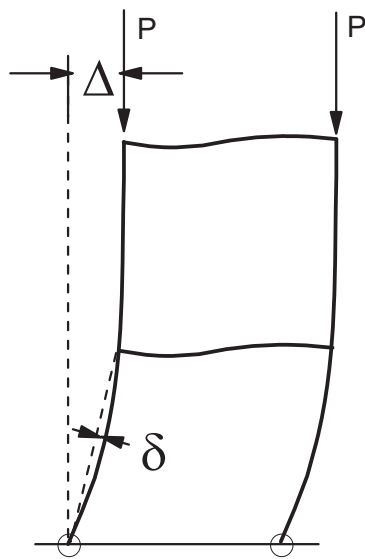
In the current transition period from the first-order linear to second-order nonlinear structural analysis and design, the second-order elastic or first-plastic hinge analysis, which assumes the design resistance is reached at the formation of the first plastic hinge, is recommended for daily non-seismic design. Second-order elastic or first-plastic hinge analysis means an analysis allowing for the second-order effects due to the change of geometry and initial stresses in members but material yielding is not allowed to be distributed after the first plastic hinge. If both the $P-\Delta$ and $P-\delta$ effects are included in the analysis, the method is termed as “second-order elastic $P-\Delta-\delta$ analysis” while only the $P-\Delta$ effect is considered, the method is termed as “second-order elastic $P-\Delta$ -only analysis”. It should be noted that the checking of member strength relies on the application of design formula since this type of methods does not take material yielding into account. Moreover, an additional member resistance checking for $P-\delta$ effect should be conducted separately for the “second-order elastic $P-\Delta$ -only analysis”. On the other hand, for the “second-order elastic $P-\Delta-\delta$ analysis”, the process of determining the effective length of the member by a formula in a design code in order to calculate the second-order moments can be skipped and the accuracy and saving in routine design effort can be achieved.

2.1 $P-\Delta$ and $P-\delta$ effects

When a structure deforms, the original geometry can no longer be employed for the formulation of the transformation matrix simply because the nodal coordinates have been changed. This effect, named $P-\Delta$ effect, may become important when the deflection and/or the conjugate force is large such as the case of a building under a heavy mass at the roof and a lateral wind load. An additional moment termed as the $P-\Delta$ moment will be induced due to this effect.

The $P-\delta$ effect is referred to as the second-order effect due to the deflection along a member and the axial force. It affects the state of stress as well as the stiffness of the member. Like the $P-\Delta$ effect, an additional moment named $P-\delta$ moment will be induced due to the $P-\delta$ effect. Its careful consideration is important for buckling analysis and design of slender skeletal structures.

In general, both the $P-\Delta$ (frame sidesway) and $P-\delta$ effects (member curvature) will occur in a structure under vertical and horizontal external forces. These effects are shown in Figure 1.



$P-\Delta$ and $P-\delta$ effects

If we consider both $P-\delta$ and $P-\Delta$ effects with member and frame initial imperfections, we need not worry about the effective length and the design is more efficient and accurate.

Figure 1 The $P-\Delta$ and $P-\delta$ effects

In this paper, the $P-\Delta$ effect is automatically considered in the incremental-iterative procedure while the $P-\delta$ effect is accounted for by the use of curved stability functions Chan and Gu (2000) at the element level.

2.2 Initial imperfections

As no structures are perfect and free from defects due to initial crookedness, residual stress, installation and erection, imperfections must be considered. One of the biggest differences between the effective length method and the second-order analysis is their consideration of initial imperfections. The effective length method considers imperfection implicitly in the use of buckling curves such as the a_0 , a , b , c and d curves in Eurocode-3(2005) whereas the second-order analysis explicitly considers imperfections in use of member initial curvatures and frame out-of-plumbness and notional forces. Two types of imperfections should be included in the nonlinear analysis and design, i.e., the member and frame imperfections.

(1) Member imperfections

Member initial imperfections are due to member initial crookedness or residual stresses. The initial geometric imperfections of members may be due to one or several aspects such as cambering, sweeping, twist, out of straightness and cross-section distortion. The residual stresses in members may be due to manufacturing and fabrication processes, erection out-of-fit, and construction sequencing. To exactly account for all the imperfections rigorously seems impossible for practical structures. Practically, they can be simulated in the analysis/design model by the equivalent initial bow imperfection which may be slightly different in the national design codes due to the difference in steel products.

According to HKSC (2005), the equivalent initial bow imperfections for different sections are specified in its Table 6.1 and Table 8.7 and also listed in the Table 1 and Table 2 respectively of this paper for clarity. These values may be used in a second order analysis for the steel members under compression. For composite column, the buckling curves and member imperfections are specified in Table 10.13 of HKSC (2005).

Buckling curves referenced in Table 8.7	$\frac{e_0}{L}$ to be used in Second-order P-Δ-δ elastic analysis
a	1/500
b	1/400
c	1/300
d	1/200

Table 1 Values of member initial bow imperfection used in design

In the proposed second-order analysis, the initial member imperfection has been formulated in the curved stability functions (see Figure 2) according to the code requirements. Therefore, its effects have been considered in the analysis part of the second-order analysis.

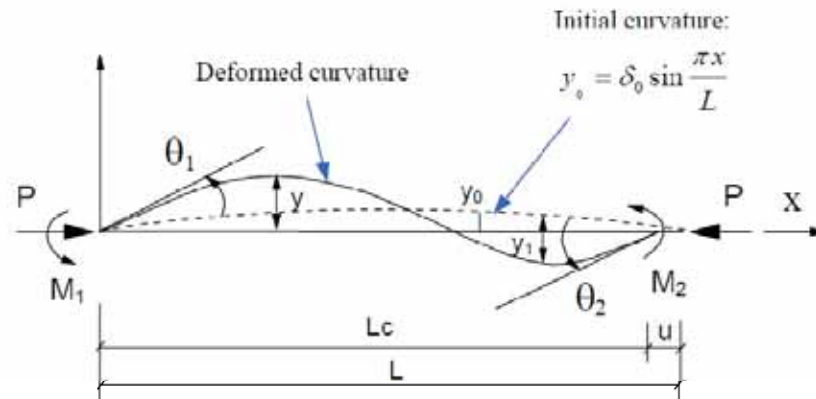


Figure 2 The Curved Stability Function Element with Initial Crookedness

(2) Frame imperfections

The frame imperfections are mainly due to the out of plumbness of frame and column in the erection processes and construction sequence, see Figure 3. This type of imperfections may increase the sway effect and induce P- Δ moments which are specially important when a structure is subjected to large vertical loads.

Type of section	Maximum thickness (see note1)	Axis of buckling	
		x-x	y-y
Hot – finished structural hollow section		a)	a)
Cold – formed structural hollow section		c)	c)
Rolled I – section	≤ 40 mm > 40 mm	a) b)	b) c)
Rolled H – section	≤ 40 mm > 40 mm	b) c)	c) d)
Welded I or H – section (see note 2)	≤ 40 mm > 40 mm	b) b)	c) d)
Rolled I – section with welded flange cover plates with $0.25 < U/B < 0.80$ as shown in Figure 8.4)	≤ 40 mm > 40 mm	a) b)	b) c)
Rolled H – section with welded flange cover plates with $0.25 < U/B < 0.80$ as shown in Figure 8.4)	≤ 40 mm > 40 mm	b) c)	c) d)
Rolled I or H – section with welded flange cover plates with $U/B \geq 0.80$ as shown in Figure 8.4)	≤ 40 mm > 40 mm	b) c)	a) b)
Rolled I or H – section with welded flange cover plates with $U/B \leq 0.25$ as shown in Figure 8.4)	≤ 40 mm > 40 mm	b) b)	c) d)
Welded box section (see note 3)	≤ 40 mm > 40 mm	b) c)	b) c)
Round, square or flat bar	≤ 40 mm > 40 mm	b) c)	b) c)
Rolled angle, channel or T-section Two rolled sections laced, battened or back-to-back Compound rolled sections		Any axis: c)	

Table 2 Designation of buckling curves for different section types

Linear analysis uses the moment amplification to enlarge the linear moment for sway effect.

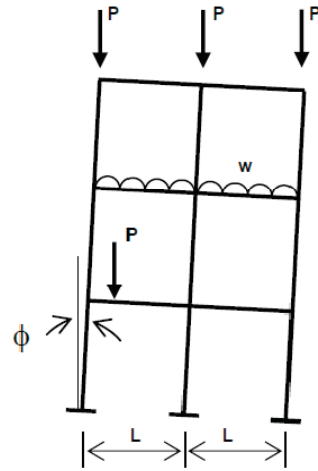


Figure 3 Frame Imperfection

In second-order analysis, wind load or notional force can be still used, but an alternative and more reliable and convenient method is to adopt the elastic buckling mode as the imperfection mode with amplitude set equal to the out-of-plumbness normally taken as height/200 according to HKSC (2005) or other justified values.

2.3 Section capacity check

In the codified linear design method a member is required for checking against member buckling and sectional strength while in the proposed second-order design method, only the section capacity check in the following symbolic expression is required.

$$\frac{P}{p_y A} + \frac{\bar{M}_y + P(\Delta_y + \Delta_{0y}) + P(\delta_y + \delta_{0y})}{M_{cy}} + \frac{\bar{M}_z + P(\Delta_z + \Delta_{0z}) + P(\delta_z + \delta_{0z})}{M_{cz}} = \varphi \leq 1 \quad (1)$$

where

P is the axial force in member;

A is the cross sectional area;

p_y is the design strength;

\bar{M}_y, \bar{M}_z are the moments about the minor and major axes obtained from a first order analysis;

M_{cy}, M_{cz} are the moment capacities about the minor and major axes. If lateral-torsional buckling is considered, the smaller of buckling moment, M_b ,

and the plastic moment M_{cz} divided by an equivalent moment factor m_{LT} should be used;

Δ_y, Δ_z are the nodal displacements due to out-of-plumbness of frame sway induced by loads;

Δ_{0y}, Δ_{0z} are the nodal displacements due to out-of-plumbness of frame imperfections;

δ_y, δ_z are the member deformations due to loads on the member;

δ_{0y}, δ_{0z} are the member deformations due to member initial bow;

φ is the section capacity factor. If $\varphi > 1$, a member fails in design strength check and if $\varphi \ll 1$, the member section can be reduced in size.

It is noted that as the effective length is used to account for the P- Δ and P- δ effects, the above Eq. (1) including both P- Δ and P- δ moments will automatically consider these effects due to buckling. Thus, the proposed second-order analysis only needs section check and eliminates the tedious member check.

3. PLASTIC HINGE METHOD

It is necessary to consider inelastic behavior in second-order plastic analysis, pushover analysis, time history analysis and progressive collapse analysis. The plasticity models for tracing nonlinear material behavior of beam-column members have fallen into two categories: distributed plasticity and concentrated plasticity. The distributed plasticity (also referred to as plastic zone) models can monitor the spread of yielding both along the member length and throughout its cross-section. This method is considered to be “exact” solution but rarely adopted in practical engineering as it consumes huge computer time. The concentrated plasticity (also referred to as plastic hinge) models assume that the plasticity is lumped only at the ends of an element, while the portion within the element is assumed to remain elastic throughout the analysis. The plastic hinge method is much simpler and needs less computational effort with acceptable accuracy, therefore, it is widely used both in research and engineering applications.

In this paper, a refined plastic hinge method is implemented by inserting two end section springs into the curved stability function element Chan and Gu (2000). The progressive strength and stiffness degradation of the structure can be captured by properly adjusting the stiffness of section spring. Thus, a simple, accurate and efficient method for determining the plastic hinge(s) is proposed to account for material nonlinearity.

The basis of the plastic hinge method is cross-section plastification. Material yielding is accounted for by zero-length plastic hinges at one or both ends of each element. Here, two predefined section springs which are used to simulate plastic hinge, will be set at the two ends of each curved stability function beam-column element Chan and

Gu (2000) and therefore a new hybrid element (see Figure 4) is formulated. The internal degrees of freedom can be eliminated by a standard static condense procedure, and therefore the bending equilibrium equations in an incremental form can be expressed as,

$$\begin{bmatrix} \Delta M_{s1} \\ \Delta M_{s2} \end{bmatrix} = \begin{bmatrix} S_{s1} - S_{s1}^2(K_{22} + S_{s2}) / \beta_s & S_{s1}S_{s2}K_{12} / \beta_s \\ S_{s1}S_{s2}K_{21} / \beta_s & S_{s2} - S_{s2}^2(K_{11} + S_{s1}) / \beta_s \end{bmatrix} \begin{bmatrix} \Delta \theta_{s1} \\ \Delta \theta_{s2} \end{bmatrix} \quad (2)$$

with

$$\beta_s = \begin{vmatrix} K_{11} + S_{s1} & K_{12} \\ K_{21} & K_{22} + S_{s2} \end{vmatrix} > 0 \quad (3)$$

and, S_{si} is the stiffness of section spring, ΔM_{si} is the incremental nodal, $\Delta \theta_{si}$ is the incremental nodal rotations, K_{ij} is the stiffness coefficients of the curved stability function element.

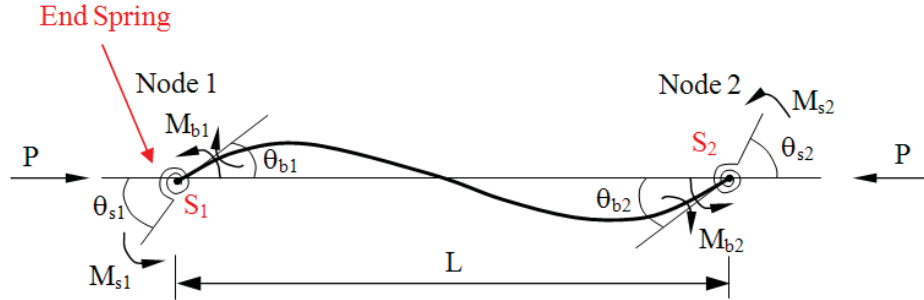


Figure 4 Internal Forces of the Curved Element with End Springs

To consider the progressive cross-section yielding, the section spring stiffness S_s is simply defined below to approximate the inelastic behavior of the steel members for design purpose,

$$S_s = \frac{6EI}{L} \frac{|M_{pr} - M|}{|M - M_{er}|} \quad (M_{er} < M < M_{pr}) \quad (4)$$

where EI is the flexural constant, L is the member length, M is bending moment due to external forces, and M_{er} and M_{pr} are the first yield and plastic moments respectively.

In computer analysis, the section spring S_s is taken as $10^{+10} EI/L$ and $10^{-10} EI/L$ for the elastic case (i.e. $M < M_{cr}$) and the plastic case (i.e. $M > M_{pr}$) respectively. In case of a force point outside the full yield surface (i.e. $M > M_{pr}$), it should be moved back onto the surface to avoid the violation of plastic state. In this paper, the path normal to the yield surface is chosen as the recovery path.

The hysteresis model for steel material used in NIDA (2010) is shown in Figure 5. As illustrated in the figure, initial yielding occurs at point A when the first yield moment capacity M_{ei} is attained. On the curve AB, the gradual yielding occurs and the plastic moment capacity M_p is reached at point B. When unloading takes place at point B, gradual yielding characteristics disappears and the path follows the line BDC in which the moment at point C is less than the initial yield moment M_{ei} at point D. On reloading, the path moves along the line CD under the perfectly elastic state and then follows the curve DE under the partial yielding state. Similarly, under unloading conditions at point E, the path moves along EFG'H.

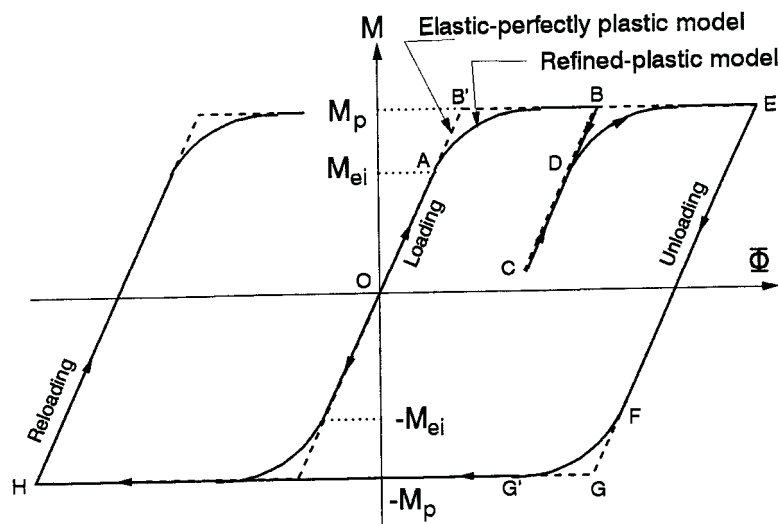


Figure 5 Elastic-Perfectly Plastic & Refined-Plastic Models Employed in NIDA

4. TIME HISTORY ANALYSIS

Many seismic design codes compulsively require a time history analysis (THA) to evaluate the structural performance. For example, GB50011 (2010) specifies that buildings in extremely irregular configuration, buildings assigned Seismic Design Category A, and tall buildings in the height shown in Table 3, a time history analysis should be performed.

Seismic Intensity & Site Class	Range of Building Height
Intensity 7, Intensity 8 with Site Class I & II	> 100 m
Intensity 8 with Site Class III & IV	> 80 m
Intensity 9	> 60 m

Table 3 Buildings Required Time History Analysis

Unlike modal response spectrum analysis (MRSA) which only gives best estimates of the peak response and generally ignores the degradation of strength and stiffness during an earthquake, THA can provide much more exact response predictions within the framework of the reliability and representativeness of the nonlinear modeling of the structure.

4.1 Direct Integration for Equation of Motion

The incremental form of the equation of motion can be written as,

$$[M]\{\Delta\ddot{u}\} + [C]\{\Delta\dot{u}\} + [K]\{\Delta u\} = \{\Delta F\} \quad (5)$$

in which $\{\Delta F\}$ is equal to $-[M]\{\Delta\ddot{u}_g\}$. For simplicity, the “(t)” in acceleration $\ddot{u}(t)$, velocity $\dot{u}(t)$ and displacement $u(t)$ is omitted.

Noted that the damping matrix $[C]$ is usually employed as the Rayleigh damping model given by,

$$[C] = a[M] + b[K] \quad (6)$$

in which a is mass proportional coefficient, and b is stiffness proportional coefficient. The two coefficients can be calculated by

$$\begin{cases} a = \frac{4\pi(\zeta_1 T_1 - \zeta_2 T_2)}{(T_1^2 - T_2^2)} \\ b = \frac{T_1 T_2 (\zeta_2 T_1 - \zeta_1 T_2)}{\pi(T_1^2 - T_2^2)} \end{cases} \quad (7)$$

in which T_1 and T_2 are the first and second natural periods of the structure respectively, and ζ_1 and ζ_2 are the damping ratios corresponding to T_1 and T_2 respectively.

MRSA solves the dynamic equilibrium equation by mode superposition while THA widely adopts numerical integration method. In NIDA (2010), the popular Newmark (1959) method is utilized for step-by-step solution of Eq. (5).

Newmark (1959) truncated the Taylor's series for displacement $\{u\}$ and velocity $\{\dot{u}\}$ as,

$$\{^{t+\Delta t}\dot{u}\} = \{^t\dot{u}\} + (1-\gamma)\Delta t\{^t\ddot{u}\} + \gamma\Delta t\{^{t+\Delta t}\ddot{u}\} \quad (8)$$

$$\{^{t+\Delta t}u\} = \{^tu\} + \Delta t\{^t\dot{u}\} + (0.5-\beta)(\Delta t)^2\{^t\ddot{u}\} + \beta(\Delta t)^2\{^{t+\Delta t}\ddot{u}\} \quad (9)$$

where $\{^tu\}$, $\{^t\dot{u}\}$ and $\{^t\ddot{u}\}$ are the total displacement, velocity and acceleration vectors at time t , and Δt is time increment. The parameters γ and β define the variation of acceleration over a time step and determine the stability and accuracy characteristics of the method. Typically, $\gamma = 0.5$ and $1/6 \leq \beta \leq 1/4$ can provide stable results.

Using Eqs. (8) and (9), the equation of motion Eq. (5) can be finally written as,

$$[K_{eff}]\{\Delta u\} = [\Delta F_{eff}] \quad (10)$$

in which

$$[K_{eff}] = c_1[M] + c_4[C] + [K] \quad (11)$$

$$[F_{eff}] = \{^t\Delta F\} - (c_2[M] + c_5[C])\{^t\dot{u}\} - (c_3[M] + c_6[C])\{^t\ddot{u}\} \quad (12)$$

with

$$\begin{cases} c_1 = \frac{1}{\beta(\Delta t)^2}; & c_2 = -\frac{1}{\beta\Delta t}; & c_3 = -\frac{1}{2\beta} \\ c_4 = \frac{\gamma}{\beta\Delta t}; & c_5 = -\frac{\gamma}{\beta}; & c_6 = -(\frac{\gamma}{2\beta} - 1)\Delta t \end{cases} \quad (13)$$

After obtaining $\{^t\Delta u\}$ from Eq. (10), the incremental velocity $\{^t\Delta \dot{u}\}$ and acceleration $\{^t\Delta \ddot{u}\}$ can be calculated by

$$\{^t\Delta \dot{u}\} = c_4\{^t\Delta u\} + c_5\{^t\dot{u}\} + c_6\{^t\ddot{u}\} \quad (14)$$

$$\{^t \Delta \ddot{u}\} = c_1 \{^t \Delta u\} + c_2 \{^t \dot{u}\} + c_3 \{^t \ddot{u}\} \quad (15)$$

Further, the total vectors for next time step are updated as

$$\begin{cases} \{^{t+\Delta t} u\} = \{^t u\} + \{^t \Delta u\} \\ \{^{t+\Delta t} \dot{u}\} = \{^t \dot{u}\} + \{^t \Delta \dot{u}\} \\ \{^{t+\Delta t} \ddot{u}\} = \{^t \ddot{u}\} + \{^t \Delta \ddot{u}\} \\ \{^{t+\Delta t} F\} = \{^t F\} + \{^t \Delta F\} \end{cases} \quad (16)$$

For nonlinear dynamic analysis, iterations for solving Eq. (10) are needed for correction of equilibrium error in which both the displacement and force norms are used as,

$$\frac{\{^t \Delta u\}_i^T \{^t \Delta u\}_i}{\{^{t+\Delta t} u\}_i^T \{^{t+\Delta t} u\}_i} < \text{TOLERANCE} \quad (17)$$

$$\frac{\{^t \Delta F^*\}_i^T \{^t \Delta F^*\}_i}{\{^{t+\Delta t} F\}_i^T \{^{t+\Delta t} F\}_i} < \text{TOLERANCE} \quad (18)$$

in which the subscript “ i ” is the number of iterations within a time step, and $\{^t \Delta F^*\}$ is the unbalanced residual force increment vector determined by

$$\{^t \Delta F^*\} = \{^{t+\Delta t} F\} - ([M]\{^{t+\Delta t} \ddot{u}\} + [C]\{^{t+\Delta t} \dot{u}\} + \{^{t+\Delta t} R\}) \quad (19)$$

where $\{^{t+\Delta t} R\}$ is the resisting force of the complete structure.

Once the conditions given in Eqs. (17) and (18) are satisfied, the procedure presented in Eqs. (10-18) is repeated for next time step until the target time is reached or the structure collapses.

4.2 Selection of Earthquake Wave

It is obvious that the artificial/recorded/simulated waves of ground motion selected for a time history analysis may significantly affect the outcome. Therefore, seismic design codes explicitly or implicitly specify some requirements for selecting earthquake waves when performing a nonlinear dynamic analysis.

The theoretical background for selection of earthquake wave is generally based on the three characteristics of ground motion, i.e. peak ground motion, time duration and frequency content. Peak ground motion, primarily peak ground acceleration (PGA), influences the vibration amplitude and has been commonly employed to scale earthquake design spectra and acceleration time histories. Time duration of ground motion affects the severity of ground shaking. For example, an earthquake with a high PGA poses a high hazard potential, but if it is sustained for only a short period of time it is unlikely to inflict significant damage to many types of structures. On the contrary, an earthquake with a moderate PGA and a long duration can build up damaging motions in certain types of structures. When the frequency content of the ground motion is close to the natural frequencies of the structure, the resonant phenomenon, in which the vibration amplitude of the structure grows significantly, will occur.

From above, the general rules for selection of earthquake waves in GB50011 (2010) are listed as below.

(1) Minimum Time Duration

The duration of the input wave should be sufficiently long, which is generally taken as not less than 5 to 10 times of the fundamental period of the structure.

(2) Minimum Number of Waves

GB50011 (2010) specifies that at least 2 sets of recorded strong earthquake waves and 1 set of artificial wave, based on the seismic intensity, design seismic group and site classification, should be employed.

(3) Minimum Base Shear

The seismic action represented by the input waves should conform, on average, to the 5% damping elastic response spectrum so that the waves used may have the statistical meaning to some extent. GB50011 (2010) states that when performing an elastic time history analysis, the base shear obtained from each wave shall not be less than 65% of that from the response spectrum method, and the average value from all waves shall not be less than 80% of that from the response spectrum method.

5. EXAMPLES

5.1 Vogel six-story frame

The two-bay six-story frame subjected to distributed gravity loads and concentrated lateral loads has been analyzed by Vogel (1985). The frame is assumed to have an initial out-of-plumb straightness with all the members assumed to possess the ECCS residual stress distribution (ECCS 1983). The structural layout and the applied loads of the frame are shown in Figure 6. This frame has been widely used to calibrate proposed plastic hinge methods of analysis.

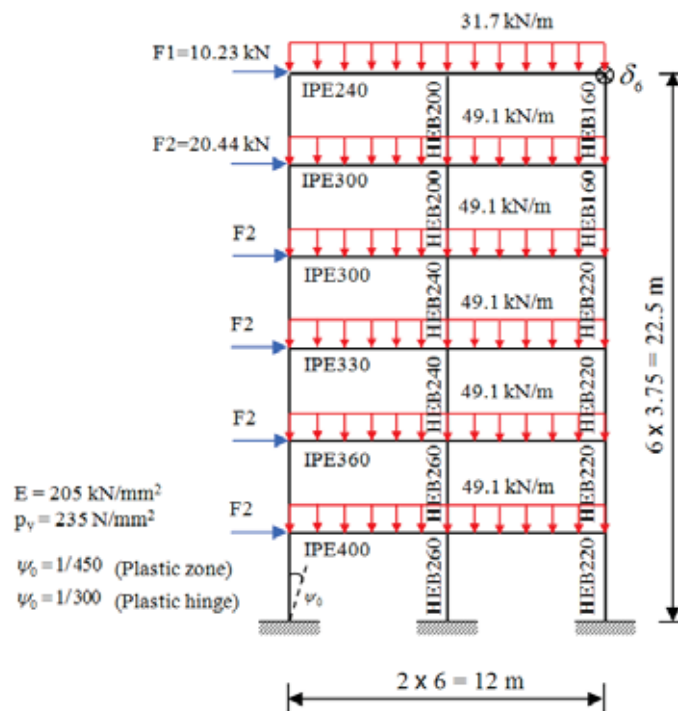


Figure 6 Section Properties and Applied Loads of Vogel Six-story frame

The structure is analyzed by the proposed second-order plastic analysis method assuming that the vertical and horizontal forces are proportionally applied. Eq. (1) has been used in many design codes as conservative yield surface of beam-columns but a more economical yield surface in the paper by Vogel (1985) is adopted here for direct comparison.

The load-deflection curve of the node at top level is plotted against the results by Vogel (1985) who used the plastic zone and plastic methods and shown in Figure 7. The load factor obtained from the proposed plastic hinge method is 1.09 compared with the maximum load factor 1.11 and 1.12 obtained by plastic zone and plastic hinge methods (Vogel 1985) respectively. The locations of plastic hinges (marked in black point) are indicated in Figure 8. From these figures, it can be seen that the proposed second-order inelastic analysis is of high accuracy against results by others.

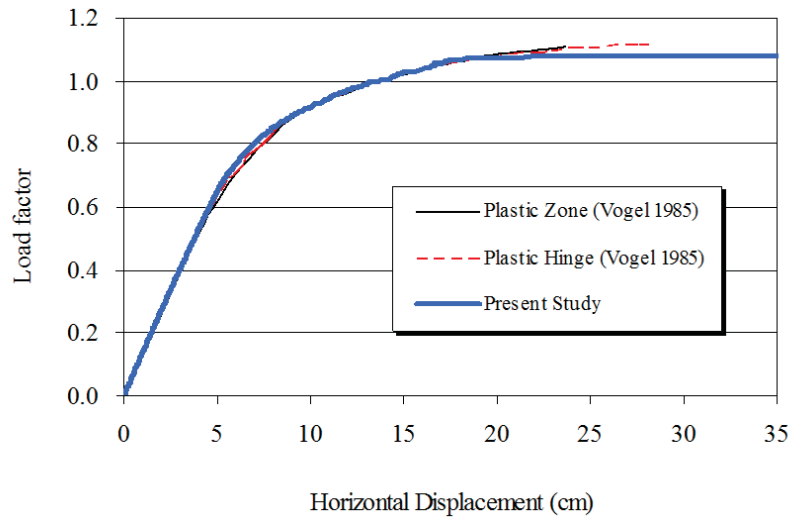


Figure 7 Comparison of Load-Deflection Curve at δ_6

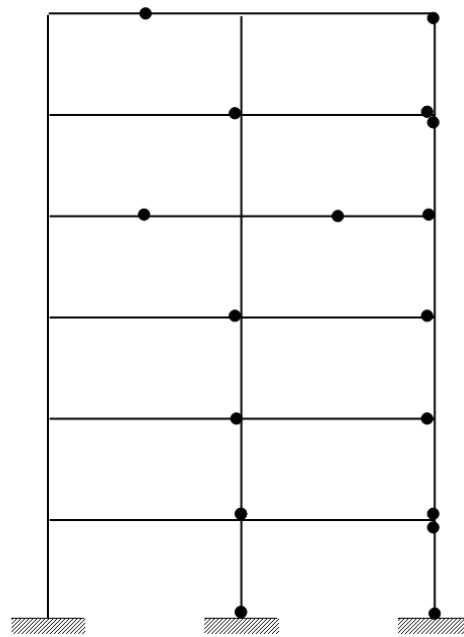


Figure 8 Locations of Plastic Hinges

5.2 Seven-Story 2D Steel Frame

A seven-story 2D steel frame shown in Figure 9 is used here for demonstration of time history analysis by NIDA (2010). The details of the 2D frame are given below.

- (a) Geometrical dimensions and section sizes: shown in Figure 9;
- (b) The material properties for all members: Young's modulus $E=2.034 \times 10^5$ MPa, Poisson's ratio $\nu=0.3$, yield strength $p_y=250$ MPa;
- (c) Applied static loads: shown in Figure 10;
- (d) Boundary conditions: all columns are fixed to foundation and member connections are rigid;
- (e) Mass: 85 812.16 kg at each story (node 5, 8, 11, 14, 17, 20 and 23);
- (f) Earthquake wave: the N-S component of the El Centro 1940.

The procedure for performing time history analysis in NIDA (2010) is detailed as below.

Step 1: Build the structural model. For example, nodal coordinates, material properties, section properties, applied loads, boundary conditions and so on;

Step 2: Define one or more than one time history functions. User can import a previous earthquake record as shown in Figure 10.

Step 3: Define the time history analysis case. Generally, user only needs to give a case name, specifies time steps and input the parameters for calculation of damping as seen in Figure 11. The default values for Newmark method can be used for many structures.

Noted that the Newton-Raphson method is used for the nonlinear incremental-iterative solution when performing a time history analysis in NIDA (2010). In some cases the structural behaviour may be highly nonlinear and therefore several cycles in each time step are needed.

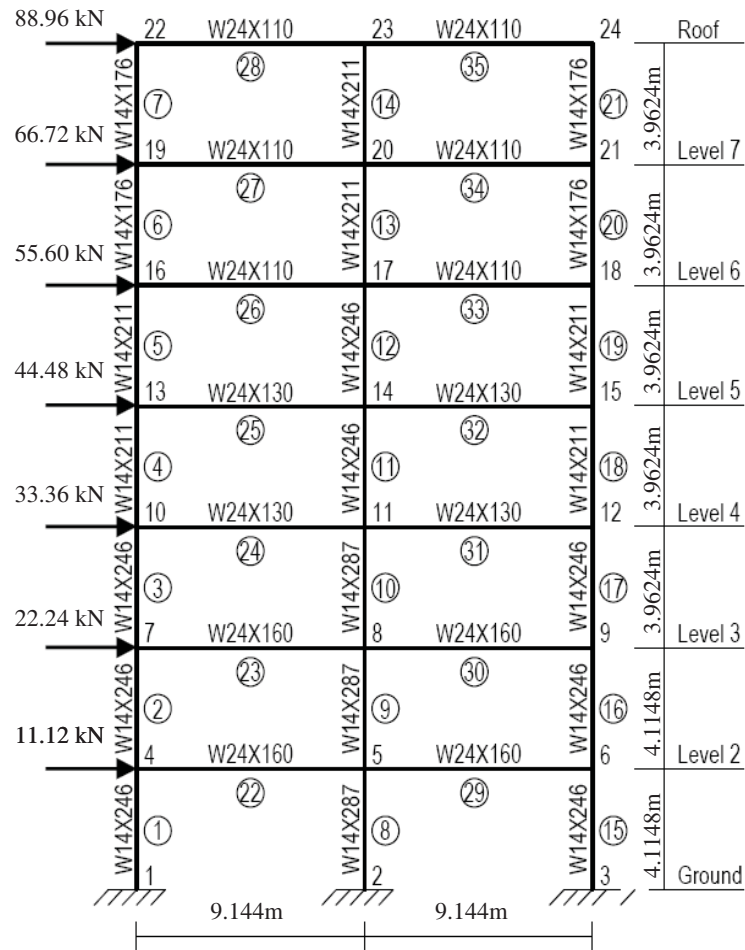


Figure 9 Seven-Story 2D Steel Frame

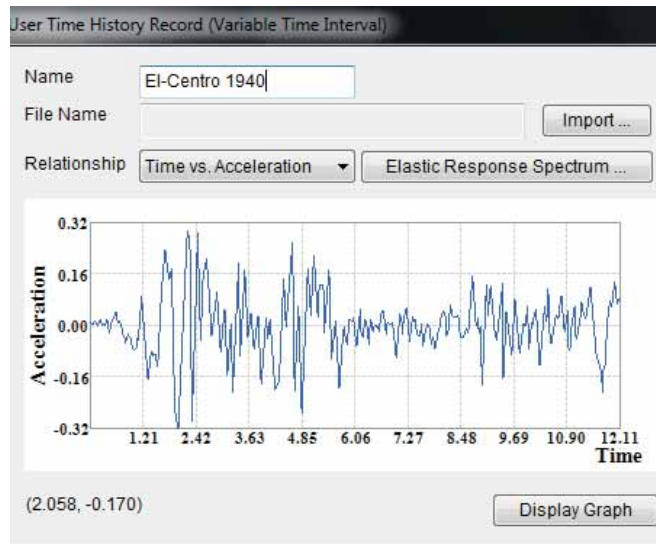


Figure 10 Defining a Time History Function in NIDA

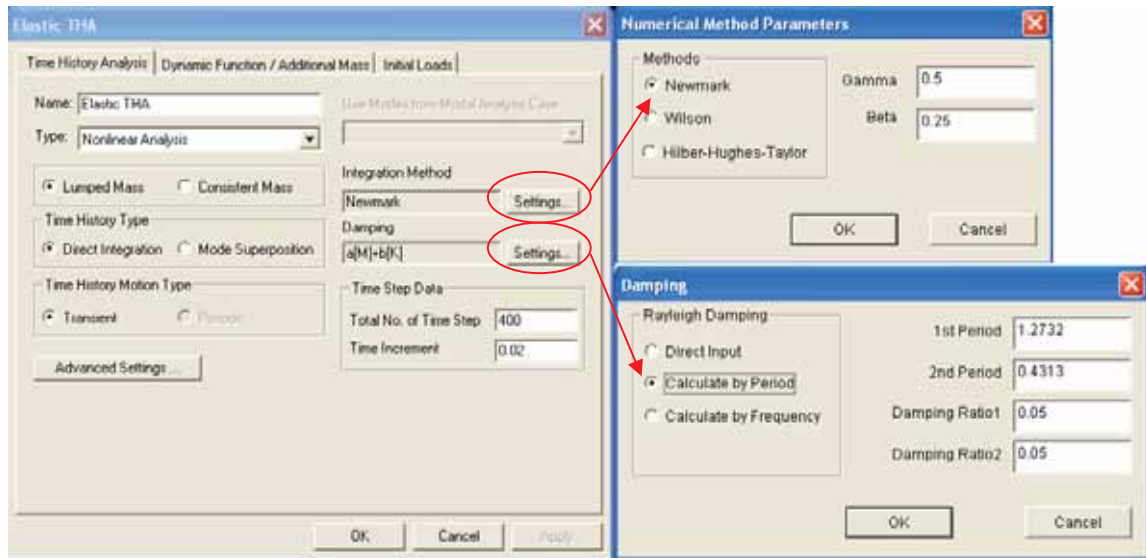


Figure 11 Define a Time History Analysis Case in NIDA

Step 4: Define the initial static loads. Besides the earthquake action, other actions such as dead loads and live loads should be taken into account. Notably, NIDA (2010) allows for initial member and frame imperfection before applying static loads.

Step 5: View the results and check the structural adequacy after completing the analysis. The member capacity has been checked at each time step in NIDA (2010). User needs to check the maximum story and building drift as well as other output indicating the structural adequacy during the time duration.

The base shear F_x , the displacement U_x of Node 24 calculated from NIDA (2010) are shown in Figures 12 and 13 respectively against those results from SAP2000 (2009). For easy comparison, the plastic behaviour does not taken into account in the two sets of results. Also, as SAP2000 (2009) does not consider initial imperfections which will also be ignored in this example so that the comparison between NIDA (2010) and SAP2000 (2009) could be on the same basis. From Figures 12 and 13, it can be seen that the results from NIDA (2010) agree well with those from SAP2000 (2009) at every time step in the elastic time response analysis.

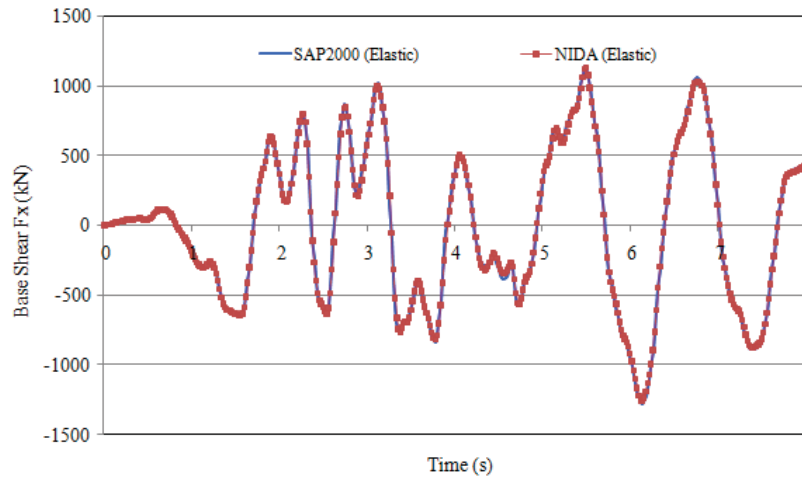


Figure 12 Comparison of Base Shear (Elastic THA)

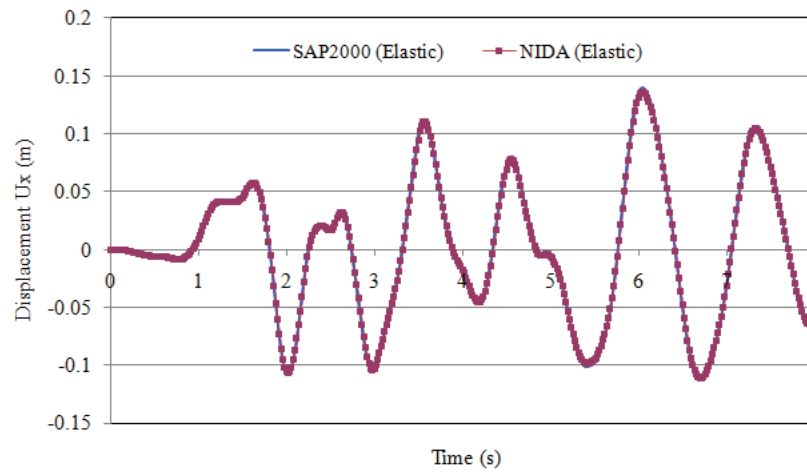


Figure 13 Comparison of Building Drift (Elastic THA)

Further, the inelastic time history analysis is performed by NIDA (2010) for this example. The plastic hinge model presented in Section 3 will be used here to capture the plastic behaviour of the beam-column elements.

Before activating the inelastic time history analysis, the PGA of El Centro 1994 is scaled to 2.0 times for easy observation of plastic hinges. The base shear F_x and the displacement U_x of Node 24 calculated from NIDA (2010) are shown in Figures 14 and 15 respectively against those results from SAP2000 (2009). From the Figures, it can be seen that NIDA (2010) can produce the same trend as SAP2000 (2009) with slight difference in some time steps. The maximum base shear and displacement responses over the entire time histories are almost the same. The discrepancy between two sets of results is due to the difference in their plastic hinge models. In this paper, the progressive cross-section yielding is captured by Eq. (4) while SAP2000 (2009) does not clearly show the tracing procedure for this effect.

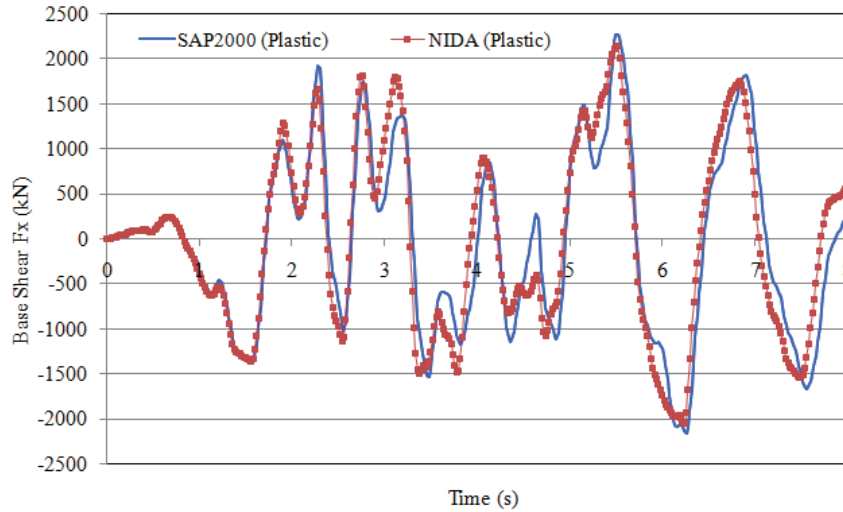


Figure 14 Comparison of Base Shear (Elastic & Plastic)

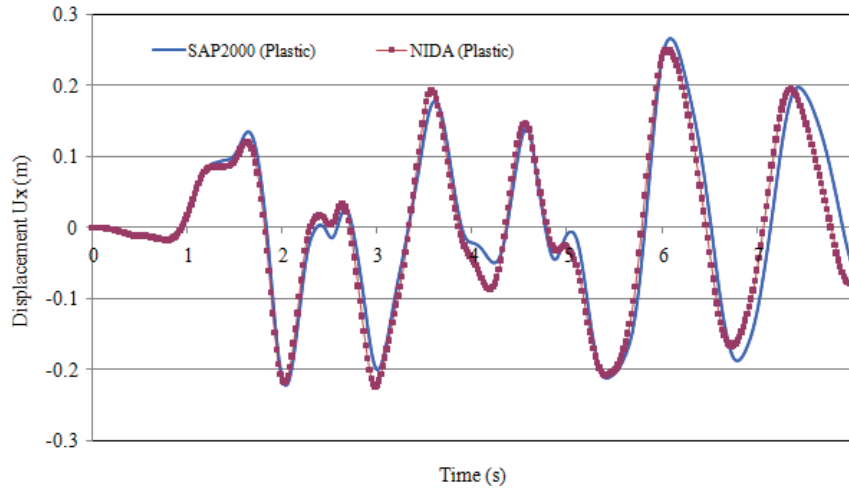


Figure 15 Comparison of Building Drift (Elastic & Plastic)

Figure 16 shows the moment-rotation curve of one of plastic hinges (marked in black point) formed in the beam during the earthquake analysis. Under the cyclic seismic action, the indicated end of the beam undergoes loading, unloading and reloading status. When the plastic hinge is formed and the bending moment is close to the plastic moment, the stiffness of the section spring is close to zero. When the plastic hinge is in the unloading status, the stiffness is recovered and the section becomes elastic. Figure 16 also shows the sequential cross-section yielding response.

This example shows that the proposed second-order plastic analysis method provides high accuracy in both static and seismic design in a consistent manner.

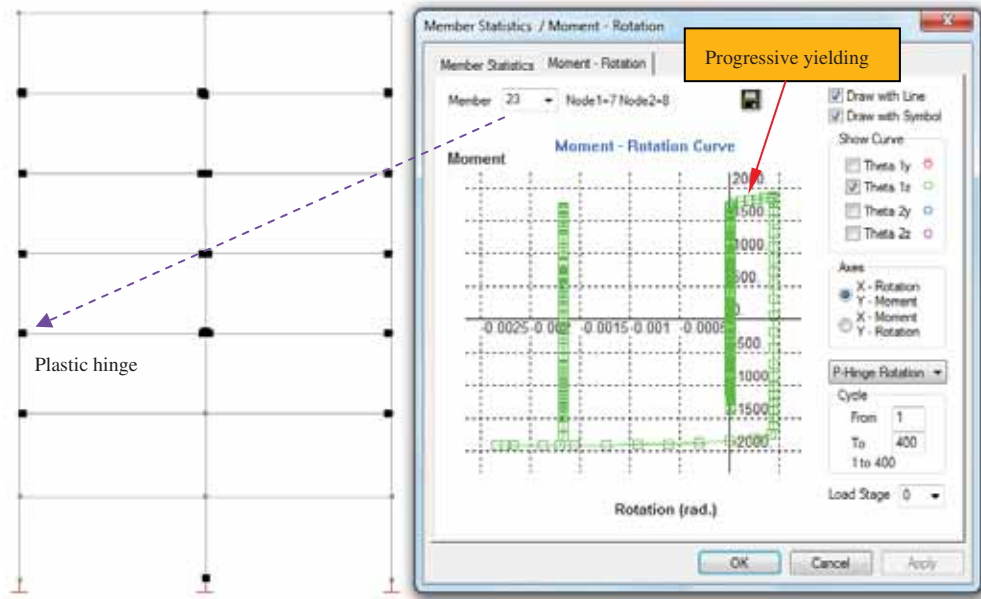


Figure 16 Moment-Rotation Curve of One Plastic Hinge

5.3 Four-Story 3D Steel Frame

The four-story 3D steel frame shown in Figure 17 is studied here for demonstration of the influence of irregular layout in plan and in elevation under earthquake attack. The geometry, section sizes and material properties are shown in Figure 17.

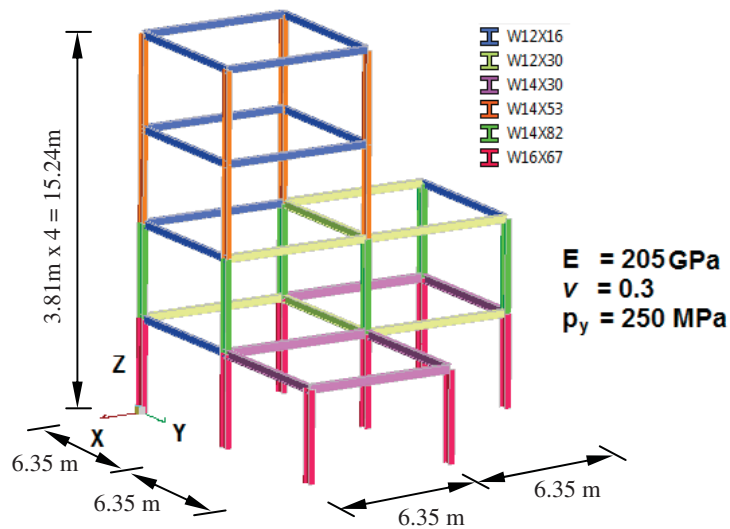


Figure 17 Four-Story 3D Steel Frame

For simplicity, the static loads on steel frame are assumed to be self weight (SW), dead loads (DL) of 2 kPa and live loads (LL) of 2 kPa at each floor. According to GB50011 (2010), only half of the live loads need to be considered in the seismic case, i.e., $1.0(SW+DL) + 0.5LL$. Similarly, the masses of the structural system are taken from $1.0(SW+DL) + 0.5LL$.

There are four earthquake records used as ground motion input, i.e., the El-Centro 1940, the San Fernando 1971, the Loma Prieta 1989 and the Northridge 1994, seen Figure 18. According to GB50011 (2010), the seismic fortification intensity of Hong Kong is 7 (0.15g), and the seismic design group is 1. The corresponding maximum acceleration under rare earthquake for time history analysis is 310 cm/s^2 . Thus, the PGAs of the four earthquake records will be scaled to 310 cm/s^2 with scale factors of 0.9072, 0.2938, 0.7932 and 0.6158 respectively. The earthquake direction is global X-axis.

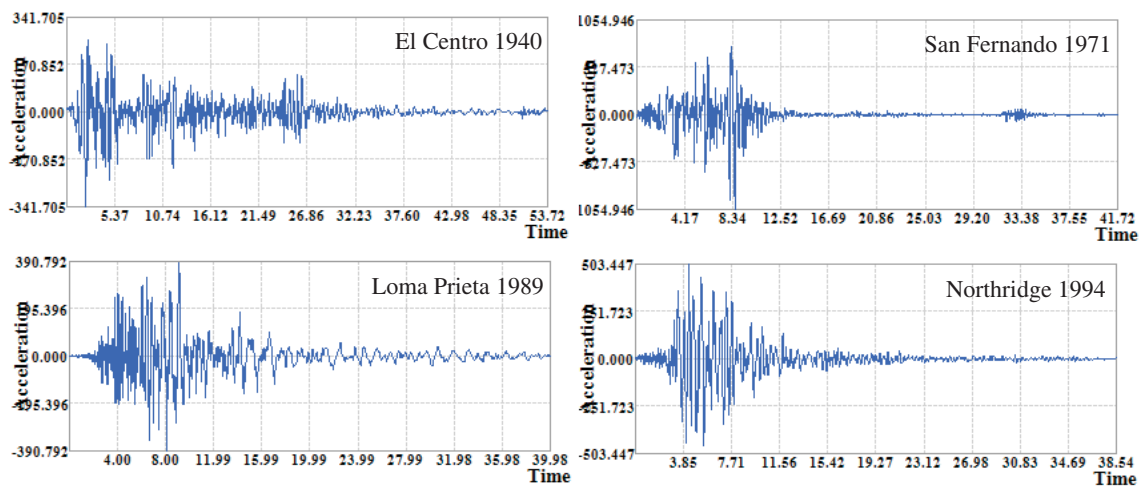


Figure 18 Four Earthquake Records (Acceleration vs. Time)

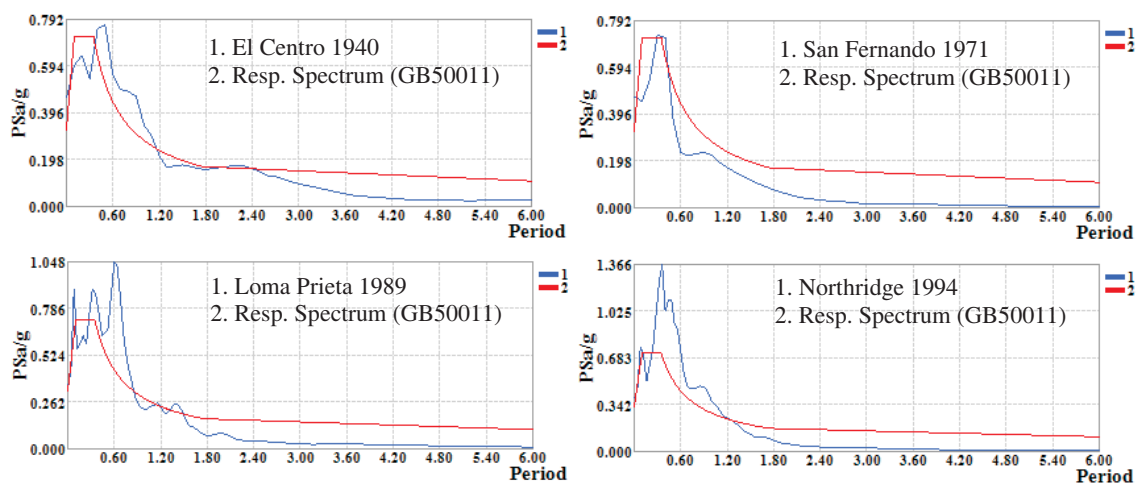


Figure 19 Elastic Acceleration Response Spectrum Curves

The elastic acceleration response spectrum curves of the four earthquakes are shown in Figure 19 compared with those from GB50011 (2010) with the maximum spectral acceleration of 0.72g and the damping ratio of 0.05.

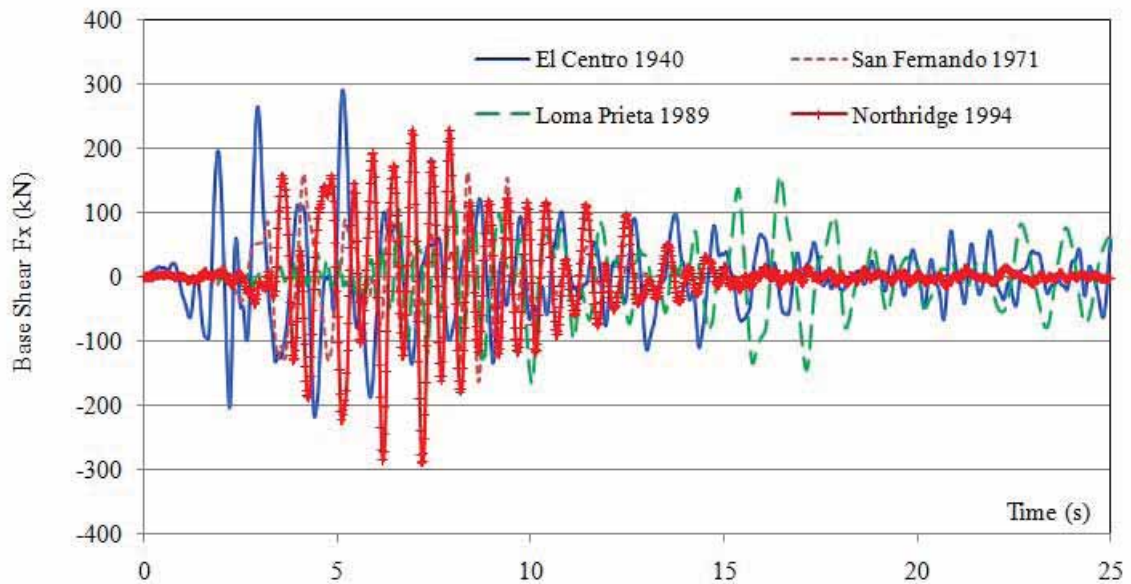


Figure 20 Comparison of Base Shear under Four Earthquakes

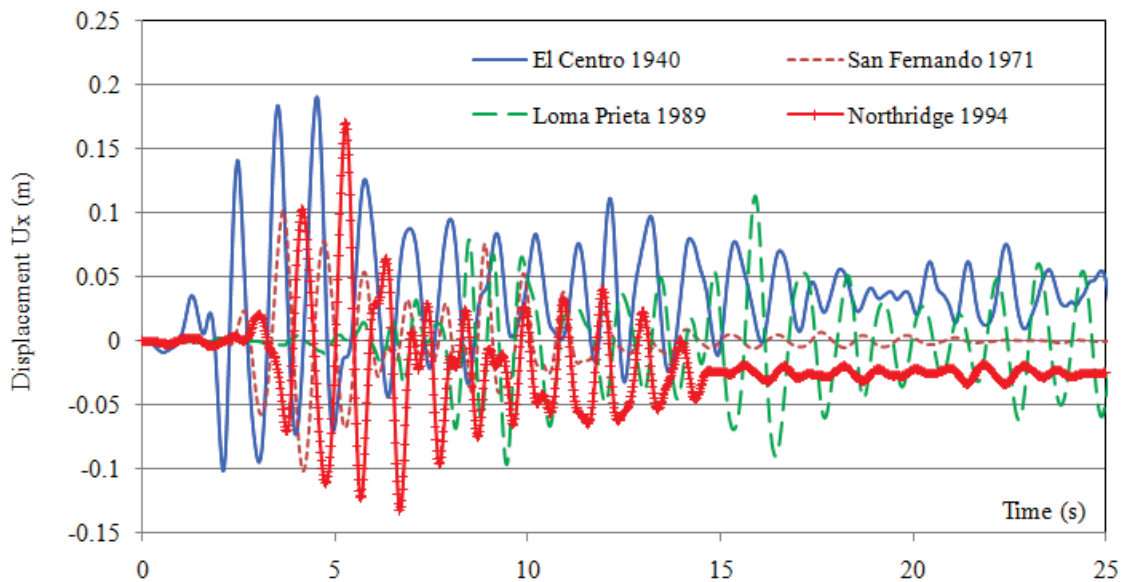


Figure 21 Comparison of Building Drift under Four Earthquakes

The base shear F_x and the displacement U_x at the roof level calculated from NIDA (2010) are shown in Figures 20 and 21 respectively. From the Figures, it can be seen that the El Centro 1940 and the Northridge 1994 will cause larger responses to the steel frame. The maximum base shear is about 300 kN both for the El Centro 1940

and the Northridge 1994 while the maximum base shear is about 160 kN both for the San Fernando 1971 and the Loma Prieta 1989. The maximum displacements U_x at the roof level are 0.190 m, 0.102 m, 0.114 m and 0.171 m for the El Centro 1940, the San Fernando 1971, the Loma Prieta 1989 and the Northridge 1994 respectively.

The plastic hinges formed in the steel structure under the four earthquakes are shown in Figure 22. It is clearly shown that many plastic hinges are formed in the beams and columns of the frame when subjected to the El Centro 1940 and the Northridge 1994 while only two plastic hinges are formed for the San Fernando 1971 and the Loma Prieta 1989. As the steel is a high ductility material with good elongation property, the structure does not collapse under each of these earthquake events. This example also shows that the irregular layout will cause severe damage to many components of the structure with corner members loaded to inelastic range.

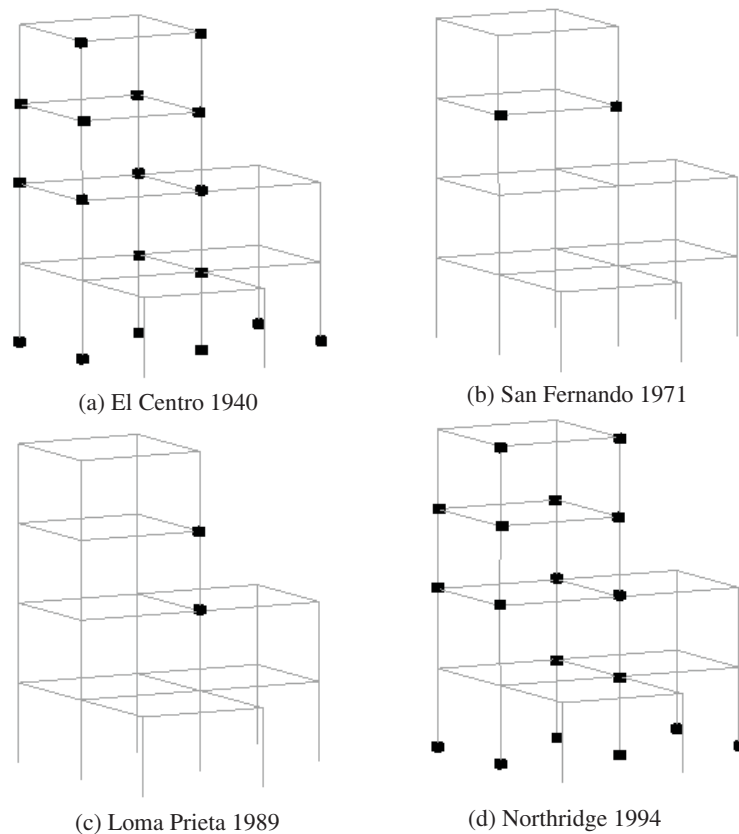


Figure 22 Plastic Hinges Formed during Four Earthquakes

Using only the elastic response spectrum analysis in Figure 19, the Loma Prieta 1989 and the Northridge 1994 will cause larger responses to the structure. However, the results of the time history analysis do not fully agree with this because yielding alter significantly the response of the structure. In other words, the response spectrum analysis without consideration of inelastic behavior and time duration cannot always give “best” estimate of the structural response.

6. CONCLUSIONS

In this paper, the basic theoretical framework of second-order analysis for conventional and seismic structural design is briefly introduced and this method has been extended to performance-based static and seismic design with the consideration of frame and member buckling and material yielding by plastic hinge approach. The application of the method covers a wide range of structural forms like steel, steel-concrete composite, slender trusses dominated by buckling, reinforced concrete frames controlled by material crushing and a variety of loading scenarios like statics and seismic load cases. It can also be used for investigation of un-conventional scenarios like progressive collapse due to local failure in a frame or accidental removal or damage of some members and structural stability under fire. As the second-order analysis attempts to model the true structural behavior, it is less restrictive to the effective length method which is based on elastic buckling at undeformed geometry. Finally, engineers should be very cautious on use of appropriate software as many important parameters like modeling of member initial crookedness by curved element and use of buckling modes as imperfection modes are not considered by many structural analysis programs, which are then inconsistently used in nonlinear time-history analysis but not in conventional linear analysis and design for member sizing.

ACKNOWLEDGEMENTS

The authors acknowledge the supports of the Research Grant Council of the Hong Kong Government on the project "Advanced Analysis Allowing for Load and Construction Sequences" funded jointly by Construction Industry Institute-Hong Kong (CII-HK) and The Hong Kong Polytechnic University and "Advanced Analysis for Progressive Collapse and Robustness Design of Steel Structures (PolyU 5115/07E)".

REFERENCES

1. Chan, S. L. and Gu, J. X. (2000). "Exact tangent stiffness for imperfect beam-column members." *Journal of Structural Engineering-ASCE* **126**(9): 1094-1102.
2. Chan, S. L., Liu, S. W. and Liu, Y. P. (2010). "Advanced Analysis of Hybrid Frame Structures By Refined Plastic-Hinge Approach." *Proceedings of 4th International Conference on Steel & Composite Structures, Sydney, Australia: 21-23 July 2010.*
3. ECCS (1983). "Ultimate Limit State Calculation of Sway Frames with Rigid Joints." *European Convention for Constructional Steelwork, Technical Working Group 8.2, Systems, Publication No. 33.*
4. Eurocode3 (2005). "EN 1993-1-1: Design of steel structures - General rules and rules for buildings." *European Committee for Standardization.*

5. GB50011 (2010). "Code for seismic design of buildings." Ministry of Construction P.R. China.
6. HKSC (2005). "Code of Practice for the Structural Use of Steel 2005." Buildings Department, Hong Kong SAR Government.
7. Liu, S. W., Liu, Y. P. and Chan, S. L. (2010). "Pushover Analysis by One Element Per Member for Performance-Based Seismic Design." *International Journal of Structural Stability and Dynamics* **10**(1): 111-126.
8. Liu, Y. P. and Chan, S. L. (2009). "Nonlinear Analysis and Design of Wall-framed Structures." *Steel Concrete Composite and Hybrid Structures*: 675-681.
9. Newmark, N. M. (1959). "A Method of Computation for Structural Dynamics." *ASCE Journal of the Engineering Mechanics Division* **85**: 67-94.
10. NIDA (2010). "User's Manual, Nonlinear Integrated Design and Analysis." NIDA 8.0 HTML Online Documentation. (<http://www.nida-naf.com>).
11. SAP2000 (2009). "CSI Analysis Reference Manual for SAP2000, ETABS and SAFE." Computers and Structures, Inc., Berkeley, California, USA
12. Savory, E., Parke, G. A. R., Zeinoddini, M., Toy, N. and Disney, P. (2001). "Modelling of tornado and microburst-induced wind loading and failure of a lattice transmission tower." *Engineering Structures* **23**(4): 365-375.
13. Vogel, U. (1985). "Calibrating frames." *Stahlbau* 54(October): 295-311.

SEISMIC STRENGTHENING OF REINFORCED CONCRETE STRUCTURES

S.S.E. Lam¹, Y.L. Wong¹, M.Z. Zhang², C.S. Li³, B. Wu⁴, A. Chen⁵, Z.D. Yang⁶, Y.Y. Wang⁷, F.Y.I. Ho⁶ and B. Li⁶

(in the order of appearance in the paper)

¹*Associate Professor, Department of Civil and Structural Engineering, The Hong Kong Polytechnic University, Hong Kong*

²*Professor, Institute of Engineering Mechanics, China Seismological Bureau, Harbin, China*

³*PhD, Ove Arup and Partners Hong Kong Limited*

⁴*Professor, School of Architectural and Civil Engineering, South China University of Technology, Guangzhou, China*

⁵*Professor, Department of Civil and Environmental Engineering, West Virginia University*

⁶*PhD student, Department of Civil and Structural Engineering, The Hong Kong Polytechnic University, Hong Kong*

⁷*Professor, China Academy of Building Research, Beijing, China*
E-mail (first author): cessleram@polyu.edu.hk

ABSTRACT

Seismic hazard in Hong Kong has traditionally been considered as low. As a result, buildings in Hong Kong have been designed with no seismic provisions. However, recent studies have consistently indicated that Hong Kong is a region with moderate seismic risk. There is a need to strengthen the existing structures in Hong Kong for proper seismic resistance. This paper outlines various practical approaches to assess or qualify (if not quantify) the seismic resistance of buildings through shaking table tests, pseudo-dynamic tests and numerical analysis. Various means to mitigate the seismic risk are demonstrated including the use of damping devices and base isolators to improve the performance of adjacent buildings in a building group and the use of high performance ferrocement to strengthen the structural members.

1. INTRODUCTION

Although the nearest active tectonic plate boundaries is relatively far away from Hong Kong, Hong Kong has experienced moderate earthquake as far back as 1874 and 1918 when it was a small village at that time. Probably due to historical perception that no serious damage has ever been caused by earthquakes, structures in Hong Kong can be designed without any seismic provisions (Lam et al 2002). However, studies by the Geotechnical Control Office (1991) of the Hong Kong Government, Pun and Ambrassey (1992), Scott et al (1994), Lee et al (1996) and Wong et al (1998a, 1998b) have consistently indicated that Hong Kong is an area with moderate seismic risk. According to the “Seismic Ground Motion Parameter Zonation Map of China” (GB 18306-2001), the recommended peak ground acceleration of Hong Kong with a return period of 475 years is 0.15g on rock site. As a major financial centre and one of the densely populated cities, interruption to critical facilities and business operations in Hong Kong may have serious social and economical consequences. Among others, Chan et al (1998), Kuang and Wong (2002), Pam et al (2002), Lam et al (2003) and Su (2008) have indicated seismic deficiency in the existing structures due to non-seismic detailing. There is a need to strengthen the existing structures in Hong Kong for proper seismic resistance.

This paper outlines various practical approaches to assess the seismic resistance of buildings through shaking table tests, pseudo-dynamic tests and numerical analysis. Further, means to mitigate the seismic risk are demonstrated including the use of damping devices and base isolators to improve the performance of adjacent buildings in a building group and the use of high performance ferrocement to strengthen the structural members.

2. SEISMIC PERFORMANCE OF BUILDINGS

Most of the buildings in Hong Kong are reinforced concrete structures and can be grossly separated into three main groups. The first group comprises high-rise buildings (constructed in or after the 80s and 90s), e.g. over 30 stories. The second group includes mid-rise buildings with 10 to 12 stories, e.g. buildings once subject to the height limit of the old Kai Tak Airport. The last group is consisted of low-rise 3-story blocks, the so-called “New Territories Exempted Buildings” with structural details specified in Cap 121. Typical structural systems of high-rise and mid-rise buildings comprise coupled shear walls with transfer systems at lower stories whereas low-rise buildings are frame structures. In general, structural layouts of buildings in Hong Kong are asymmetric and incorporate transfer system. These are undesirable and cause the structure vulnerable to earthquake. It is necessary to assess structural performance of buildings, for example, by tests and numerical analysis. The following are some examples relevant Hong Kong.

2.1 *Asymmetric structures*

It is necessary to reduce the torsional effect and asymmetric structural layout has to be avoided as much as possible. Dai et al (2000) examined the torsional effect of a 9-story asymmetric building model. The model represents a reinforced concrete frame in 1/6 scale. The model was tested on a shaking table under different levels of earthquake action. It has been shown that torsional effect is more destructive when the building is damaged. Dai (2002) conducted shaking table tests on three 1/3 scale single-story reinforced concrete building models (see Figure 1). The models were designed according to the local code without seismic provisions. Due to the presence of asymmetric structural layout, torsion is introduced making the structure vulnerable to seismic action.



Figure 1: Asymmetric building model



Figure 2: 1/20-scale building model

2.2 *Transfer plate system*

A transfer plate system may cause abrupt change in the lateral stiffness at the transfer, e.g. from a stiffer shear wall system above to a relatively flexible column-girder system below. This creates a soft (or weak) story and violates the seismic design concept of “strong column weak beam” (Aoyama 2001) or concept of capacity design (Paulay and Priestley 1992).

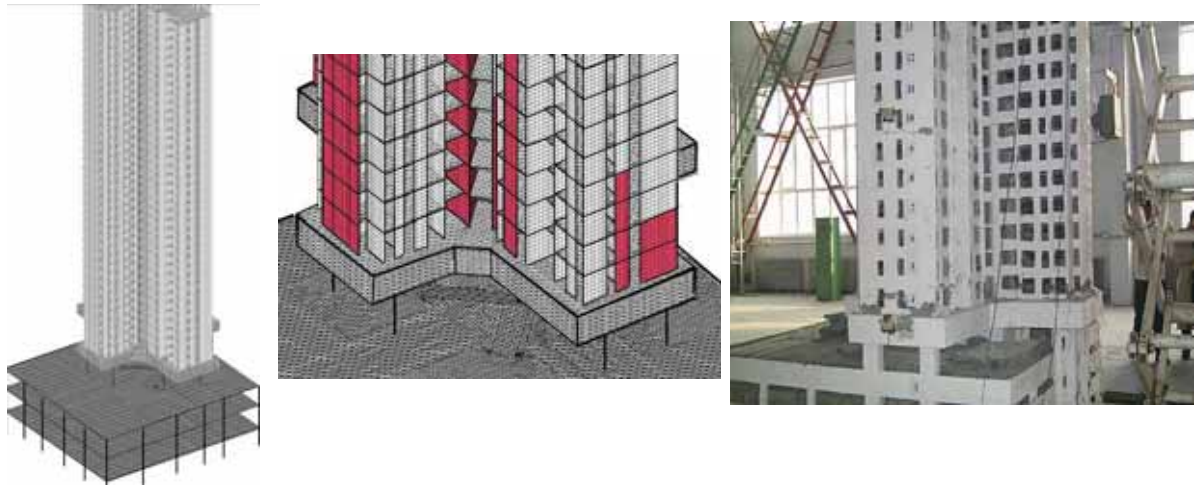


Figure 3: Numerical model (left), damage (in red) predicted by the model (center) and damage observed from the shaking table tests (right)

Li et al (2006) performed shaking table tests on a 1/20 scale reinforced concrete building model (see Figure 2). The model represents a reinforced concrete building with 34 typical floors supported by a 2.7m thick transfer plate sitting over a 3-level podium. The high-rise building model appeared to have sufficient strength in resisting a strong earthquake action that could be encountered in Hong Kong. Simulations were conducted using numerical models (see Figure 3) to identify the extent and locations of damage.

Pseudo-dynamic tests with substructure techniques were conducted by Li et al (2008). Figure 4 shows the 1/4 scale test specimen representing the first 2 stories of an 18-story high-rise building with a transfer plate to simulate the earthquake action. Performance of upper stories was simulated numerically while conducting the tests. Columns of the test specimen were strengthened to prevent failure under the pseudo-dynamic tests. Three types of time-history records were applied, including triangular waves and El-Centro earthquake record. Finite element model was developed using a commercial package, ABAQUS version 6.3.1, to verify the experimental results obtained from the pseudo-dynamic tests, see Figure 5. Based on the experimental results, it is concluded that the transfer plate may have sufficient strength to resist possible earthquake action that could be expected in a moderate seismic region, i.e. 16% g of the El-Centro earthquake record. However, there is insufficient seismic resistance if maximum acceleration of the El-Centro earthquake record is greater than 32% g. The above is subject to the condition that the columns do not collapse at all levels of earthquake action.

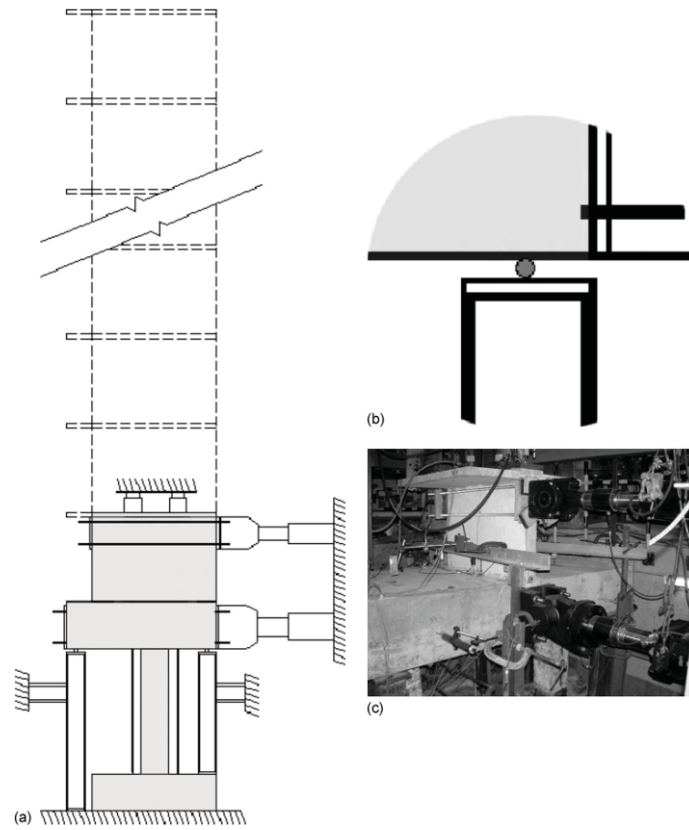


Figure 4: Experimental setup: (a) numerical simulation (in dotted line) and the test specimen; (b) details of a roller at the corner of transfer plate; and (c) the test specimen.

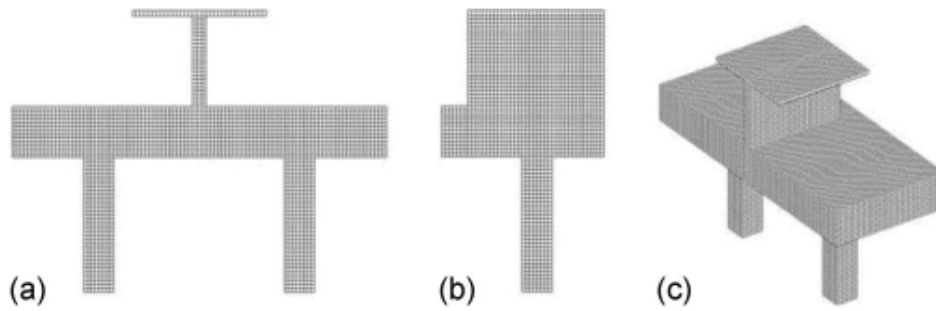


Figure 5: Finite-element model using ABAQUS.

3. BASE ISOLATORS

As land is limited in Hong Kong, many mid-rise buildings are erected next to each other without having any separation. Due to aging problems of existing buildings, there is a genuine need for redevelopment. However, it is very difficult and almost impossible to redevelop a group of buildings at the same time (Lam 2009). It is usually commenced with redevelopment of one building within a building group. Even so, existing buildings adjacent to the new building could be “protected” by designing the new building to mitigate the adverse effect due to earthquake action.

Specifically, the new building is equipped with base-isolators and connected to the existing buildings by inter-building dampers. To verify the above, numerical studies were carried out using simplified two-dimensional models.

Dynamic responses of adjacent buildings joined by energy dissipating devices, including hinged links (Westermo 1989) and dampers, were investigated (e.g. Chau and Wei 2001). Active and semi-active control devices were proposed to couple the adjacent buildings in order to reduce the dynamic response (Seto 1994, Yamada et al 1994, Christenson et al 2007). For instance, Kim et al (2006) used visco-elastic dampers to connect 2 or 3 structures together. Bhaskararao and Jangid (2006) studied the seismic responses of two adjacent structures connected with friction dampers. Xu et al (1999) used fluid dampers to connect the adjacent buildings. Efficiency of the dampers is affected by the ratio of shear stiffness of adjacent buildings and it is desirable to increase the ratio of shear stiffness as much as possible. Matsagar and Jangid (2005) recommended the use of base isolators for providing large ratio of shear stiffness and verified using dampers to connect a 4-storey fixed-base building to a neighbor 4-storey base-isolated building. Based on the above, we suggest to install dampers between the adjacent buildings and base-isolators to the new building.

3.1 Structural configuration of the building group and analytical model

Figure 6(a) shows the building group. It comprises three 12-story frames of 36 m height, namely an existing left frame with fixed base, an existing right frame with fixed base (collectively “the side frames”), and a new middle frame with base isolators. Left frame and right frame are 30 m by 30 m on plan and with same structural arrangement. The middle frame is 30 m by 18 m on plan. The frames are connected by visco-elastic dampers at each and every floor. Grade C30 concrete is assumed and Modulus of Elasticity is 30.0 kN/mm². Floor systems use traditional beam-slab construction with 200 mm thick two-way slabs. Columns are 0.75 m × 0.75 m and beams are 0.6 m × 0.6 m. Total masses of the left frame, the middle frame and the right frame are 14,036 ton, 11,959 ton and 14,036 ton respectively.

Two types of base isolators are installed in the middle frame including: plain roller bearings and lead rubber bearings. For plain roller bearings, coefficient of friction is around 0.003. Their effect on and contribution to the restoring force is ignored in the analysis (Fujitani and Saito 2006). Bilinear model is used to simulate the response of lead rubber bearings. Properties of the lead rubber bearings are defined by 3 parameters (in terms of total contributions per frame): yield force $f_y=2.5648$ MN, shear stiffness $k_1=199.2$ MN/m when elastic and $k_2=19.9$ MN/m in post-yield region. Visco-elastic dampers are used as the inter-building connectors. Dampers are modeled by linear springs and linear dashpots acting in parallel. Properties of the dampers are to be determined in the analysis that follows.

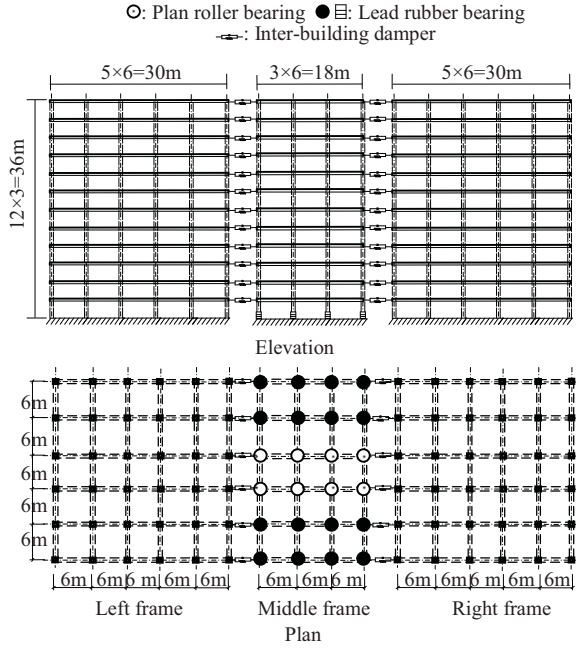


Figure 6(a): Elevation and floor plan.

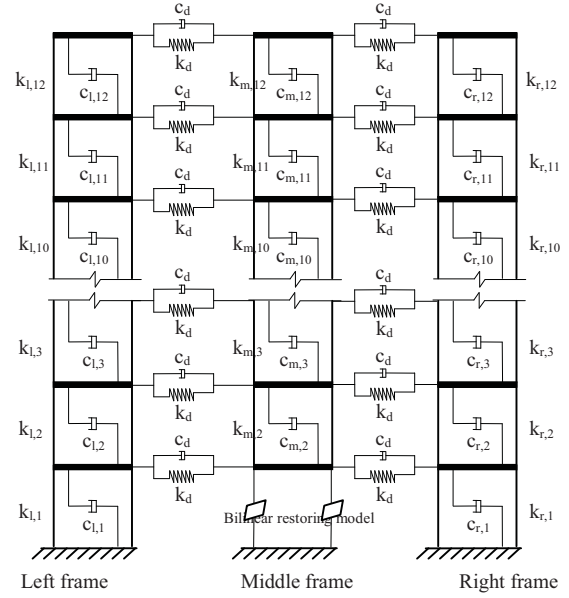


Figure 6(b): Simplified analytical model.

Ground motion is assumed to be acting in the direction along the frames such that the model is simplified to a two dimensional problem. In the analysis, frames are assumed to behave linear elastic throughout the loading history. Simplified shear model is used to represent each frame. In the model, masses are assumed to be lumped at each floor level. Lateral stiffness of each frame is calculated by the D-value method (Cheng et al 2003).

3.2 Equations of motion

Equations of motion of the structural system as shown in Figure 6(b) are developed based on a two-dimensional formulation (Chopra 2006) in the form of

$$M\ddot{X} + C\dot{X} + KX + R_u = -M\mathbf{I}a \quad (1)$$

\mathbf{M} , \mathbf{C} and \mathbf{K} are the respective mass matrix, damping matrix, and stiffness matrix of the system. Rayleigh damping is assumed with damping ratios of the first and second modes both at 0.03. \mathbf{R}_u is a vector representing the nonlinear restoring force of the lead rubber bearings. X , \dot{X} and \ddot{X} are the respective system vector for displacement, velocity and acceleration relative to the ground. \mathbf{I} and \mathbf{a} are unit vector and ground acceleration vector respectively. Equation (1) is rewritten in incremental form and solved numerically so as to obtain the response at any time t using the Newmark- β method.

3.3 Parametric studies

Three earthquake records are considered: TAF021 component of Kern County 1952 earthquake, I-ELC180 component of Imperial Valley 1940 earthquake and HOL090 component of Northridge 1994 earthquake. Peak ground accelerations of the earthquake records are scaled to 4 m/s^2 representing rarely occurred earthquakes. Considering the nonlinear properties of the base isolators, small time interval is used at 1000 time steps per earthquake reading. For Taft earthquake and El Centro earthquake (at 100 readings per second), time step $\Delta t = 0.01/1000 = 1 \times 10^{-5} \text{ s}$, and for Northridge earthquake (at 50 readings per second), time step $\Delta t = 0.02/1000 = 2 \times 10^{-5} \text{ s}$.

Figure 7 shows variation of maximum displacement and maximum base shear of the side frames excited by Taft earthquake against stiffness of inter-building dampers at different damping of inter-building dampers.

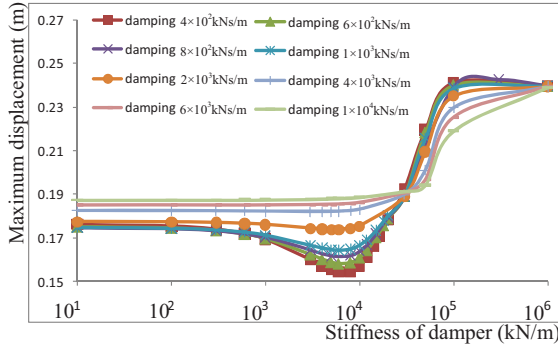


Figure 7(a): Maximum displacement of the side frames against stiffness of dampers

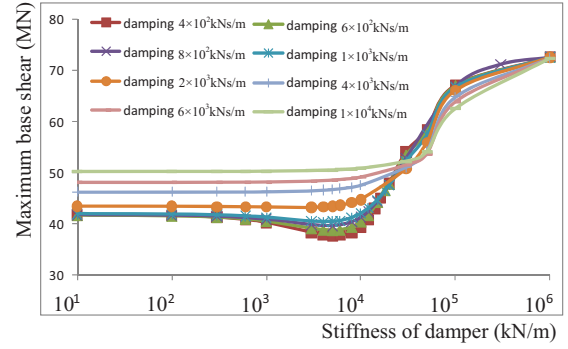


Figure 7(b): Maximum base shear of the side frames against stiffness of dampers

- (1) Case of damping larger than critical damping $c_{critical} = 2 \times 10^3 \text{ kNs/m}$: If the stiffness of dampers is larger than $5 \times 10^4 \text{ kN/m}$, increasing the stiffness of dampers significantly increases maximum displacement and maximum base shear of the side frames.
- (2) Case of damping less than or equal to critical damping $c_{critical} = 2 \times 10^3 \text{ kNs/m}$: If the stiffness of dampers is larger than $1 \times 10^3 \text{ kN/m}$, increasing the stiffness of dampers decreases maximum displacement and maximum base shear. Further increasing the stiffness of dampers to above $6 \times 10^3 \text{ kN/m}$ increases maximum displacement and maximum base shear significantly.
- (3) Maximum displacement and maximum acceleration occur at the top floor whereas maximum drift occurs at the second floor.

In general, the above also applies to maximum drift and maximum acceleration. Based on the above, optimum stiffness k_{taft} of dampers is $6 \times 10^3 \text{ kN/m}$. In the same

way of estimating the critical damping and optimum stiffness of dampers for Taft earthquake, critical damping and optimum stiffness of dampers when subjected to different earthquakes can be estimated. Table 1 summarizes the optimum stiffness of dampers for different earthquakes.

Table 1: Optimum stiffness for different earthquakes

Earthquake	Optimum stiffness (kN/m)
Taft	6×10^3
El Centro	1×10^4
Northridge	5×10^3

Optimum stiffness of dampers applicable to all earthquakes can be estimated by taking the average of the three optimum values as given in Table 1, i.e. 7×10^3 kN/m. When the stiffness of dampers is 7×10^3 kN/m, variation of maximum displacement and maximum base shear of the side frames against damping of dampers are shown in Figure 8. The optimum damping coefficient is recommended to be in the range of 5×10^2 kNs/m to 7×10^2 kNs/m.

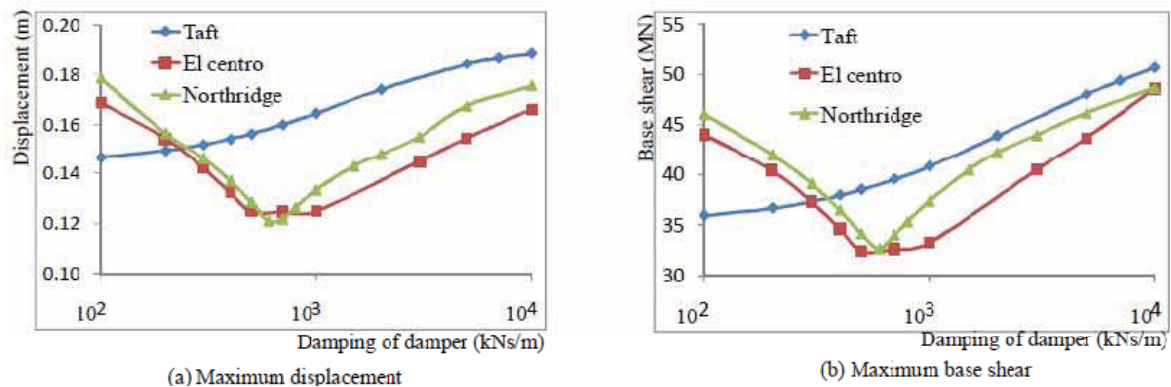


Figure 8: Maximum response of the side frames against damping of damper.

3.4 Comparison of base condition

Responses of the frames without dampers and with fixed bases are given in Table 2, as case (A). The responses are compared with the new building group (with stiffness and damping of dampers at 7×10^3 kN/m and 6×10^2 kNs/m respectively), as case (B). Maximum displacement, maximum base shear, maximum drift and maximum acceleration of the side frames are reduced by around 29% to 46%, 9% to 40%, 17% to 42% and 13% to 38% respectively (Table 3).

Relative displacements between the left frame and the center frame are computed and the maximum values are given in Table 4. In the absence of inter-building dampers and base isolators (case (A) in Table 4), pounding will occur between the frames (for example, when subjected to Taft earthquake or El Centro Earthquake).

Table 2: Comparison of middle frame's response

		(A) Without damper	(B) New building group	(B)/(A)
Maximum base shear (MN)	Taft	27.92	5.97	21.4%
	El Centro	35.26	5.95	16.9%
	Northridge	27.32	6.02	22.0%
Maximum drift (m)	Taft	0.0291	0.0072	24.9%
	El Centro	0.0224	0.0078	34.6%
	Northridge	0.0328	0.0083	25.4%
Maximum acceleration (m/s^2)	Taft	7.38	6.33	85.8%
	El Centro	7.65	6.41	83.8%
	Northridge	6.84	5.98	87.4%

Table 3: Comparison of side frame's response

		(A) Without damper	(B) New building group	(B)/(A)
Maximum displacement (mm)	Taft	225	158	70.3%
	El Centro	235	125	53.2%
	Northridge	175	121	69.1%
Maximum base shear (MN)	Taft	42.97	39.05	90.9%
	El Centro	54.33	32.37	59.6%
	Northridge	42.09	32.65	77.6%
Maximum drift (m)	Taft	0.0248	0.0206	83.0%
	El Centro	0.0294	0.0168	57.1%
	Northridge	0.0226	0.0171	75.6%
Maximum acceleration (m/s^2)	Taft	10.92	6.75	61.9%
	El Centro	8.11	7.01	86.5%
	Northridge	8.90	7.17	80.6%

Table 4: Maximum relative displacements between the side frames and center frame

Earthquake	(A) Without damper (mm)	(B) New building group (mm)
Taft	324.4	150.7
El Centro	265.2	128.6
Northridge	184.3	198.9

4. STRENGTHENING OF REINFORCED CONCRETE MEMBERS BY FERROCEMENT

On the subject of strengthening reinforced concrete members, many methods have been proposed including, inter alia, steel and concrete jacketing (Ersoy et al 1993); pre-stressed concrete jacketing (Bracci et al 1995); steel/FRP jacketing (Wu et al 2006); and CFRP jacketing (Harries et al 2006). When applied to buildings, fire rating has always been a concern making it less desirable to implement the above-mentioned methods (e.g., Han et al 2006, Tadeu and Branco 2000). As viable alternative,

ferrocement has good fire resistance compatible to concrete (Williamson and Fisher 1983, Kaushik et al 1996). Other advantages include ease of construction, requiring no special technique and cost effective.

Ferrocement is defined in ACI 549.1R-93 as “a form of reinforced concrete using closely spaced multiple layers of mesh and/or small-diameter rods completely infiltrated with, or encapsulated, in mortar.” It has been successfully applied as an alternative to strengthen reinforced concrete members (Shah et al 1986, Paramasivam et al 2000, Kumar and Kumar 2005) and is codified in CECS 242:2008, a technical specification in China.

High performance ferrocement (“HPF”) is a type of ferrocement with improved strength-to-weight ratio and increased tensile strength. It has been used to enhance both ductility and load carrying capacity of columns (Kondraivendhan and Pradhan 2009, Jiang et al 2009, Kim and Choi 2010). Among others, Cao et al (2007) applied high strength steel wire meshes and polymer mortar to strengthen beam-column joints.

Figures 9 and 10 show the respective sequence of strengthening a reinforced concrete column and a beam-column joint using ferrocement or HPF. In general, application of HPF comprises three consecutive steps: (a) proper preparation of surface, (b) installation of wire meshes and (c) application of rendering material. The following are the salient points:-

1. Surface of the substrate should be properly prepared to receive the rendering material. Mechanical scratching, bonding agent, abrasive blasting, shot blasting and bush hammering are some of the methods to improve roughness of the substrate. The substrate should be cleaned and free from all fine particles, dust, oil, grease, rust stains, before application of the rendering material.
2. Wire meshes should be effectively anchored to the substrate by stainless steel nails. Overlapping of wire meshes should be at least 100mm or 4 times width of mesh lattice, whichever the larger.
3. Maximum particle size of the rendering material should not be more than $\frac{1}{4}$ of the mesh lattice width. Properly prepared rendering material should be applied from top to bottom. In any event, sagging/sliding of the rendering material and/or spreading/belling out effect at the bottom (e.g. caused by self-weight of the rendering material) should be avoided.
4. Thickness of HPF should be thickness of the rendering material and the recommended tolerance should be within $\pm 10\%$ thickness of HPF.

To evaluate the mechanical properties of HPF, the following tests are recommended: (a) compressive strength of rendering material (ASTM C39/C39M), (b) static modulus of elasticity of rendering material (ASTM C469-02e1), (c) tensile strength of wire meshes (Naaman 2000), and (d) flexural strength of ferrocement prisms (Naaman 2000).

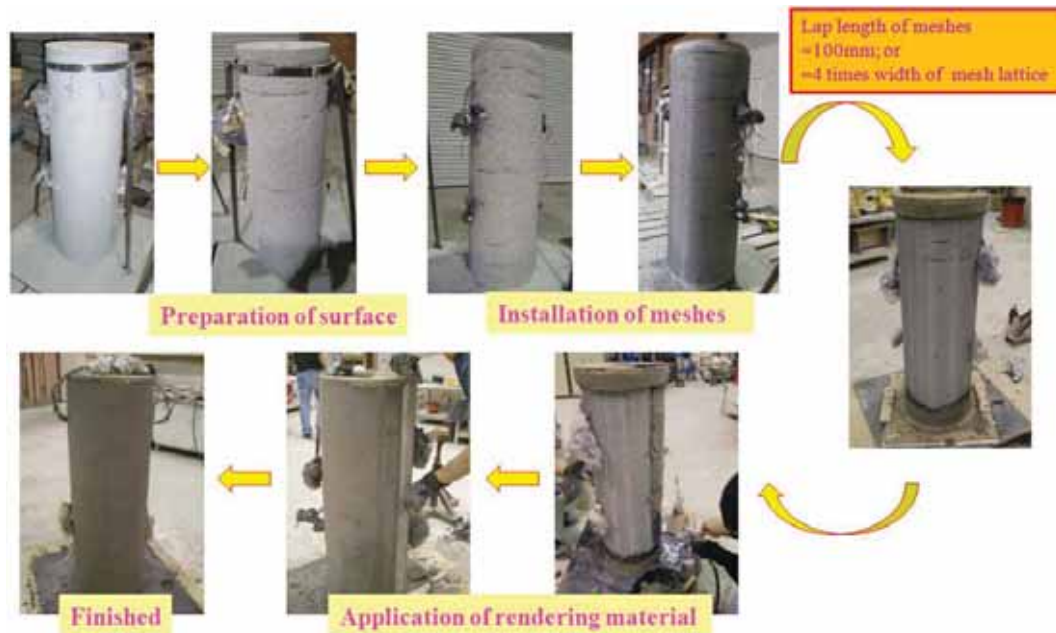


Figure 9: Sequence of HPF strengthening of columns

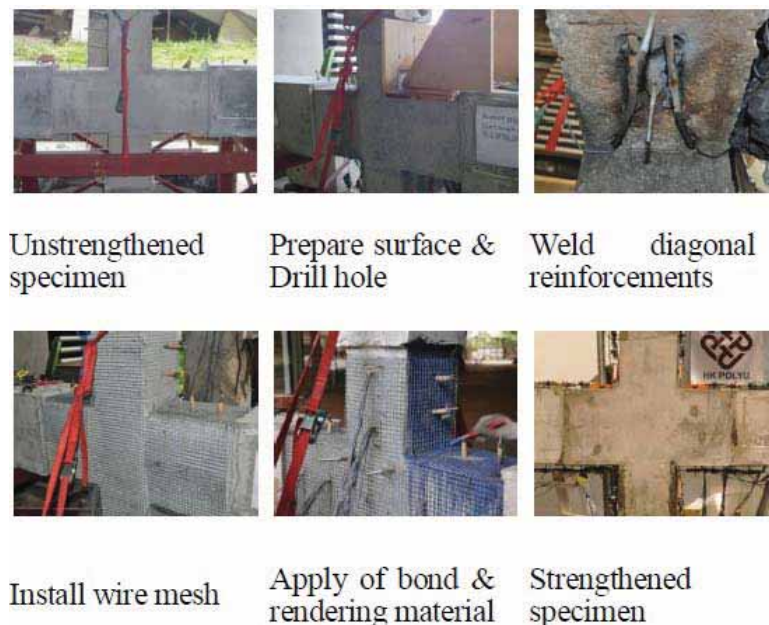


Figure 10: Sequence of HPF strengthening of beam-column joints

4.1 Strengthening of reinforced concrete columns

Columns designed according to the Code of Practice for Structural Use of Concrete 2004 (“CoP2004”) are usually detailed with high volumetric ratio of transverse

reinforcement when compared with those designed to the Code of Practice for Structural Use of Concrete 1987 (“CoP1987”). The substantial increase in volumetric ratio of transverse reinforcement is primarily due to a reduction in transverse reinforcement spacing. As a result, load carrying capacity of columns is enhanced due to confinement action (Richart et al 1928, Balmer 1949, Popovics 1973, Sheikh and Uzumeri 1980, Ahmad and Shah 1982, Mander 1983, Mander et al 1988 and Li 1994). To strengthen the columns designed to CoP1987, HPF is used to provide the necessary confinement. To relate the degree of confinement with properties of HPF, a test programme was instigated by performing compression tests on 19 full-scale specimens. The specimens are 350mm diameter and 980mm height using grade C30/20 concrete. They were tested to failure under axial compression. The test results were reported in Ho and Lam (2010), (2011).

The specimens are categorized into Group 1 and Group 2 since they were casted from two batches of concrete (Table 5). Except the two control specimens TCP1 and TCP2, all specimens are reinforced with 8T25 as main reinforcements (or 4% main reinforcement ratio). Two types of transverse reinforcement detail are considered, namely R8@75 with 135⁰ hooks to CoP2004 and R8@300 with 90⁰ hooks as per recommended by CoP1987. Volumetric ratios of transverse reinforcement (ρ_s) are 0.918% and 0.230% respectively.

6 combinations of HPF with 2 mesh densities and 3 types of rendering materials are considered. 4 parameters are studied including (i) angle of hooks, (ii) spacing of transverse reinforcement, (iii) tensile strength of rendering materials and (iv) mesh densities. Rendering materials include cement-sand screeding, polymer modified cementitious based repair mortar and epoxy based repair mortar (denoted as “CS”, “PMC” and “EM” respectively in the tables). Welded square wire mesh (having 12.6mm grids) is used. Measured values of diameter and ultimate strength of wires in the circumferential direction are 1.14 mm and 548 MPa respectively.

Table 6 lists the peak strengths P and capacity ratio R obtained by all the specimens. R is defined as peak strength divided by the peak strength of specimen type TB75 in the same group. For plain concrete specimens with HPF, R is with reference to the peak strength of plain concrete specimen TPC2. If R is larger than 1, it means that the specimen has a load carrying capacity comparable to a column designed according to CoP2004. Figure 11 shows the load-strain plots of all the specimens. The following are observed:-

1. By comparing the peak strengths of specimens TA300C-1 and TB300C, angle of hooks (i.e. 90⁰ hooks in specimen TA300C-1 versus 135⁰ hooks in specimen TB300C) does not have significant influence on the load carrying capacity. As far as axial load is considered, the use of 90⁰ hooks in lieu of 135⁰ hooks causes minor effect to the confinement action.

2. Reinforced concrete specimens (like specimen TA300SD1-2) detailed to CoP1987 and strengthened with HPF can achieve peak strength up to 23.3% higher than that achieved by reinforced concrete specimens detailed to CoP2004.
3. Improvement in peak strength of specimens T0ST1 and T0ST3 is 29.8-37.7% and of specimens T0SD1 and T0SD3 is 50.6-58.7%. Hence, epoxy based rendering material provides better confinement to enhance the compressive strength of concrete when compared with polymer modified cementitious based rendering material.

Test results have shown that HPF strengthening is an effective way to improve the load carrying capacity of columns. HPF using epoxy based rendering material provides better confinement due to higher tensile strength (at 3-4 times higher than polymer modified cementitious based rendering material).

Table 5A: Basic properties of specimens – Group 1

Specimen	Transverse reinforcement (hook)	Rendering mortar	Layers of wire mesh
TPC1	Plain concrete		
TA300C-1	R8@300 (90 ⁰)	Nil	Nil
TB75C-1	R8@75 (90 ⁰)	Nil	Nil
TB300C	R8@300 (135 ⁰)	Nil	Nil
TA300CS3	R8@300 (90 ⁰)	CS	3
TA300SD1-1	R8@300 (90 ⁰)	EM	1
TA300SD3-1	R8@300 (90 ⁰)	EM	3
TA300ST3-1	R8@300 (90 ⁰)	PMC	3

Table 5B: Basic properties of specimens – Group 2

Specimen	Transverse reinforcement (hook)	Rendering mortar	Layers of wire mesh
TPC2	Plain concrete		
TA300C-2	R8@300 (90 ⁰)	Nil	Nil
TB75C-2	R8@75 (90 ⁰)	Nil	Nil
TA300SD1-2	R8@300 (90 ⁰)	EM	1
TA300SD3-2	R8@300 (90 ⁰)	EM	3
TA300ST1	R8@300 (90 ⁰)	PMC	1
TA300ST3-2	R8@300 (90 ⁰)	PMC	3
T0ST1	Nil	PMC	1
T0ST3	Nil	PMC	3
T0SD1	Nil	EM	1
T0SD3	Nil	EM	3

Table 6: Peak strength P and capacity ratio R of specimens

Group 1			Group 2		
Specimen	P (kN)	R	Specimen	P (kN)	R
TPC1	2833.4	-	TPC2	3957.7	-
TA300C-1	3632.9	80.2%	TA300C-2	4717.3	85.7%
TB75C-1	4529.8	-	TB75C-2	5502.5	-
TB300C	3736.3	82.5%	TA300SD1-2	6782.2	123.3%
TA300CS3	4036.7	89.1%	TA300SD3-2	6574.1	119.5 %
TA300SD1-1	4765.0	105.2%	TA300ST1	5433.8	98.8%
TA300SD3-1	4918.9	108.6%	TA300ST3-2	5774.1	104.9 %
TA300ST3-1	4368.5	96.4%	T0ST1	4003.4	137.7%
			T0ST3	3774.8	129.8%
			T0SD1	4615.8	158.7%
			T0SD3	4378.1	150.6%

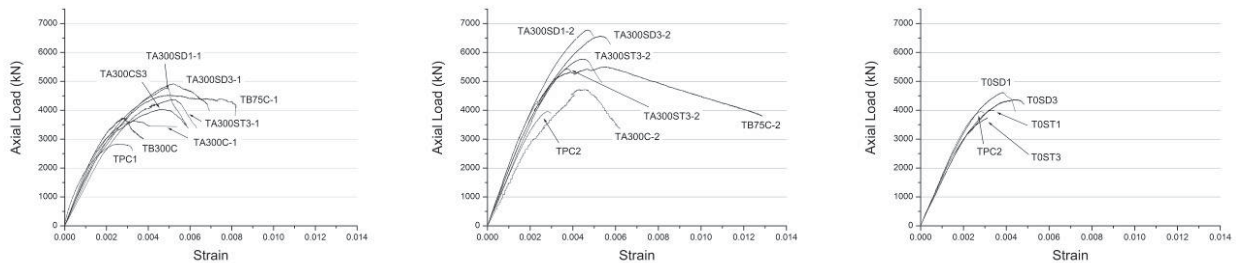


Figure 11: Load-strain plots of specimens.

4.2 Strengthening of beam-column Joints

Beam-column joint is a key member that affects the overall behavior of buildings under seismic action. Evidence from previous earthquakes has shown that failure of beam-column joints may cause the collapse of buildings and that beam-column joints designed without transverse reinforcement in the joint core (i.e. designed to gravity action similar to those commonly found in Hong Kong) exhibit poor performance (Pampanin et al 2002). Concrete jacketing, one of the earliest and common methods, has been used for strengthening beam-column joints for many years, e.g. Hakuto et al (2000), Wang and Hsu (2009). The technique has space limitation. Steel jacketing (e.g. Ghobarah et al 1997) and FRP jacketing (e.g. Ghobarah and Said (2002), Pantelides et al (2008), Lee et al (2010)) were developed, but it is vulnerable to fire. As a viable alternative, a method of strengthening beam-column joint using ferrocement jackets and diagonal reinforcements is proposed (see Figure 12).

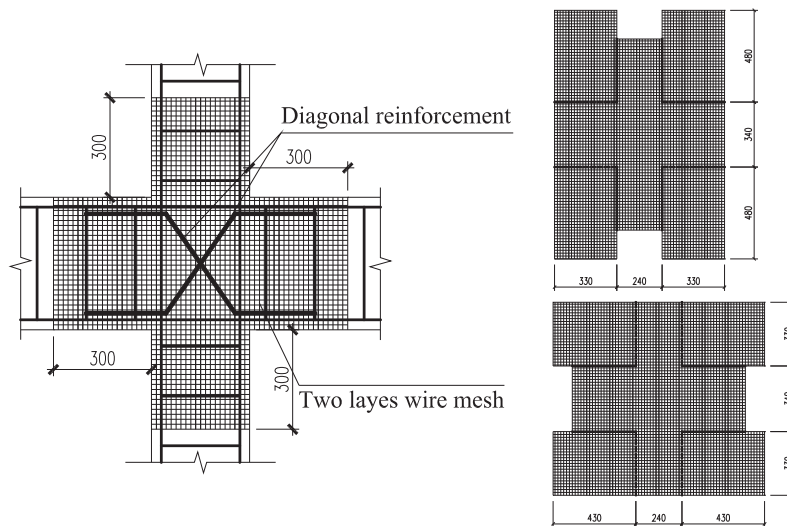


Figure 12: Proposed strengthening scheme for beam-column joints

Firstly, ferrocement is used to replace the concrete cover in the beam-column joint region. Two layers of wire mesh (see Figure 12) are installed by folded along the dotted lines and cut along the solid lines. Welded square mesh is used with averaged wire diameter of 1.45 mm and spacing at 13.23 mm in both directions. Afterwards, rendering material is applied. Secondly, two diagonal reinforcements of 10 mm diameter (yield stress at 800 MPa) are installed in the joint and anchored to the main reinforcements of the beams to reduce the force transferred to the joint.

Two specimens in 2/3 scale representing non-ductile beam-column joints were tested. Details of specimen are shown in Figure 13. The specimens replicate lower stories of a building. Specimen C1 is the control specimen without strengthening whereas specimen S1 is strengthened by ferrocement jackets and diagonal reinforcements. Ends of the specimens coincide with mid-span and mid-height of the actual frame. Columns are 2,385mm height and 300mm by 300mm in cross-section. Main reinforcements comprise 12T16 (or 2.7% main reinforcement ratio). Beams are 2,700mm long and 300mm by 400mm in cross-section. Transverse reinforcements comprise R8 rectangular ties at 150mm spacing. Same reinforcement ratio (4T16) is provided as top and bottom reinforcement (or 1.35% main reinforcement ratio).

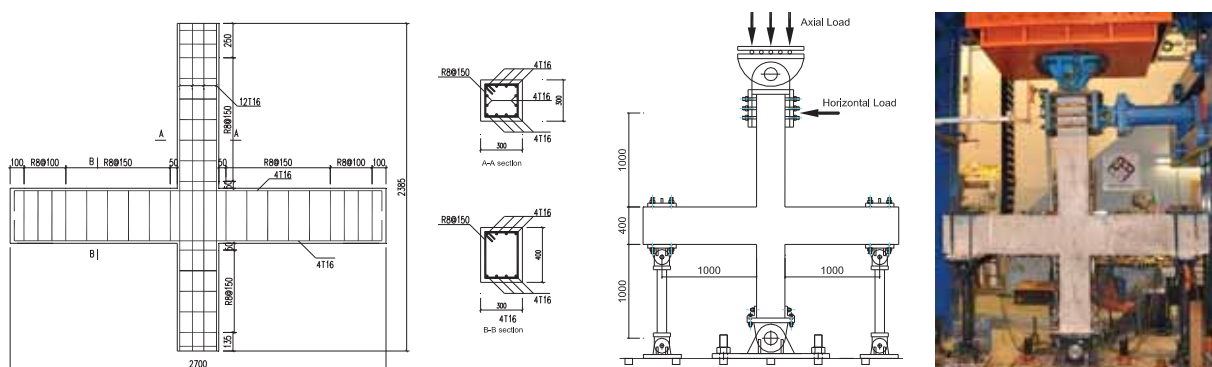


Figure 13: Reinforcement detail and test setup

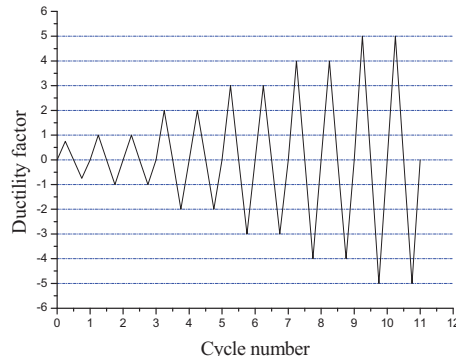


Figure 14: Loading routine

Test setup is shown in Figure 13. The specimens are tested by a displacement control multi-purpose testing system with a maximum loading capacity of 10,000kN. The bottom column is hinged at the base and is allowed to rotate. Both ends of the beam are supported by rollers and are free to move horizontally, but not vertically. Axial load is applied at the top of the upper column at $0.6f_c A_g$ and is kept constant throughout the loading test. Afterwards, cycles of horizontal displacement are applied from the top of the upper column by displacement control. Displacement ductility factor μ (ratio of actual displacement to yielding displacement) is used to control the loading cycles. Each loading cycle is repeated twice until the horizontal load dropped to 85% of its maximum value. Loading routine is shown in Figure 14. It is noted that high axial load is applied due to the high main reinforcement ratio in the columns.

Modes of failure of both specimens are due to insufficient shear strength in the joint and buckling of main reinforcement of the columns. Specimen C1 failed with two vertical cracks along the main reinforcements of the columns, diagonal cracks in the joint and flexural cracks in the beams. For specimen S1, delamination of ferrocement occurred at the joint. Cracks were distributed more uniformly in specimen S1 demonstrating better crack control.

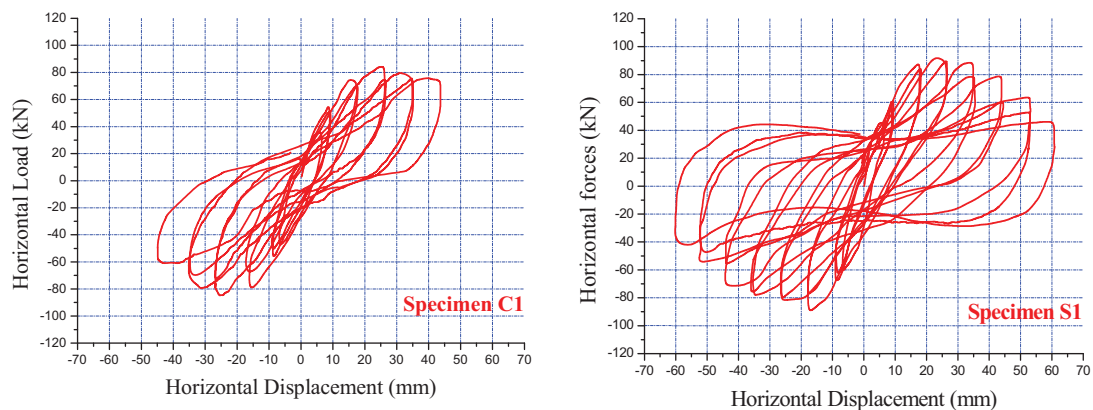


Figure 15: Column tip load-displacement relationship

Figure 15 shows horizontal load-displacement relationships obtained from the column tips. Specimen S1 reaches its ultimate load of 92.4kN (at 23.20mm) and -90.1kN (at -17.40mm). Specimen C1 reaches its ultimate load of 84.3kN (at 25.4mm) and -84.7kN (at -25.35mm). Here, positive and negative displacements represent pull and

push direction respectively. Ultimate strength is enhanced by 9.6% in the pull direction and 6.4% in the push direction. Increase in strength is limited due to spalling of rendering material at early stage of the loading history. As shown in Figure 16, energy dissipation capacity is enhanced at higher loading stage. In other words, if the same energy dissipation is required during an earthquake, specimen S1 will have smaller horizontal displacement as compared with specimen C1. At higher loading, energy dissipation of specimen S1 is larger than that of specimen C1. Specimen S1 sustains a larger increase in energy dissipation as the horizontal displacement cycle increases.

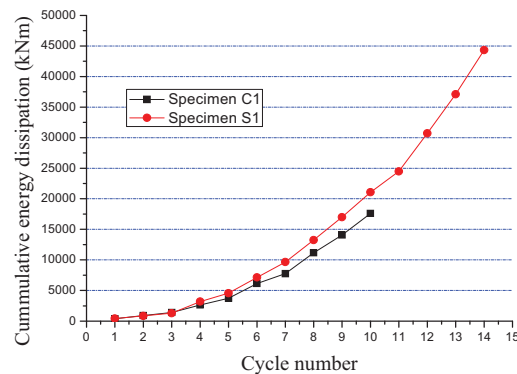


Figure 16: Cumulative energy dissipation at each cycle

Based on the observations and experimental results of two interior beam-column joints, it can be conclude that seismic performance of interior beam-column joints is improved by the proposed strengthening method with enhancement on ultimate strength, energy dissipation, stiffness and drift. Improvement on the proposed strengthening method will be carried out through using high performance mortar, applying varying layers of wire mesh and improving the bond behavior between ferrocement and the joint.

5. CONCLUSIONS

Through the joint efforts by academics and engineers, there is progress, within a short period of time, to address the issue of earthquake resistant design of buildings in Hong Kong. Still, there remain many important issues that have not been satisfactorily solved or have not yet been addressed. For instance, there is an urge to develop and implement means to strengthen the existing buildings. New technologies currently available worldwide, including damping devices and high performance materials can be used to improve the seismic performance of our building stock. By carrying out shaking table tests on scaled models, pseudo-dynamic tests on key members and numerical analysis, it is possible to qualify (if not quantify) the performance of existing buildings when subjected to earthquake action. The paper serves to bring out a few new options of strengthening for engineers to consider, including the use of damping devices to improve the performance of adjacent buildings in a building group and the use of high performance ferrocement to strengthen the structural members.

ACKNOWLEDGEMENTS

The authors are grateful to the financial support from the Research Grants Council of Hong Kong (RGC No: PolyU 5026/98E, 5038/99E, 5042/02E, 5206/08E) and The Hong Kong Polytechnic University. The authors would like to thank for the technical assistance provided by the Heavy Structural Laboratory of the Hong Kong Polytechnic University. In particular, the authors would like to thank the Institute of Engineering Mechanics, China Seismological Bureau, Harbin, China, for jointly conducting the shaking table tests.

REFERENCES

1. ABAQUS version 6.3.1. The Abaqus Software is a product of Dassault Systèmes Simulia Corp., Providence, RI, USA.
2. ACI 549.1R-93. "Guide for the Design, Construction, and Repair of Ferrocement". Reported by ACI Committee 549, reapproved 1999.
3. Ahmad S.M. and Shah S.P. (1982). "Stress-strain curves of concrete confined by spiral reinforcement". *Am. Concr. Inst. J.*, 79(6), 484-490.
4. Aoyama H. (2001). "RC High-rise Buildings in Seismic Areas". Editor Aoyama H., *Design of Modern High-rise Reinforced Concrete Structures*, Imperial College.
5. ASTM C39/C39M. "Standard Test Method for Compressive Strength of Cylindrical Concrete Specimens". ASTM International, 2009.
6. ASTM C469-02e1. "Standard Test Method for Static Modulus of Elasticity and Poisson's Ratio of Concrete in Compression". ASTM International, 2002.
7. Balmer G.G. (1949). "Shearing strength of concrete under high triaxial stress - computation of Mohr's envelope as a curve". *Structural Research Laboratory Report SP 23*, US Bureau of Reclamation, 1949-10-28.
8. Bhaskararao A.V. and Jangid R.S. (2006). "Seismic analysis of structures connected with friction dampers". *Engineering Structures*, 28(5), pp. 690-703.
9. Bracci J.M., Reinhorn A.M. and Mander J.B. (1995). "Seismic Retrofit of RC Buildings Designed for Gravity Loads: Performance of Structural Model". *ACI Structural J*, 92(6), 711-723.
10. Cap 121, *Buildings Ordinance (Application to the New Territories)*.
11. Cao Z., Li A., Wang Y.Y., Zhang W. and Yao Q. (2007). "Experimental study on RC space beam-column joints strengthened with high strength steel wire mesh and polymer mortar". *J of Southeast University (Natural Science Edition)*, 37(2), pp 235-239.
12. CECS 242:2008. "Technical specification for strengthening concrete structures with grid rebar and mortar". *China Association for Engineering Construction Standardization*. (in Chinese)
13. Chan H.C., Pan A.D.E., Pam H.J. and Kwan A.K.H. (1998). "Seismic detailing of reinforced concrete buildings with relevance to Hong Kong design practice, Part 1 and Part 2". *Transactions of the Hong Kong Institute of Engineers*, vol. 5(1), 6-20.

14. Chau K.T. and Wei X.X. (2001). "Pounding of structures modeled as nonlinear impacts of two oscillators". *Earthquake Engineering and Structural Dynamics*, vol. 30(5), 633-651.
15. Cheng W.X, Yan D.H., Kang G.Y. and Jiang J.J. (2003). "Concrete structure Part II: structure design of concrete building". Beijing: China architecture & building press.
16. Chopra K.A. (2006). "Dynamics of Structures: Theory and Applications to Earthquake Engineering". New Jersey: Prentice Hall.
17. Christenson E.R., Spencer F.B., Jr. and Johnson A.E. (2007). "Semiactive Connected Control Method for Adjacent Multidegree-of-Freedom Buildings". *Journal of Engineering Mechanics*, 133(3), pp. 290-298.
18. CoP1987. "Code of Practice for Structural Use of Concrete 1987". Building Authority Hong Kong.
19. CoP2004. "Code of Practice for Structural Use of Concrete 2004". Second Edition, The Government of the Hong Kong Special Administrative Region.
20. Dai J.W., Wong Y.L. and Zhang M.Z. (2000). "Torsion Response of Reinforced Concrete Building Under Shaking Table Test". *Advances In Structural Dynamics*, Vol. II, pp859-865.
21. Dai J.W. (2002). Research on Nonlinear Seismic Performance of Asymmetric RC Building Structure, Ph.D. Thesis, Institute of Engineering Mechanics, China Seismological Bureau.
22. Ersoy U., Tankut A.T. and Suleiman R. (1993). "Behavior of Jacketed Columns". *ACI Structural Journal*, 90(3), pp 249-261.
23. Fujitani H. and Saito T. (2006). "Devices for seismic isolation and response control". *Response control and seismic isolation of buildings*, London and New York: Taylor & Francis, pp 3-37.
24. GB 18306-2001. Seismic ground motion parameter zonation map of China. China, 2001
25. Geotechnical Control Office (1991). Review of Earthquake Data for the Hong Kong Region, Publication No.1/91, Geotechnical Control Office of Hong Kong.
26. Ghobarah A., Aziz T.S. and Biddah A. (1997). "Rehabilitation of reinforced concrete frame connections using corrugated steel jacketing". *ACI Structural Journal*, Vol. 94, No. 2, May-June 1997, pp 283-293.
27. Ghobarah A. and Said A. (2002). "Shear strengthening of beam-column joints". *Engineering Structures*, Vol. 24, Issue 7, pp. 881-888.
28. Hakuto S., Park R. and Tanaka H. (2000). "Seismic load tests on interior and exterior beam-column joints with substandard reinforcing details". *ACI Structural Journal*, Vol. 97, No. 1, pp. 11-25.
29. Han L.H., Zheng Y.Q. and Teng J.G. (2006). "Fire resistance of RC and FRP-confined RC columns". *Magazine of Concrete Research*, 58(8), pp 533-546.
30. Harries K.A., Ricles J.R., Pessiki S. and Sause R. (2006). "Seismic retrofit of lap splices in nonductile square columns using CFR jackets". *ACI Structural J*, 103(6), pp 874-884.
31. Ho I.F.Y. and Lam S.S.E. (2010). "Strengthening Reinforced Concrete Columns by High Performance Ferrocement". Proc. Joint Conf. of 7th Int. Conf. on Urban Earthquake Engng. & 5th Int. Conf. on Earthquake Engng., March 3-5, 2010, Tokyo Institute of Technology, Tokyo, Japan.

32. Ho I.F.Y. and Lam S.S.E. (2011). "Revitalization of Circular Concrete Columns by High Performance Ferrocement". Proc. Joint Conf. of 8th International Conference on Urban Earthquake Engng., March 7-8, 2011, Tokyo Institute of Technology, Tokyo, Japan.
33. Jiang L., Shang S. and Liu F. (2009). "Research on Axially compressed Behavior of RC Strengthening Round Columns Using High Performance Composite Cement Mortar Reinforced with Mesh Reinforcements". Journal of Hunan University of Technology, Vol. 23, No. 1. (in Chinese)
34. Kaushik S.K., Singh K.K., Kumar R. and Sharma T.P. (1996). "Performance of ferrocement encased concrete under fire exposure". Journal of ferrocement, 26(3), pp 191-196.
35. Kim J., Ryu J. and Chung L. (2006). "Seismic performance of structures connected by viscoelastic dampers". Engineering Structures, 28, pp.183–195.
36. Kim S.H. and Choi J.H. (2010), "Repair of Earthquake Damaged RC Columns with Stainless Steel Wire Mesh Composite", Advances in Structural Engineering, Vol. 13, No.2, April 2010, 393-402.
37. Kondraivendhan B. and Pradhan B. (2009). "Effect of ferrocement confinement on behavior of concrete". Construction and Building Materials, Vol. 23, Issue 3, 2009, 1218-1222.
38. Kuang J.S. and Wong H.F. (2002). "Enhancing the Ductility of RC Columns: A Case Study of Hong Kong". Proceedings of Recent Developments in Earthquake Engineering, HKIE Structural Division, 17 May 2002, 46-57.
39. Kumar G.R. and Kumar P.R. (2005). "A stress-strain model for standard concrete confined with ferrocement shell in addition to lateral ties". Journal of Ferrocement, 35(4), 655-669.
40. Lam S.S.E., Xu Y.L. Chau K.T., Wong Y.L., and Ko J.M. (2002). "Progress in earthquake resistant design of buildings in Hong Kong". Structural Engineering World Congress, Yokohama, Japan, October, 2002.
41. Lam S.S.E., Wu B., Wong Y.L., Wang Z.Y., Liu Z.Q. and Li C.S. (2003). "Drift capacity of rectangular reinforced concrete columns with low lateral confinement and high-axial load". Journal of Structural Engineering, 129(6), 733-742.
42. Lam S.S.E. (2009). "Estimating the economic life span of a reinforced concrete building". Proceedings of the 3rd International Conference on Concrete Repair – Concrete Solutions, Venice, 29 June to 2 July 2009.
43. Lee C.F., Ding Y.Z., Huang R.H., Yu Y.B., Guo G.A., Chen P.L. and Huang X.H. (1996). Seismic Hazard Analysis of the Hong Kong Region. Publication No 65, Geotechnical Engineering Office of Hong Kong.
44. Lee, W.T., Chiou, Y.J. and Shih, M.H. (2010). "Reinforced concrete beam-column joint strengthened with carbon fiber reinforced polymer". Composite Structures, Vol. 92, issue 1, pp. 48-60.
45. Li B. (1994). "Strength and Ductility of Reinforced Concrete Members and Frames Constructed Using High Strength Concrete". Research Report/ Dept. of Civil Engineering, University of Canterbury, Christchurch New Zealand, ISSN 0110-3326.
46. Li C.S., Lam S.S.E., Zhang M.Z. and Wong Y.L. (2006). "Shaking Table Test of a 1:20 Scale High-Rise Building with a Transfer Plate System". Journal of Structural Engineering, Vol. 132, No. 11, November 2006, pp. 1732-1744.

47. Li C.S., Lam S.S.E., Chen A. and Wong Y.L. (2008). "Seismic Performance of a Transfer Plate Structure". *Journal of Structural Engineering*, Vol. 134, No. 11, November 2008, pp. 1705-1716.
48. Mander J.B. (1983). "Seismic Design of Bridge Piers". thesis of PhD at the University of Canterbury, Christchurch New Zealand, 1983.
49. Mander J.B., Priestley M.J.N. and Park R. (1988a). "Theoretical Stress Strain Model of Confined Concrete". *Journal of Structural Engineering*, ASCE, Vol. 114, No. 8, pp. 1804-1826.
50. Mander J.B., Priestley M.J.N. and Park R. (1988b). "Observed Stress Strain Behavior of Confined Concrete". *Journal of Structural Engineering*, ASCE, Vol. 114, No. 8, pp. 1827-1849.
51. Matsagar V.A. and Janid R.S. (2005). "Viscoelastic damper connected to adjacent structures involving seismic isolation". *Journal of Civil Engineering and Management*, 6(4), 2005, pp. 309-322.
52. Naaman A. E. (2000). "Ferrocement and Laminated Cementitious Composites". Techno Press 3000, 2000.
53. Pam H.J., Su R.K.L., Lam W.Y., Li J., Au F.T.K., Kwan A.K.H. and Lee P.K.K. (2002). "Designing Coupling Beams and Joints in Concrete Buildings for Improved Earthquake Resistance". *Proceedings of Recent Developments in Earthquake Engineering*, HKIE Structural Division, 17 May 2002, 91-105.
54. Pampanin S., Calvi G.M. and Moratti M. (2002). "Seismic behavior of RC beam-column joints designed for gravity loads". 12th European Conference on Earthquake Engineering, Paper Reference 726.
55. Pantelides C.P., Okahashi Y. and Reaveley L.D. (2008). "Seismic rehabilitation of reinforced concrete frame interior beam-column joints with FRP composites". *Journal of composites for construction*, ASCE, July/August 2008, pp. 435-445.
56. Paramasivam P., Lim C.T.E. and Ong K.C.G. (2000). "Ferrocement in structural upgrading and rehabilitation – an overview". *Proc. of 4th Int. Conf. on Repair, Rehabilitation, and Maintenance of Concrete Structures*, Seoul, Korea, 253-269.
57. Paulay T. and Priestley M.J.N. (1992). "Seismic Design of Reinforced Concrete and Masonry Building". John & Sons, Inc.
58. Popovics S. (1973). "A numerical approach to the complete stress-strain curves for concrete". *Cement and Concr. Res.*, 3(5), 583-599.
59. Pun W.K. and Ambrasseys N.N. (1992). "Earthquake data review and seismic hazard analysis for the Hong Kong region". *Earthquake Engineering and Structural Dynamics*, vol. 21, 1-11.
60. Richart F.E., Brandtzaeg A. and Brown R.L. (1928). "A study of failure of concrete under combined compressive stresses". *Engineering Experiment Station Bulletin No. 185* (1928) Urbana, IL.
61. Scott D.M., Pappin J.W. and Kwok K.Y. (1994). "Seismic Design of Buildings in Hong Kong". *Transactions of Hong Kong Institution of Engineers* 1(2), p37-50.
62. Seto K. (1994). "Vibration Control Method for Flexible Structures Arranged in Parallel". *Proceedings of 1st world conference on structural control*, 2, 62–71.

63. Shah S.P., Lub K.B. and Ranzoni E. (1986). "A summary of ferrocement construction and a survey of its durability". RILEM Committee 48-FC, *Materials and Structures*, 19(4), pp 297-321.
64. Sheikh S.A. and Uzumeri S.M. (1980). "Strength and ductility of tied concrete columns". *J. Struct. Div., A.S.C.E.*, 106(5), 1079-1102.
65. Su R.K.L. (2008). "Seismic Behaviour of Buildings with Transfer Structures in Low-to-Moderate Seismicity Regions". *Electronic Journal of Structural Engineering Special Issue, Earthquake Engineering in the low and moderate seismic regions of Southeast Asia and Australia (2008)*.
66. Tadeu A.J.B. and Branco F.J.F.G (2000). "Shear tests of steel plates epoxy-bonded to concrete under temperature". *J of Materials in Civil Engineering*, 12(1), pp 74-80.
67. Wang Y.C. and Hsu K. (2009). "Shear Strength of RC Jacketed Interior Beam-Column Joints without Horizontal Shear Reinforcement". *ACI Structural Journal*, March-April 2009, pp. 222-232.
68. Westermo B. (1989). "The dynamics of interstructural connections to prevent pounding". *Earthquake Engineering and Structural Dynamics*, 18(5), pp. 687-99.
69. Williamson R.B. and Fisher F.L. (1983). "Fire resistance of a load bearing ferrocement wall". Report no UCB-FRG-83-1, Dept of Civil Eng, U of California, Berkeley, Feb 1983.
70. Wong Y.L., Zhao J.X., Chau K.T. and Lee C.M. (1998a). "Assessment of seismicity model for Hong Kong region". *The HKIE Transactions*, vol. 5(1), 50-62.
71. Wong Y.L., Zhao J.X., Lam S.E.E. and Chau K.T. (1998b). "Assessing seismic response of soft soil sites in Hong Kong using microtremor records". *HKIE Transactions*, vol. 5(3), 70-79.
72. Wu Y.F., Liu T. and Oehlers D.J. (2006), "Fundamental principles that govern retrofitting of RC columns by steel and FRP jacketing". *Advances in Str Eng*, 9(4), pp 507-532.
73. Xu Y.L., Zhan S., Ko J.M. and Zhang W.S. (1999a). "Experimental investigation of adjacent buildings connected by fluid dampers". *Earthquake Engineering and Structural Dynamics*, vol. 28, 609-631.
74. Xu Y.L., He Q. and Ko J.M. (1999b). "Dynamic response of damper-connected adjacent buildings under earthquake excitation". *Engineering Structures*, 21, pp. 135-148.
75. Yamada Y., Ikawa N., Yokoyama H., and Tachibana, E. (1994). "Active Control of Structures using the Joining Member with Negative Stiffness". *Proceedings of 1st world conference on structural control*, 2, 41-49.

Acknowledgements

The organizing committee would like to express heartfelt thanks to the following sponsors for their generous support to the One-day Symposium on 2nd Contemporary Seismic Engineering 2011:

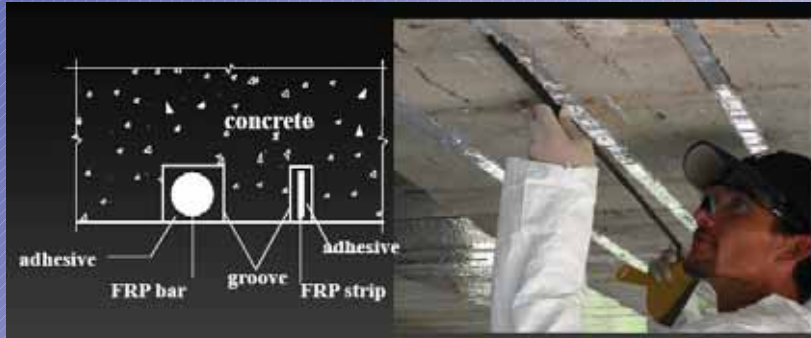
- Dextra Pacific Limited
- Genetron Engineering Company Limited
- K.Y.H. Steel Company Limited
- Meinhardt Consulting Engineers
- Ove Arup and Partners Limited
- Wong Pak Lam & Associates Consulting Engineers & Architects Limited



Dextra Pacific

SOLUTION FOR THE **CONSTRUCTION**

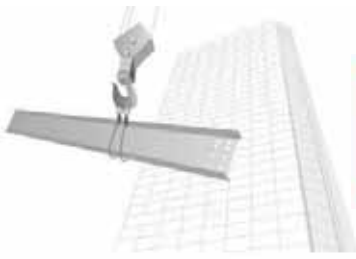
Aslan Pacific



FRP REINFORCEMENT AND STRENGTHENING SYSTEM



**SPLICING SYSTEM TO BE USED IN ANY
LOCATION OF THE STRUCTURE IN
ACCORDANCE WITH AC133 CRITERIA**



KYH 金源行



ISO 9001 : 2008
Certificate No.: CC 2930



ISO 9001 : 2008
Certificate No.: CC 2930



Supply of Steel Products:
H-bearing piles, Sheet piles,
Universal Beams/Columns,
Plates, Hollow sections,
Galvanized pipes, Angles,
Channels, Corrugated sheets,
Reinforcement bars...

K.Y.H. Steel Company Limited
11E Skyline Tower, 18 Tong Mei Road, Mongkok, Kowloon, Hong Kong.
Tel: (852) 34732300 Fax: (852) 27891366 E-mail: kyhsteel@kyh.com.hk

*TAMAR Development Project –
A Central Government Complex &
a Legislative Council Complex*



Meinhardt is a leading international multi-disciplinary engineering and project management firm, offering ultimate engineering solutions and added value to a vast range of construction initiatives.

Established for over 55 years with over 35 years leading the way throughout Asia, **Meinhardt** works with all of the best architects from around the world creating landmarks across Asia.

AVIC Plaza, Shenzhen

Taihu Plaza, Wuxi

Nanjing CBD, Nanjing



Wuxi Hang Lung Plaza, Wuxi

Hangzhou MIXC Phase 2, Hangzhou



MEINHARDT

Consulting Engineers • Planners • Managers

Offices in Asia, Australia, Middle East & UK

www.meinhardtgroup.com

Email: mcehk@meinhardt.com.hk

A tall, slender skyscraper, the China World Tower, is illuminated at night, showing a grid of windows and a distinctive top section. The building is set against a dark blue sky. In the foreground, there are other buildings, including a large, modern structure with a curved facade and a large green and white graphic on its side. The overall scene is a cityscape at night.

Optimising safety with innovation

With extensive experience and unparalleled industry insight, Arup is at the leading edge of seismic engineering, providing smart and cost-effective protection for many of the world's most innovative structures.

◀ China World Tower
Beijing's tallest building at 330m



WONG PAK LAM & ASSOCIATES
CONSULTING ENGINEERS & ARCHITECTS
黃柏林建築工程師有限公司



Tseung Kwan O Hospital Extension



*3D Reinforced Concrete Structure Frame
created by BIM Program*



*Proposed Hotel Development at
Tseung Kwan O Station*

Your **Reliable Partner** in **Structural Steelwork Construction**

Established for 20 years, **Genetron Engineering** has been one of the leading specialist contractors in structural steelwork, committed to providing practical solutions to Clients and Consultants for every unique design. We have developed a reputation of delivering quality products on time, and to the highest standards of workmanship.



Steel footbridge (52m in length) across Lung Cheung Road, Wong Tai Sin
Construction of pedestrian steel bridge with innovative design of slim cable truss and highly transparent façade



駿明工程有限公司
Genetron Engineering Co., Ltd.

Room 1161, 11/F., Hong Kong International Trade & Exhibition Centre,
1 Trademart Drive, Kowloon Bay, Kowloon, Hong Kong
Tel: (852) 2389 9900 Fax: (852) 2343 4373 Email: genetron@genetron.com.hk



香港
鋼結構學會

Hong Kong Institute of
Steel Construction

10th Anniversary

Hong Kong Institute of Steel Construction (HKISC) was established in November 2000. It has been registered as a non-profit making organization with its board members from universities, consultants, contractors laboratories, etc. in Hong Kong. HKISC serves the steel construction industry in Hong Kong and the region and carries the following specific missions.

Missions:

- Channeling of technology transfer between academics and the steel construction industry for improved quality in design, analysis and construction;
- Making university research more practical and useful for practitioners;
- Informing and sharing of new technology worldwide among members ;
- Organizing seminars for local and overseas experts for dissemination of their technological know-how ;
- Developing and fostering friendship among members for exchange of opinions

Website: <http://www.hkisc.org>